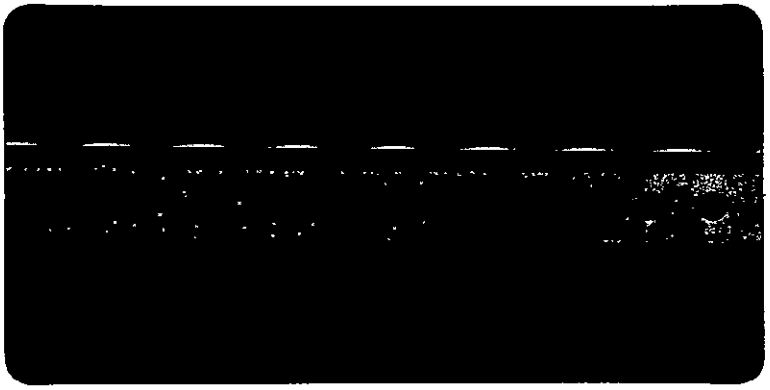

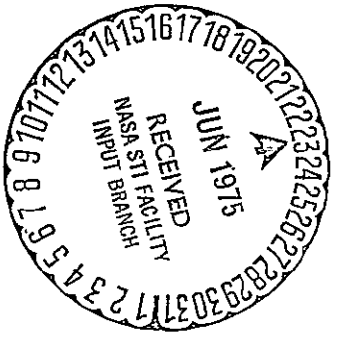

UNIVERSAL ANALYTICS, INC.

Los Angeles

FINAL REPORT

For

THE NASTRAN SRB SLAPDOWN . WATER IMPACT ANALYSIS

Presented to:

NATIONAL AERONAUTICS AND SPACE ADMINISTRATION
Marshall Space Flight Center, Alabama

Contract No. NAS8-29665

May 12, 1975

Prepared by

UNIVERSAL ANALYTICS, INC.
7740 West Manchester Boulevard
Playa Del Rey, California 90291
(213) 822-4422

FOREWORD

This document presents the Final Report for the contract, "Flexible Body/Water Interaction During Water Impact," Contract NAS8-29665. The project was originated by the Marshall Space Flight Center (MSFC) of the National Aeronautics and Space Administration (NASA), and performed by Universal Analytics, Inc. (UAI).

The principal investigator for the project was Mr. D. N. Herting. Messrs. R. L. Hoesly, K. Kahyai, E. G. Sergoyan, and D. R. Williamson contributed in various phases of the effort. UAI would like to extend its appreciation to Mr. D. A. Kross, the NASA contract technical monitor, for his able guidance during the performance of the contract and Mr. A. R. Thoren of Teledyne Brown Engineering for his assistance in the program checkout.

ABSTRACT

This report describes the computer analysis of the hydroelastic interaction between a shell structure representing the Space Shuttle Solid Rocket Motor Case and an incompressible fluid during the slapdown phase of water impact. The large motions and hydroelastic response of the system is obtained by numerical integration of the combined hydrodynamics and structural equations of motion. The computerization of the slapdown hydroelastic capability has been incorporated into the general purpose NASTRAN Computer Code.

Included in this report are the development of the theoretical basis, a guide to the program's usage, results of correlation and parameter studies, and a detailed description of the computer code.

The effort, performed by Universal Analytics, Inc., under NASA/MSFC Contract No. NAS8-29665, is a continuation of the previous task of developing water impact loads for the SRB nozzle entry and broadside impact cases. Whereas the previous effort treated localized impacts over short time periods, the slapdown analysis capability will perform the analysis of large motions of the entire booster case for a selected interval after the initial nozzle impact.

TABLE OF CONTENTS

LIST OF FIGURES

1.0 INTRODUCTION

The Space Shuttle concept calls for a parachute descent of the expended booster solid rocket motors into the sea, followed by recovery. The water impact portion of this operation will impart severe loadings which could influence the structural design requirements of the solid rocket motors. Marshall Space Flight Center (MSFC) has begun a test and analysis program to study the dynamic response characteristics of the booster structures and define envelopes of acceptable water entry and recovery conditions.

After the initial impact of the booster nozzle, the vehicle translates and rotates into the slapdown impact condition whereby large pressure loads may be applied to the cylindrical shell. The slapdown phase of the space shuttle solid rocket booster (SRB) during water entry is a potentially critical condition which depends not only on the initial impact condition but also on the structural characteristics of the vehicle.

This report has been prepared by Universal Analytics, Inc. (UAI) to describe the theoretical basis, coding design, and results for a computer program to analyze the slapdown impact of a flexible cylindrical structure. The slapdown analysis begins after the initial nozzle impact effects have subsided. The user selects the initial position and velocities at the start of the slapdown phase and the total period for the analysis. The computational scheme incorporated into NASTRAN analyzes the following effects at each instant of time:

1. The hydrodynamic pressures
2. The shell response which includes deformations (velocities and accelerations) and stresses in the flexible body
3. Vehicle rigid body motion for the total vehicle load

The interaction of these functions forms the coupled hydroelastic analysis. The structural model for the impact problem consists of cylindrical finite shell elements. The effects of the fluid is modeled by analytically calculating the fluid pressures from the structure motions and applying the resultant loads directly to the structure.

The analytic development of the fluid equations is contained in Section 2.0. The effects of hydrodynamic pressures, buoyancy, drag, and large angle changes in the vehicle orientation are included. The equations are derived with the goal of developing the forces on the structural finite element model which will, in turn, be dependent on the motions of the structural degrees of freedom. The resulting expressions have been cast in a form conducive to efficient computer processing. The chapter concludes with a discussion of the numerical stability of the transient integration method. The method of providing more exact and stable solutions to the nonlinear iterations is developed.

A description of the testing of the computer analysis with finite element models of actual structures is given in Section 4.0. Experimental results are compared with the analytic values for the 120-inch diameter (77%) test vehicle. Appendix B contains an extensive set of these comparisons. A full scale SRB analytic model was also tested for various impact conditions. Also included in this chapter are the conclusions and recommendations based on the results and the experience with the program.

The detailed user guide and programming descriptions for the new water imapct analysis capability are described in Sections 3.0 and Appendix A respectively. The code is implemented in the Level 15.5 NASTRAN structure analysis program as an extension of the existing direct transient analysis capability. The format of the descriptions is similar to the format used in the NASTRAN User's and Programmer's Manuals and may be inserted in the appropriate manuals.

2.0 THEORETICAL DEVELOPMENT

2.1 DEFINITION OF THE SLAPDOWN WATER IMPACT PROBLEM

When a flexible shell such as the space shuttle solid rocket motor case (SRM) impacts upon water, high pressures are generated on the shell surface, causing rapid local deformations of the shell and large overall displacements and rotations of the center of mass. These deformations and their time rates of change interact with the fluid to modify the pattern of flow about the shell and, consequently, the pressure profiles and subsequent shell deformations. It is essential to accurately predict the forces acting on the vehicle and the vehicle's motion during water impact in order to satisfy the structural design requirements of proposed configurations.

In the slapdown phase of the SRM water impact the following forces act on the structure:

1. The submerged portion of the structure interacts with the water to produce a three-dimensional flow field dependent on the vehicle position and velocity. The resulting pressures on the shell will produce "hydrodynamic" forces which produce local deformations and acceleration of the overall rigid body motions.
2. Hydrostatic and gravitational forces are produced due to buoyancy effects of the submerged volume and mass of the vehicle respectively. These forces will primarily contribute to the overall vehicle motion; their effect on local deformations is small.
3. Although the viscous fluid drag forces (i.e., "skin friction") will be small when compared to the hydrodynamic forces, they will act as damping forces on the overall vehicle motion and affect the results when the analysis is performed over the full slapdown time period.

These forces are absorbed by the vehicle as a combination of structure deformations and inertial reactions, dependent on the structure stiffness and mass properties.

The structure to be analyzed consists of a cylindrical shell with an arbitrary axisymmetric interior structure. The ends of the cylinder are enclosed by a nose section and a bulkhead/nozzle structure. The structure may be represented by an axisymmetric finite element model whereby the local displacements at each station are represented by a Fourier series. This allows a matrix formulation using uncoupled harmonics and a relatively small number of degrees of freedom. Because of the large overall displacements and rotations, the dynamics of the structure will be separated into nonlinear rigid body motion and linear local deformations. The deformations will be measured in a coordinate system moving with the center of gravity.

The impact problem must be analyzed by numerical integration of the equations of motion with respect to time. At each point in time the positions, velocities, and accelerations of the structure are used to calculate the corresponding fluid dynamics. The resulting fluid pressures may then be resolved into forces on the structure which, in turn, affect the structure motion.

This numerical transient procedure is developed to achieve accuracy and stability within the constraints of economics and computer hardware. Because of the large changes in the fluid-structure interface, the fluid forces must be treated as nonlinear loads which depend on displacement, velocity, and acceleration, rather than as known functions of time. When the nonlinear terms become predominant and conventional numerical transient methods are used, a numerical stability problem results. In the effort previous to this contract [Ref. 1] the standard NASTRAN nonlinear capability proved to have limits on the physical parameters of the problem to be solved.

In the following sections the theoretical development of the equations of motion and the water impact loads will be presented, followed by a description of the numerical integration procedure. An overall summary of the computational steps concludes the theoretical report.

2.2 EQUATIONS OF MOTION

In the following development, the motion of the SRB structure will be separated into two types of displacements. The rigid body motion of the structure will be measured by the displacements and rotation at the center of gravity in a fixed coordinate system shown in Figure 1. In addition, the deformations of the structure are assumed to be linear small motions measured in a moving coordinate system fixed to the body as shown in Figure 2.

The structure itself is assumed to be an axisymmetric shell. At each station along the axis, the displacement field is defined by the coefficients u_r^n, u_ϕ^n, u_z^n of the Fourier series,

$$
\begin{aligned}
u_r(\phi) &= \sum_{n=0}^{N} u_{ri}^n \cos n\phi \\
u_\phi(\phi) &= \sum_{n=0}^{N} u_{\phi i}^n \sin n\phi \\
u_z(\phi) &= \sum_{n=0}^{N} u_{zi}^n \cos n\phi
\end{aligned}
\tag{1}
$$

where $u_r(\phi)$, etc., are the actual displacements at angle, ϕ, as shown in Figure 2. For a more detailed description of this method of structure modeling, and the options available, see Reference 2.

In order to separate the local displacements from the rigid body motion it is necessary to develop a transformation where:

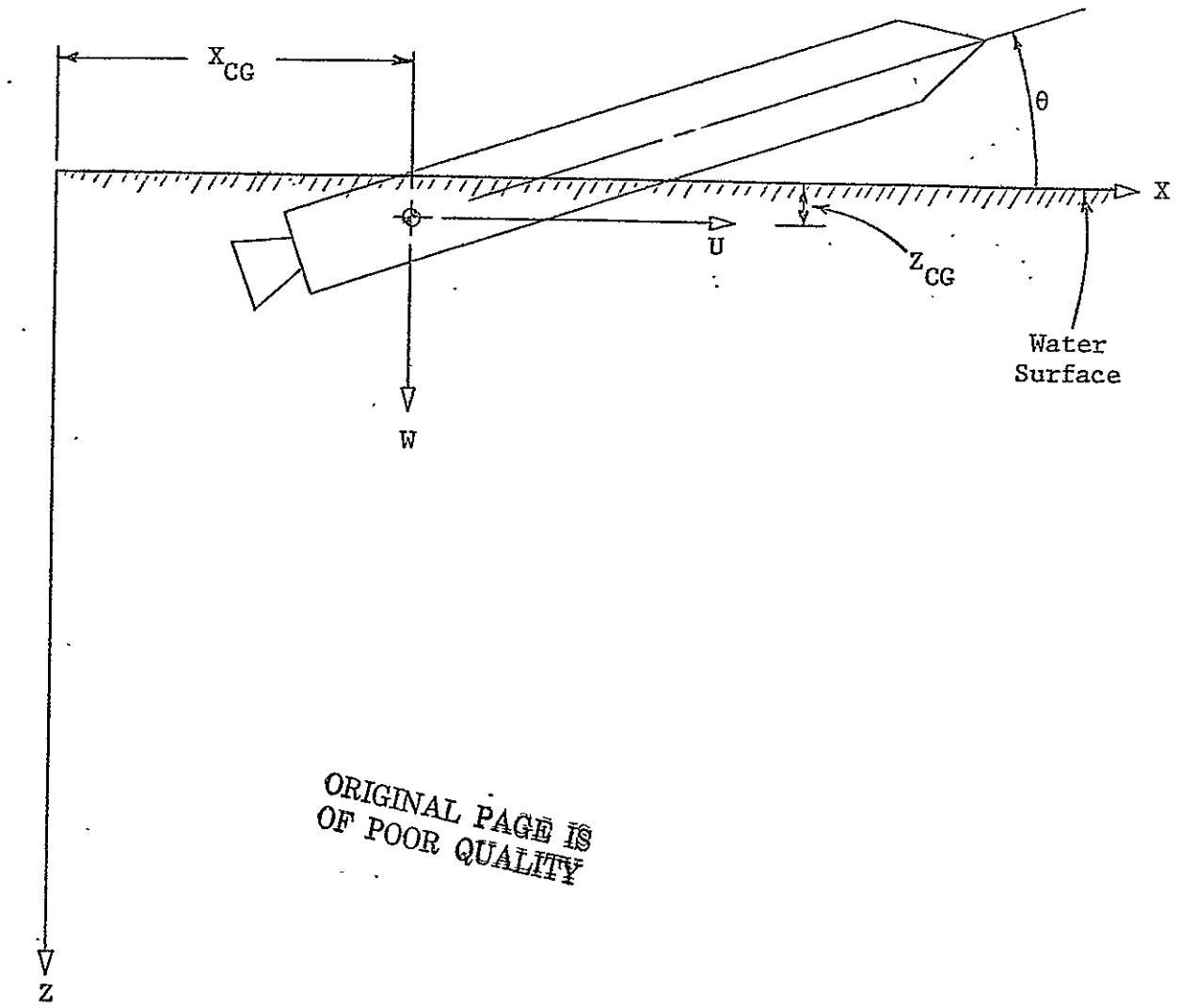

FIGURE 1. RIGID BODY COORDINATE SYSTEM

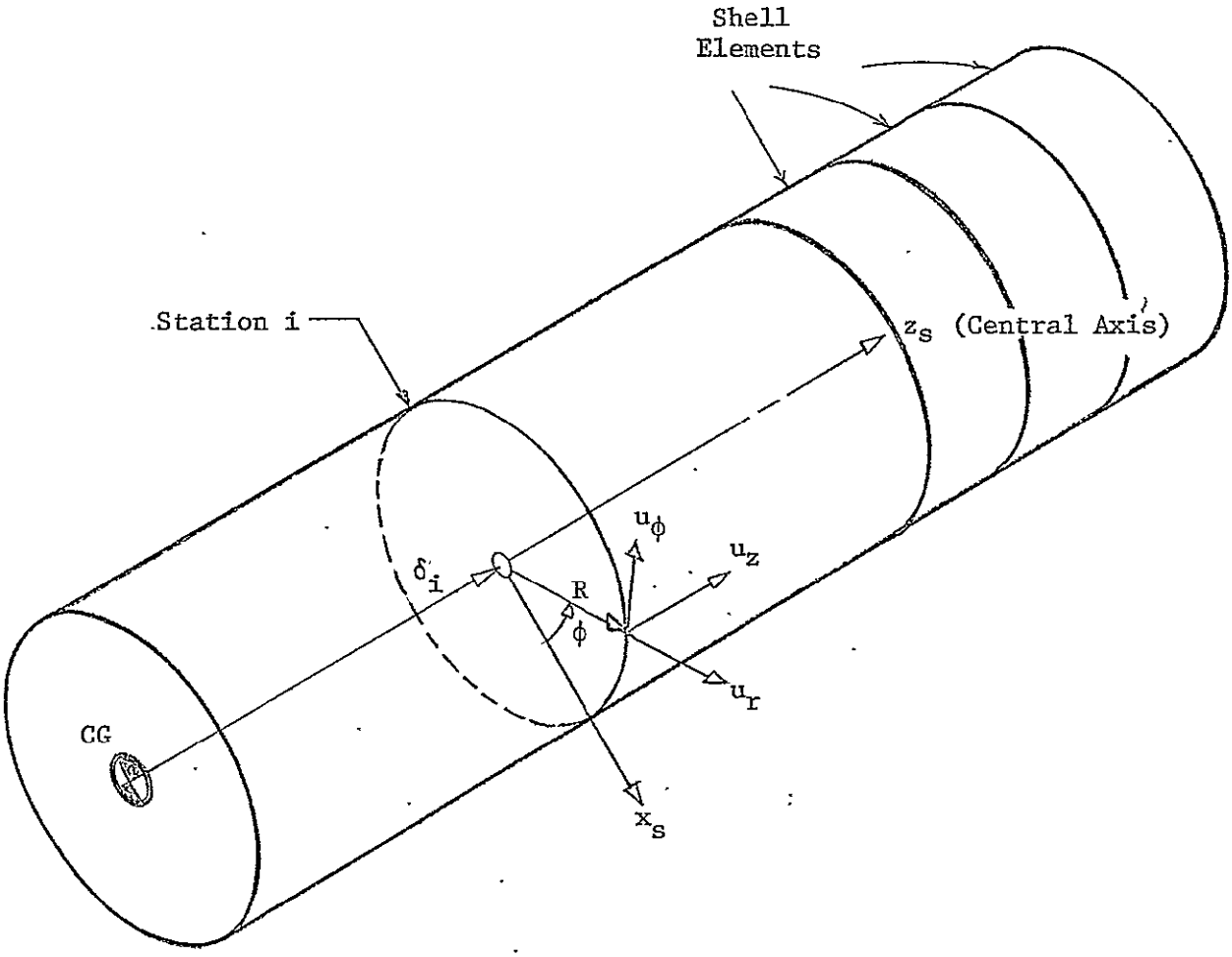

FIGURE 2. VEHICLE AND ELEMENT COORDINATE SYSTEMS

$$\{u_i\}_{abs} = \{u_i\}_{local} + [D_i] \begin{Bmatrix} U \\ W \\ \theta \end{Bmatrix}_{CG} \tag{2}$$

The matrices, D_i, in effect, are the free-body modes of the structure. Since energy is preserved in the transformation, the net forces on the center of gravity are

$$\begin{Bmatrix} F_x \\ F_z \\ M \end{Bmatrix}_{CG} = \Sigma [D_i]^T \{F_i\} \tag{3}$$

When the transformation given above is obtained, the equations of motion may be separated into the free body and deflected components as shown in the following development.

The structure is defined by a stiffness matrix [K], a structural damping matrix [B], and a mass matrix [M] where

$$[M] \{\ddot{u}\}_{abs} + [B] \{\dot{u}\}_{abs} + [K] \{u\}_{abs} = \{P\} \tag{4}$$

where {u} is the vector of absolute displacements at all points on the structure and {P} is the corresponding set of applied loads.

Substituting Eqs. (2) and (3) into Eq. (4), and noting that a rigid body displacement does not produce internal loads on the stiffness or damping matrices, two separate equations of motion are obtained.

The equation for local deformation is:

$$[M] \{\ddot{u}\}_{local} + [B] \{\dot{u}\}_{local} + [K] \{u\}_{local} = \{P\} - [M] [D] \{\ddot{U}\}_{CG} \tag{5}$$

Since the damping and stiffness matrices do not restrain rigid body motions, the equation for rigid body motion is:

$$[D]^T [M] [D] \{\ddot{U}\}_{CG} = [D]^T \{P\} \tag{6}$$

Equations (5) and (6) provide the basis for the solution of the problem. A set of loads {P} are generated from the fluid pressures, gravity, etc. and

transformed to rigid body loads for use in Eq. (6). The rigid body accelerations, $\{\ddot{U}\}$, are obtained from Eq. (6) and integrated to produce rigid body velocities and position. The right-hand side of Eq. (5) is a set of loads on the structure which includes the inertial loads due to the rigid body motion. The load vector is in equilibrium and, when applied to the structure transient algorithm, theoretically will produce no free body motions.

Note that the matrix [D] is the collection of all partitions $[D_i]$ described by Eqs. (2) and (3). If the body is undergoing large rotations the [D] matrix changes with time, however, the matrix product on the left side of Eq. (6) remains constant, since the rigid body mass matrix at the CG is defined as:

$$[D]^T [M] [D] = \begin{bmatrix} M & 0 & 0 \\ 0 & M & 0 \\ 0 & 0 & I \end{bmatrix} \tag{7}$$

where M is the total mass of the structure and I is the inertia.

Since the matrices [M], [B], and [K] are created by the finite element model and are developed in Reference 2, Eq. (5) may be solved with the linear structure analysis. The remaining tasks are to define the load vector, {P}, and the transformation matrix [D]. The latter is derived quite easily in terms of the geometry and equilibrium of forces as described below.

The forces on the structure may be defined as coefficients F^n_{ri}, $F^n_{\phi i}$, F^n_{zi} in the Fourier series representing the circumferential force distribution at each station i. The total force vector in vehicle coordinates at each station may be obtained by the equations:

$$\begin{aligned} F_{xi} &= \int_0^{2\pi} [F_{ri}(\phi) \cos\phi - F_{\phi i}(\phi) \sin\phi] \, d\phi \\ &= F^1_{ri} - F^1_{\phi i} \end{aligned} \tag{8}$$

$$F_{zi} = \int_0^{2\pi} F_{zi}(\phi) \, d\phi = F^0_{zi}$$

The total force acting at the center of gravity is the sum of the resultant force at each station. The total moment about the CG is obtained by multiplying the forces by the distance from the center of gravity.

Rotating the forces into the absolute coordinate system results in the following equation for the net force at the center of gravity:

$$\begin{Bmatrix} F_X \\ F_Z \\ M \end{Bmatrix}_{CG} = \sum_i \begin{bmatrix} \sin\theta & -\sin\theta & \cos\theta \\ \cos\theta & -\cos\theta & -\sin\theta \\ \delta_i & \delta_i & 0 \end{bmatrix} \begin{Bmatrix} F^1_{ri} \\ F^1_{\phi i} \\ F^0_{zi} \end{Bmatrix} \tag{9}$$

where δ_i is the location of station i relative to the center of gravity.

The transformation matrices $[D_i]$ defined in Eq. (3) are the transpose of the matrix on the right side of Eq. (9). In the actual calculation algorithm these matrices need not be generated explicitly; the loads and accelerations are transformed as they are needed.

2.3 VEHICLE LOADS

In this section the dynamic loads applied to the structure will be developed from the position of the vehicle and its displacements, velocities, and accelerations. At any point in time the position of the vehicle is illustrated in Figure 1. The pressures on each vehicle station are calculated individually from the local properties, transformed to loads on the structure, and used to calculate the vehicle response.

2.3.1 Coordinate System Relationships

At the point of intersection of the vehicle and the water surface at each station, two coordinate systems are erected. The types of systems to be used in the fluid analysis are shown in Figures 3 and 4. In Figure 3, the basic

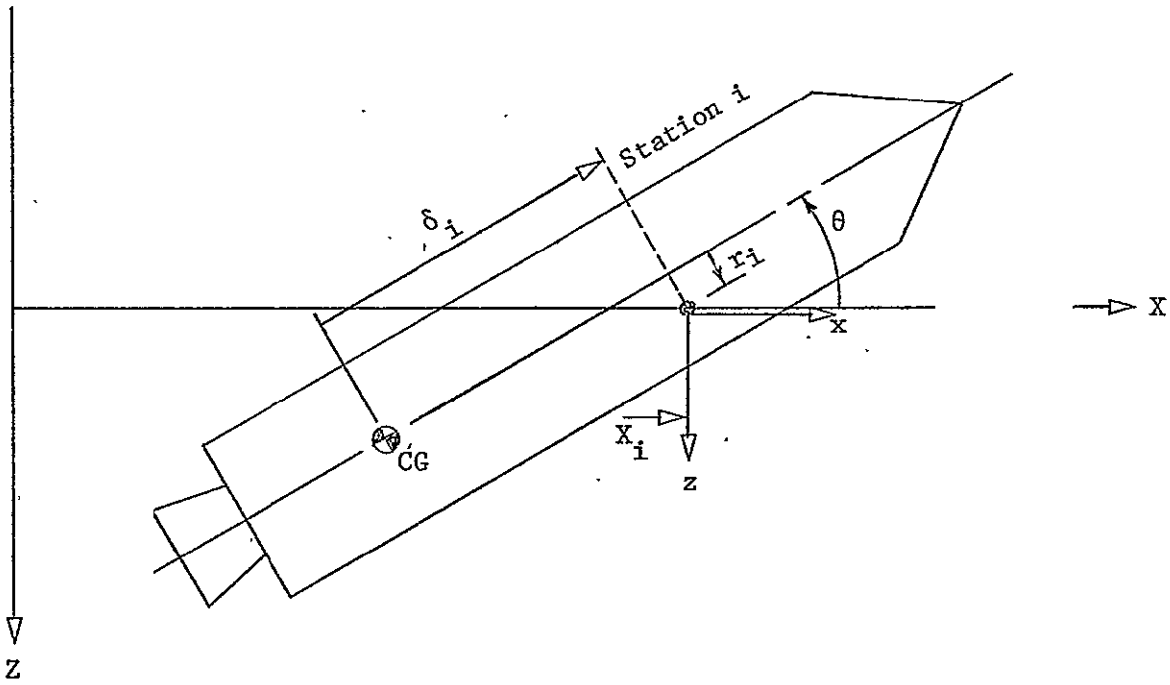

FIGURE 3. LOCAL FLUID SYSTEM AT EACH VEHICLE STATION

rigid body positions are used to define the penetration of each section of the structure. In Figure 4, a local coordinate system is placed on the surface to define the flow in the region of each station.

Referring to Figure 3, the distance from the center line to the water surface, r_i, and the location of the intersection, X_i, may be obtained from the equations:

$$X_i = X_{CG} + \delta_i \cos\theta + r_i \sin\theta$$

and

$$r_i \cos\theta = \delta_i \sin\theta - Z_{CG} \qquad (10)$$

or

$$X_i = X_{CG} + (\delta_i - Z_{CG} \sin\theta) / \cos\theta \qquad (11)$$

2.3.2 Hydroelastic Impact Loads

The solution for the potential flow problem assuming impact of a cylindrically shaped body will be summarized in this section. This case is representative of the broadside slapping condition assuming the booster to be a cylindrical shell. Expressions will be developed for three-dimensional pressure distributions which will include the interactive effects between the flexible shell and the fluid. These loads are calculated for penetration depths which are less than the radius of the cylinder.

Following the procedure described in Reference 1 for determining the velocity potential ϕ, we shall represent the wetted surface of the penetrating shell by an expanding flat plate having a variable width 2a at each vehicle station.

In Figure 4, the coordinate system used for analyzing the potential flow is illustrated. The elliptic coordinates η and ξ are defined by the equations:

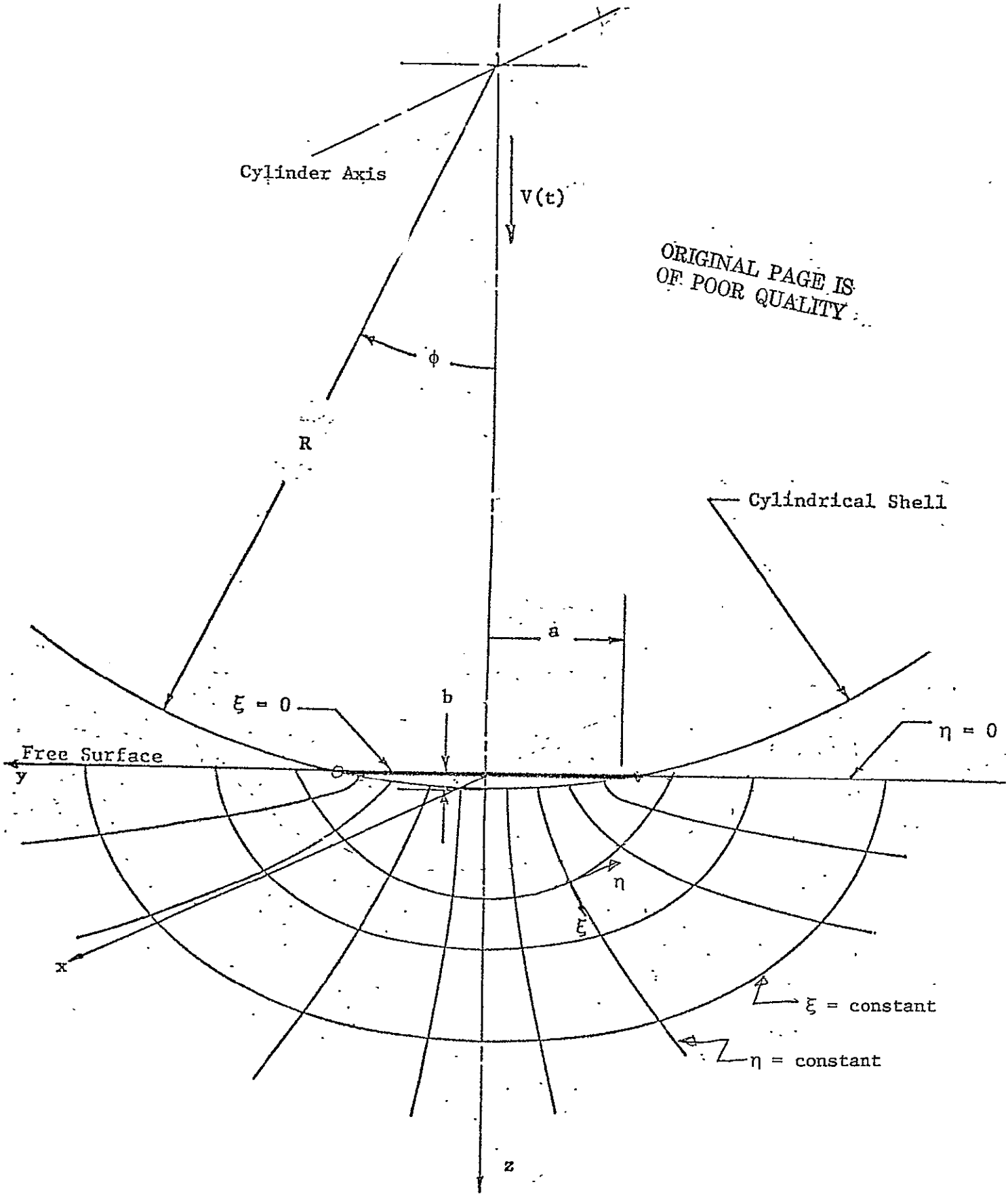

FIGURE 4. ELLIPSOIDAL COORDINATE SYSTEM AT EACH STATION FOR SLAPDOWN IMPACT

$$y = a \cosh\xi \cos\eta$$
$$z = a \sinh\xi \sin\eta \qquad (12)$$

where a is the half-width of the intersection of the vehicle and the fluid surface.

Referring to Figure 4, the half-width, a, of the wetted surface is related to the radius of curvature of the shell, R, and to the distance to the water line, r_i. If the shell's change in curvature is small in the neighborhood of the water line, the following equation results:

$$a = (R^2 - r_i^2)^{\frac{1}{2}} \quad , \quad (r_i < R) \qquad (13)$$

where a and r_i will vary along the length of the cylinder.

The use of an elliptic coordinate system is found to be convenient, since both the plate and planar free surface are distinct coordinate surfaces. The focal distance is equal to the width of the plate. In the elliptic coordinate system, Laplace's Equation is:

$$\nabla^2 \Phi = \frac{1}{(\sinh^2 \xi + \sin^2 \eta)} \left[\frac{\partial^2 \Phi}{\partial \xi^2} + \frac{\partial^2 \Phi}{\partial \eta^2}\right] + \frac{\partial^2 \Phi}{\partial x^2} = 0 \qquad (14)$$

where Φ is the velocity potential function.

A set of solutions to the above equation which conform to the boundaries defined in Figure 4 are defined by the equation:

$$\phi = \sum_m \left(B_m + B'_m(X - X_i)\right) e^{-(2m+1)\xi} \sin(2m+1)\eta \qquad (15)$$

where the coefficients B_m and B'_m, to be determined from the velocities, represent linear variations in the x direction. Note that the choice of a linear function for the x direction restricts the velocity parallel to the cylinder axis to a constant for each section of the structure. In effect, this is a finite difference method for evaluating the effects of flow parallel to the axis.

At the moving surface ($\xi = 0$) the coefficients B_m and B'_m may be evaluated with the following relation between potential and velocity:

$$\nabla\Phi|_{\xi=0} = \frac{\partial\Phi}{\partial z} = -V_n \tag{16}$$

and

$$\frac{\partial\Phi}{\partial z} = \frac{\partial\Phi}{\partial\xi}\frac{\partial\xi}{\partial z} = \frac{1}{a \sin\eta}\frac{\partial\Phi}{\partial\xi} \tag{17}$$

Equation (15) is evaluated using Eqs. (10) and (17) at $\xi = 0$. Using the orthogonality condition produces the following equations for the coefficients:

$$B_m = \frac{2a}{(2m+1)\pi}\int_0^{\pi} V_n^i(\eta)\, \sin(2m+1)\eta\, \sin\eta\, d\eta \tag{18}$$

$$B'_m = \frac{\Delta B_m}{\Delta X} = \frac{B_m^{i+1} - B_m^{i-1}}{X_{i+1} - X_{i-1}} \tag{19}$$

where V_n^i is the equivalent velocity function at the surface. These velocities are the sum of both rigid body motion and local deformations.

Since the known velocities occur as Fourier coefficients on the surface of the cylinder it is necessary to develop an approximate method of transferring them to the flat surface, $\xi = 0$. If V_r is a velocity normal to the shell at an angular position ϕ, the flow, dQ_r, from the shell surface is:

$$dQ_r = V_r(\phi)\, (Rd\phi)\, (dx \cos\theta) \tag{20}$$

The flow through a corresponding section of the flat surface is:

$$dQ_s = V_n\, dxdy \tag{21}$$

At this point we introduce a transformation between the points on the shell surface and the flat plate. Using a constant one-to-one transformation results in the equation:

$$y = a\cos\eta = \frac{a\phi}{\sin^{-1}(\frac{a}{R})} \tag{22}$$

Equating the flow through the two surfaces and including the inclination effect results in the following velocity transformation:

$$V_n(\eta) = \frac{R}{a} \sin^{-1}\left(\frac{a}{R}\right) \cos\theta \; V_r(\phi) \qquad (23)$$

The velocity at the shell surface is defined by the Fourier displacement coefficients u_r^n, where:

$$V_r(\phi) = \sum_{n=0}^{N} \dot{u}_r^n \cos n\phi \qquad (24)$$

Substituting Eqs. (23) and (24) into Eq. (18) results in a more convenient definition of the flow coefficients:

$$B_m = \frac{2R \sin^{-1}\left(\frac{a}{R}\right) \cos\theta}{\pi(2m+1)} \sum_{n}^{N} I_{mn} \dot{u}_r^n \qquad (25)$$

where

$$I_{mn} = \int_0^{\pi} \cos n\phi \sin(2m+1)\eta \sin\eta \, d\eta \qquad (26)$$

and

$$\phi = \sin^{-1}\left(\frac{a}{r}\right) \cos\eta \qquad (27)$$

Note that the dimensionless integrals I_{mn} are functions only of the width a, and may be precomputed numerically as tabular functions. The coefficient B_m' is obtained from the numerical difference between two stations.

The pressure field in the fluid may be obtained from the potential solution using the linearized Bernoulli equation:

$$= \rho \frac{d\Phi}{dt} \qquad (28)$$

where the derivative of Φ must be evaluated at a point fixed in space. The value of the potential Φ at the flat surface $\xi = 0$ is obtained by substituting Eq. (25) into Eq. (16) resulting in:

$$\Phi(\eta)_{\zeta=0} = \sum_m \sum_n \frac{2R\, I_{mn} \sin^{-1}\left(\frac{a}{R}\right)}{\pi(2m+1)} \cos\theta \sin(2m+1)\eta\, \dot{u}_r^n \qquad (29)$$

Since the coordinate system in which we are measuring Φ is moving and expanding, the following terms are functions of time.

Because the velocities are measured on the moving body:

$$\frac{d\dot{u}_r^n}{dt} = \ddot{u}_r^n + \frac{d\dot{u}_r^n}{dx}\dot{X} \qquad (30)$$

Because the body is moving relative to the fluid:

$$\dot{a} = \frac{\partial}{\partial t}\left(\sqrt{R^2 - r_i^2}\right) = -\frac{r_i \dot{r}_i}{a} \qquad (31)$$

$$\dot{r}_i = \frac{\partial}{\partial t}\left[\delta_i \sin\theta - Z_{CG} / \cos\theta\right] \qquad (32)$$

$$= (r_i \tan\theta + \delta_i)\dot{\theta} - \frac{\dot{Z}_{CG}}{\cos\theta} \qquad (33)$$

$$\dot{I}_{mn} = \frac{\partial I_{mn}}{\partial a}\dot{a} \text{ (obtained by numerical difference)} \qquad (34)$$

$$\dot{\eta} = \frac{d}{dt}\left[\cos^{-1}\left(\frac{y}{a}\right)\right] = \frac{\dot{a}}{a}\cot\eta \qquad (35)$$

After performing the appropriate substitutions and differentations in Eqs. (28) and (29), the pressure equation becomes:

$$p|_{\xi=0} = \frac{2}{\pi}\rho R \sin^{-1}\left(\frac{a}{R}\right)\cos\theta \sum_n \sum_m \left\{\left[I_{mn}\left(\dot{u}_r^n - \frac{\partial u_r^n}{\partial x}\dot{x}\right) + \left(\frac{\partial I_{mn}}{\partial a} + \frac{I_{mn}}{\sqrt{R^2 - a^2}}\right)\dot{a}\,\dot{u}_r^n\right]\frac{\sin(2m+1)\eta}{(m+1)} + I_{mn}\left(\frac{\dot{a}}{a}\right)\dot{u}_r^n \cos(2m+1)\eta \cot\eta\right\} \qquad (36)$$

The above pressure distributions could be evaluated as a set of points along the flat surface, multiplied by the area to produce forces, and added

to the structure. However, since the structure loads must be in the form of Fourier coefficients, it will be more convenient to perform a direct transformation from Eq. (36) to the harmonic load, P_r^k, on the K^{th} harmonic, where:

$$P_r^k = R\Delta X \int_0^{2\pi} \ddot{p}(\phi) \cos k\phi \, d\phi \qquad (k > 0) \tag{37}$$

$$P_r^o = R\Delta X \int p(\phi) \, d\phi \qquad (k = 0) \tag{38}$$

In order to conserve energy in the transfer of pressure from the flat surface to the shell we observe that if the flow is equal, the pressures must be equal, or

$$p(\phi) = p\big|_{\xi=0} \tag{39}$$

Also, in Eq. (37), the integration variable, $d\phi$, may be transformed by the equation

$$dy = -a \sin\eta \, d\eta = \frac{a d\phi}{\sin^{-1}\left(\frac{a}{R}\right)} \tag{40}$$

$$d\phi = -\sin^{-1}\left(\frac{a}{R}\right) \sin\eta \, d\eta \tag{41}$$

Substituting Eqs. (36) and (41) into Eq. (37) we obtain the k^{th} harmonic of the load on station i of the surface of the shell, P_r^k, where:

$$P_r^k = -\frac{2}{\pi}\rho R^2 \Delta X \sin^{-1}\left(\frac{a}{R}\right)^2 \cos\theta \sum_m \sum_n \left\{\left[\left(\ddot{u}_r^n - \frac{\partial \dot{u}_r^n}{\partial x}\dot{X}\right) + \left(\frac{1}{I_{mn}}\frac{\partial I_{mn}}{\partial a} + \frac{1}{\sqrt{R^2 - a^2}}\right)\dot{a}\,\dot{u}_r^n\right]\frac{I_{mn}I_{mk}}{2m+1} + \frac{\dot{a}}{a}\dot{u}_r^n I_{mn}J_{mk}\right\} \tag{42}$$

and

$$J_{mk} = \int_0^{\pi} \cos k\phi \cos(2m + 1)\, \eta \cos \eta \, d\eta \qquad (43)$$

Note that the same integral functions I_{mk} are used to transfer loads as were used to transfer velocities. The J_{mk} integrals are related complementary functions.

Equation (42) may be used to calculate the fluid impact loads directly. The integral functions I_{mn} and J_{mn} are precalculated by numerical integration for a set of values of a. At each station the values r_i, a, $\dot{a}$, and $\dot{x}$ are obtained from the rigid body displacements and velocities. If $0 < r_i < R$ and $\dot{a} > 0$, the velocities and accelerations, $\dot{u}_r^n$ and $\ddot{u}_r^n$ are obtained from the previous solution. The integral values I_{mn}, J_{mn}, and $\frac{\partial I_{mn}}{\partial a}$ are obtained by interpolating the precalculated values using the local value of a. Equation (42) is then evaluated for all harmonics to produce the load vector.

2.3.3 Additional Loads

Although the previously developed hydrodynamic impact loads are the major cause of structure deformation and internal stresses, the rigid body dynamics, required for the above calculations, are also dependent on other sources of loading. These loads are the buoyancy, gravity, and fluid damping forces. In addition, the above development is only valid for partially submerged sections of the structure. Forces due to attached virtual fluid mass on the submerged structure will affect the structural response. The above effects are described individually in the following discussion.

Buoyancy Loads

The buoyancy loads will be added to the dynamic loads at each station. At each station, i, the displaced volume is:

$$\Delta V = \frac{S}{2}\left[\delta_{i+1} - \delta_{i-1}\right] \tag{44}$$

where the cross sectional area, S, is:

$$S = \frac{R^2}{2}\left[\pi - 2 \sin^{-1} \frac{r_i}{R}\right] - r_i \sqrt{R^2 - r_i^2} \tag{45}$$

$$(-R < r_i < R)$$

The incremental loads, in structure coordinates, are:

$$\begin{aligned} \Delta P_r^1 &= -\rho g \Delta V \cos\theta \\ \Delta P_z^o &= \rho g \Delta V \sin\theta \end{aligned} \tag{46}$$

Gravity Loads

The net gravity load at the center of gravity is:

$$P_{zg} = M \cdot g \tag{47}$$

where M is the total structural mass and g is the acceleration of gravity.

Viscous Drag Loads

The viscous drag loads will be applied to the individual structure stations in order to provide realistic damping to the structural deformation The user provides the coefficients C_{Dz} and C_{Dr}. The resulting forces at each station are:

$$\begin{aligned} \Delta P_z^o &= -\frac{1}{2}\rho C_{Dz}\left(\dot{u}_z^o\right)^2 c_i \\ \Delta P_r^1 &= -P'_\phi = \frac{1}{2}\rho C_{Dr}\left[\frac{1}{2}\left(\dot{u}_r^1 - \dot{u}_\phi^1\right)\right]^2 \end{aligned} \tag{48}$$

where the effective surface area, c_i, is:

$$c_i = R\left(\pi - 2 \sin^{-1} \frac{r_i}{R}\right) \quad (-R < r_i < R) \tag{49}$$

Note that the superscripts 0 and 1 refer to the harmonic and the subscripts refer to direction of the motion and force.

Virtual Mass Effects

When a section of structure is more than one-half submerged, the hydrodynamic impact loads are negligible. However, a certain portion of the surrounding fluid remains attached to the vehicle and will modify the structure dynamics. The magnitude of the mass may be obtained from the solution of two-dimensional flow about a cylinder. A solution to Laplace's equation in cylindrical coordinates is:

$$\Phi = \sum_{n=1}^{N} \left(A_n r^{-n} + B_n r^n\right) \cos n\phi \tag{50}$$

The boundary conditions are:

$$\begin{aligned} \Phi &= 0 \quad \text{as} \quad r \to \infty \\ \nabla\Phi &= -V_r = \Sigma \dot{u}_r^n \cos n\phi \quad \text{at } r = R \end{aligned} \tag{51}$$

The potential coefficients A_n and B_n are therefore:

$$\begin{aligned} A_n &= \frac{R^{n+1}}{n} \dot{u}_r^n \\ B_n &= 0 \end{aligned} \tag{52}$$

The pressure function at r = R is therefore:

$$P = \rho\dot{\Phi} = \rho \frac{R}{n} \ddot{u}_r^n \cos n\phi \quad n > 0 \tag{53}$$

The force on each harmonic is defined by the equation:

$$P_r^n = \frac{R\Delta\ell}{\pi} \int_0^{2\pi} P(\phi) \cos n\phi \, d\phi \qquad n > 0$$

$$P_r^o = \frac{R\Delta\ell}{2\pi} \int_0^{2\pi} P(\phi) \, d\phi \qquad n = 0 \tag{54}$$

where $\Delta\ell$ is the length of a section and R is the radius. Substituting Eq. (53) into Eq. (54) results in the equation defining the virtual mass on each harmonic n as:

$$P_n^n = M_{nn} \ddot{u}_r^n \tag{56}$$

where

$$M_{nn} = \frac{\rho R^2 \Delta\ell}{n} \qquad n > 0 \tag{57}$$

On the zeroth harmonic, a special case, the virtual mass is:

$$M_{oo} = 2\rho R^2 \Delta\ell \tag{58}$$

Because these masses change when the vehicle moves into the water, the resulting loads, P_n^n, are calculated directly. The masses are scaled according to the wetted area for depths between one-half and fully submerged.

2.3.4 Loading Application

The loads P_r^n and P_z^n on the structure developed in the previous sections are resolved into loads on the rigid body, and the rigid body accelerations are obtained (from Eq. (6)). Using the transformations developed in Section 2.2 the inertial reactions are obtained and added to the structure load vector, resulting in a set of loads that will produce only displacements relative to the center of gravity (Eq. (5)). These loads are used in the load vector, N_e, applied to the structure at each time step.

The fluid loads are produced by structure accelerations and velocities which, in turn, are dependent on the loads. These equations are solved by the transient integration algorithm described below which calculates the response one time step at a time.

2.4 TRANSIENT RESPONSE NUMERICAL METHODS

In most NASTRAN problems, the transient analysis of regular structures having predetermined loads is a stable, accurate numerical procedure. However, when the loads are functions of the velocities and accelerations, such as the water impact of a flexible structure, the numerical stability of the system becomes critical. The basic parameters for choosing an integration method are:

1. Stability: For certain combinations of data, most nonlinear transient integration methods may produce a set of errors which grow with time until a numerical overflow occurs, indicating a lack of stability.
2. Accuracy: In some cases, the errors remain bounded but eventually dominate the solution, causing poor accuracy.
3. Efficiency: For a given problem size the efficiency of a method generally decreases with increased stability and accuracy. Unconditionally stable and accurate methods generally tend to require very small time steps, many matrix inversions, or extensive manipulations for each time step.

In order to solve the overall problem of hydroelastic fluid/structure response during a water impact, a modification of the NASTRAN direct transient analysis rigid format has been chosen.

The basic equation of motion for the water impact analysis is expressed by the following matrix equation:

$$[M]\{\ddot{u}(t)\} + [B]\{\dot{u}(t)\} + [K]\{u(t)\} = \{P(t)\} + \{N_{\ell}(u,\dot{u},\ddot{u})\} \qquad (59)$$

where [M], [B], and [K] are the structural mass, damping, and stiffness matrices, $\{u(t)\}$ is the vector of displacements of the structural degrees of freedom, $\{P(t)\}$ is a vector of pre-defined loads, and $\{N_{\ell}\}$ is the velocity and acceleration-dependent fluid load vector which depends on the current state

of the system. The method and equations are described in Section 11 of the NASTRAN Theoretical Manual.

2.4.1 NASTRAN Algorithm

In the application of the water impact analysis to the NASTRAN algorithm, the loads created by the fluid pressures, including the rigid body forces, are entered in the $\{N_\ell\}$ vector. At each point in time, the displacement, velocity, and accelerations of the structure points and CG motions are estimated from the previous time step. The new loads are calculated using the equations given in the previous chapters and an improved set of displacements, velocities, and accelerations is computed. The process continues until Eq. (59) is satisfied and the time step is incremented.

The numerical form of the equations of motion in the NASTRAN algorithm is:

$$[A_2]\{u_{i+1}\} = \overline{P}_i + N_\ell(u_i,\dot{u}_i,\ddot{u}_i) + [A_1]\{u_i\} + A_o\{u_{i-1}\} \qquad (60)$$

where i is the time step index, i.e.:

$$\{u_i\} = \{u(t_i)\}$$

$$[A_2] = \left[\frac{1}{\Delta t^2} M + \frac{1}{2\Delta t} B + \frac{1}{3} K\right]$$

$$[A_1] = \left[\frac{2}{\Delta t^2} M - \frac{1}{3} K\right] \qquad (61)$$

$$[A_o] = \left[-\frac{1}{\Delta t^2} M + \frac{1}{2\Delta t} B - \frac{1}{3} K\right]$$

$$\overline{P}_i = \frac{1}{3}(u_{i+1} + u_i + u_{i-1})$$

and $\Delta t = t_{i+1} - t_i$ is the time step size. Note that the solution vector $\{u_{i+1}\}$ is required to calculate the fluid load $\{N_\ell\}$ since:

$$\ddot{u}_i \cong \frac{1}{\Delta t^2}(u_{i+1} - 2u_i + u_{i-1})$$
$$\dot{u}_i = \frac{1}{2\Delta t}(u_{i+1} - u_{i-1}) \tag{62}$$

If a vector $\{u_{i+1}\}$ is found such that Eq. (60) is satisfied it may be shown that the NASTRAN transient integration is unconditionally stable. However, if only an approximation from the previous solution for the load, N_ℓ, is used, the process may diverge as described in Reference 1.

A method for solving the above problems and correcting for divergent characteristics will be developed in the following sections.

2.4.2 Nonlinear Load Iteration

At each time step in the transient integration it is desired to obtain a displacement vector $\{u_{i+1}\}$ that provides a solution to Eq. (60). A direct method would be to expand the nonlinear loads $\{N_\ell\}$ in terms of their derivatives, i.e.:

$$\{N_\ell\} = -[M_f]\{\ddot{u}_i\} - [B_f]\{\dot{u}_i\} \tag{63}$$

where

$$\left.\begin{aligned} M_{f_{ij}} &= -\frac{\partial N_{\ell i}}{\partial \ddot{u}_j} \\ B_{f_{ij}} &= -\frac{\partial N_{\ell i}}{\partial \dot{u}_j} \end{aligned}\right\} \text{ at } u_i \tag{64}$$

Substituting the finite difference forms of $\dot{u}_i$ and $\ddot{u}_i$ into Eq. (60) we obtain:

$$[A_2]\{u_{i+1}\} = -\left[\frac{1}{\Delta t^2}M_f + \frac{1}{2\Delta t}B_f\right]\{u_{i+1}\} + \{\overline{P}\}$$

$$+\left[-\frac{2}{\Delta t^2}M_f + A_1\right]\{u_i\} + \left[\frac{1}{\Delta t^2}M_f - \frac{1}{2\Delta t}B_f + A_2\right]\{u_{i-1}\} \quad (65)$$

Note that the equation has a direct solution if the matrices associated with $\{u_{i+1}\}$ are combined and inverted. This procedure would be costly, however, since a matrix generation and inversion would be required at each time step.

An iterative method may be used to solve Eq. (65) implicitly whereby the solution vector is obtained by repeated substitutions into Eqs. (62) and (60). If y_n is the n^{th} approximation to u_{i+1}, the iterative equations are:

$$[A_2]\{y_{n+1}\} = \{N_\ell(y_n)\} + \{C\} \quad (66)$$

where the constant terms are collected in the vector {C} which is:

$$\{C\} = \{P_i\} + [A_1]\{u_i\} + [A_o]\{u_{i-1}\} \quad (67)$$

and the process is started by extrapolating from the last time step by the equation:

$$\{y_o\} = n_i + \dot{u}_{i-1}\Delta t + \frac{1}{2}\ddot{u}_{i-1}\Delta t^2 \quad (68)$$

Starting with the initial estimate, y_o, the fluid loads are calculated. Equation (66) is solved for the next approximation. The process is repeated until the loading error is sufficiently small. The error vector, $\{\varepsilon_n\}$, is:

$$\{\varepsilon_n\} = \{N_\ell(y_n)\} + \{C\} - [A_2]\{y_n\} \quad (69a)$$

or, substituting Eq. (66) with n - 1 for y_n we obtain:

$$\{\varepsilon_n\} = \{N_\ell(y_n)\} - \{N_\ell(y_{n-1})\} \quad (69b)$$

2.4.3 Stability Analysis

In some cases the load iteration procedure may be unstable itself. In effect, we are solving Eq. (65) in the form:

$$[A_2]\ \{y_{n+1}\} = -[F]\ \{y_n\} + \{C_2\} \tag{70}$$

where

$$[F] \cong \left[\frac{1}{\Delta t^2} M_f + \frac{1}{2\Delta t} B_f\right] \tag{71}$$

and

$\{C_2\}$ = the constant terms

Equation (70) is very similar to the equation used in eigenvalue analysis whereby the vector contains a set of modes $\{\phi_j\}$ defined by the equation:

$$\lambda_j\ [A_2]\ \{\phi_j\} = -[F]\ \{\phi_j\} \tag{72}$$

The vector, $\{y_n\}$, will be a combination of the exact solution, y_e, and the modes in the form:

$$\{y_n\} = \{y_e\} + \Sigma\ \alpha_j^n\ \{\phi_j\} \tag{73}$$

where y_e is the exact solution to Eq. (70), and α_j^n are the error coefficients.

Substituting Eq. (73) into Eq. (70) we obtain:

$$\alpha_j^{n+1}\ [A_2]\ \{\phi_j\} = -\alpha_j\ [F]\ \{\phi_j\} \tag{74}$$

therefore, comparing Eq. (74) to Eq. (72) we observe that:

$$\alpha_j^{n+1} = \lambda_j \alpha_j^n \tag{75}$$

If $|\lambda_j| > 1$, the error coefficient α_j will grow and the process will diverge. Examining Eq. (72) we observe that if the matrix [F] contains larger terms than the matrix $[A_2]$, some λ values will cause divergency. This is very possible in a water impact problem when the mass of the attached fluid represented in the matrix [F] is larger than the structure mass represented in the matrix $[A_2]$

A similar problem was solved in Reference 3 by the method of extracting the actual system modes at each time step using a single step iteration procedure for a fixed number of modes. This allowed the explicit solution of Eq. (59) and supressed the divergent characteristics. In the following discussion a similar method will be derived which, in effect, will directly measure and remove the errors from the solution.

2.4.4 Error Elimination Procedure

In the discussion above it is noted that the load iteration procedure produces error vectors that are dominated by the eigenvectors of the matrix equation. If a series of the vectors $y_1, y_2, \ldots, y_n$ are obtained by a series of iterations, their differences will be rich in the dominant error modes. As an alternative to Eq. (73), the solution may be expressed as a combination of these vectors or:

$$\{y_e\} = \{y_n\} - [U]\ \{\alpha\} \tag{76}$$

where

$$[U] = [y_1 - y_o \mid y_2 - y_1 \mid \cdots \mid y_n - y_{n-1}] \tag{77}$$

The errors are contained in the matrix U, obtained by the iterations, and y_e is the exact solution. If the coefficients, α, the weighing factors which may be determined from the equations below, are obtained, the solution y_e is available.

If Eq. (70) is substituted into the basic iteration equation, Eq. (70), the result is:

$$[A_2]\ \{y_n\} - [A_2]\ [U]\ \{\alpha\} = N(y_e) + \{C\} \tag{78}$$

assuming that the vector $\{N\}$ is linear for small changes in y, the exact load is:

$$\{N(y_e)\} = \{N(y_n)\} - [F]\ [U]\ \{\alpha\} \tag{79}$$

and from the last iteration:

$$\{N(y_n)\} = [A]\{y_{n+1}\} - \{C\} \tag{80}$$

therefore

$$\left[[F][U] - [A_\Delta][U]\right]\{\alpha\} \doteq [A]\{y_{n+1} - y_n\} \tag{81}$$

The matrix [F] need not be evaluated explicitly since each column, $\{U_n\}$, of [U] may be modified by the identity:

$$[F]\{U_n\} = [F]\{u_n - y_{n-1}\} = -[A]\{y_{n+1} - y_n\} \tag{82}$$

Combining the above equations results in an expression for the unknown coefficients α

$$-[A]\left[y_2 - 2y_1 + y_o \;\vdots\; \cdots \;\vdots\; y_{N+1} - 2y_N + y_{N-1}\right]\{\alpha\} = [A]\{y_{N+1} - y_N\} \tag{83}$$

$$\text{or} \qquad [A][\Delta]\{\alpha\} = [A]\{\delta y\}$$

The above equation results in an exact solution only if the left-hand matrix can be inverted. Since the matrix on the left is rectangular it must be transformed to a square matrix. This is performed by pre-multiplying both sides of Eq. (83) by the load matrix U^T. The coefficients α are approximated by the equation:

$$\{\alpha\} \doteq \left[[U]^T[A][\Delta]\right]^{-1}[U]^T[A]\{\delta y\} \tag{84}$$

The exact solution is approximated by Eq. (76) where the above coefficients are used directly. This method will produce good approximations even though the basic iteration equations are diverging. The only requirement for satisfactory results is that the number of iterations be larger than the number of divergent modes, which, in most cases, is a small number. Also, note that the matrix to be inverted is of the order N-1, where N+1 is the number of iterations. The matrix is typically small and may be inverted in core.

3.0 USER'S MANUAL

3.1 SUMMARY

This section describes the NASTRAN data deck set up required to execute the hydroelastic analysis of a booster vehicle impacting a calm sea. The water impact analysis capability in NASTRAN is basically a set of subroutines which calculate the fluid loads in a direct transient analysis. The structure is modeled with standard NASTRAN elements. The execution of the program follows the normal execution path except for the generation of loads on the structure. Three impact conditions of the structure are allowed: (a) broadside, (b) tail-first, and (c) slapdown. The finite element idealizations for these impact conditions are illustrated in Figures 5 and 6.

The broadside analysis is used to analyze the impact of a cylinder section of structure. This case is a two-dimensional representation of the three-dimensional slapdown impact when pressures and local deflections at the point of impact are considered. The analysis is valid only for small penetration depths.

The nozzle impact analysis is used for the impact of a conical shell structure. Both vertical and limited non-vertical cases are allowed. Additional structural elements above the nozzle elements may be included to represent the full vehicle dynamics.

The slapdown option is used to analyze the water impact of a cylindrical shell which enters the water at a more general set of initial conditions. The initial height, angle, and velocities may be specified by the user. Hydroelastic, hydrostatic, and fluid drag loads are automatically generated. The analysis is three-dimensional. Large angular rotation and fluid penetration effects are included.

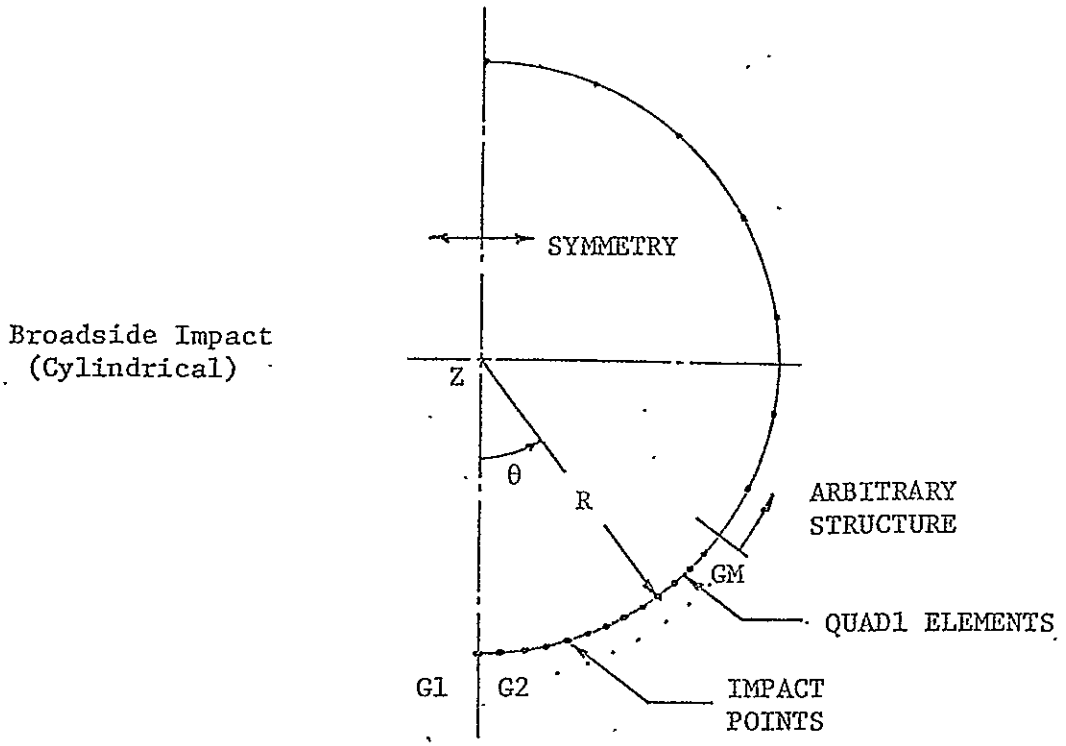

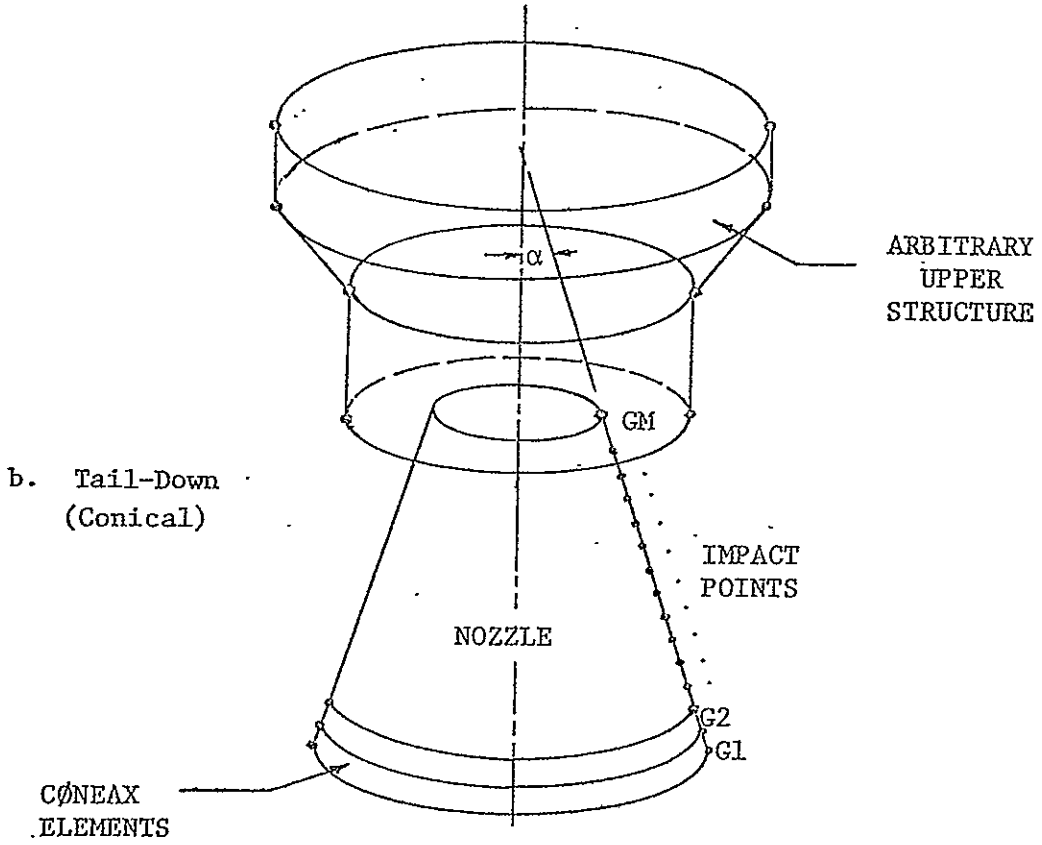

FIGURE 5. FINITE ELEMENT STRUCTURE MODELS FOR BROADSIDE AND TAIL-DOWN CONFIGURATIONS

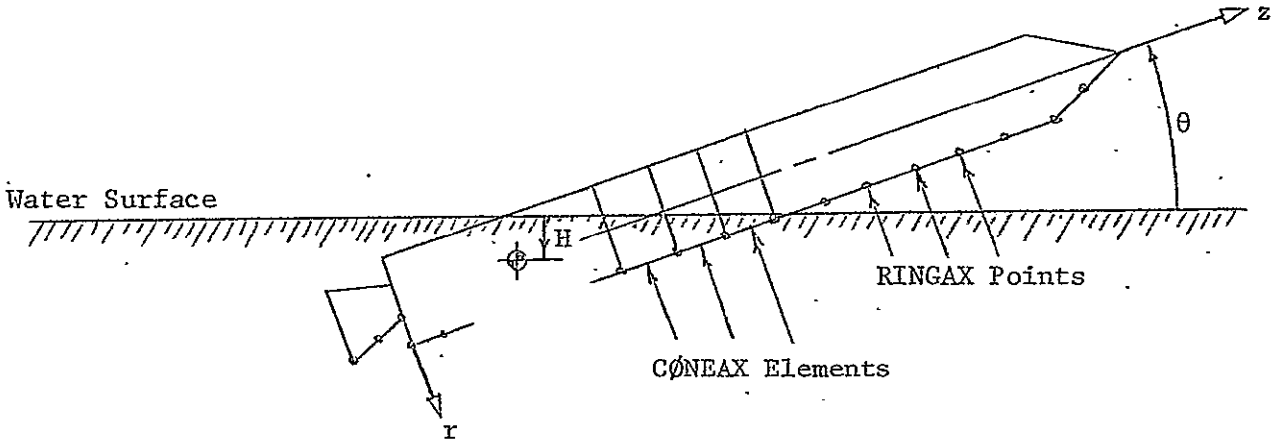

FIGURE 6. FINITE ELEMENT STRUCTURE MODE FOR SLAPDOWN CONFIGURATION

A standard NASTRAN data deck is constructed with EXECUTIVE CONTROL, CASE CONTROL, and BULK DATA sub-decks, prepared as though a direct transient response analysis was requested, with the additions of one case control flag (NØNL) and two new bulk data sets (IMPACT and either IMPLIST or SLPLIST) to initiate and define the generation of water impact loads.

3.2 DATA PREPARATION

This section describes the detailed input data necessary for execution of the water impact problems. Features for requesting certain non-standard and intermediate output for the impact problems are discussed together with some of the more familiar aspects of preparing a NASTRAN transient analysis data deck.

3.2.1 Model Idealization and Executive Control Deck and Preparation

For the broadside impact case (Figure 5a) the cylindrical booster shell may be modeled in a normal fashion with standard NASTRAN grid points and BAR or QUAD1 elements. The axisymmetric CØNEAX elements must be used exclusively for the tail-first nozzle configuration (Figure 5b) or the slapdown case (Figure 6).

The usual arbitrary selection of grid point locations is allowed, with the exception that points which are expected to interact with the fluid during the impact process should be spaced uniformly and close together for the broadside or nozzle impact models. For the slapdown case, the spacing of the elements is arbitrary.

The modeling tasks of the user include providing the necessary boundary conditions and constraints to the structural model. Symmetry in the case of broadside impact is defined by modeling one-half of the structure and providing single-point constraints on the boundary points. In the nozzle impact and

slapdown cases, the singular rotational displacements must be constrained. Samples of input data preparation will be provided in Section 3.3.

The standard Executive Control data deck is used with the exception that a DIAG = 12 card is interpreted as a flag to delete output of hydrodynamic pressures.

3.2.2 Case Control Deck Preparation

A typical CASE CONTROL deck includes necessary title information, one TSTEP set ID card, and a control flag to exercise the hydroelastic shell/fluid impact analysis (NØNL = 99999). Printed and plotted output of displacements, velocities, accelerations, non-linear forcing functions, stresses, etc. are obtained with standard NASTRAN output request options. Note when axisymmetric elements (CØNEAX) are used for the nozzle and slapdown impact analyses, grid point labels for output sets are processed by the internal coded format

$$ID_{internal} = ID_{list} + 10^6 * (n + 1)$$

when n = 0, 1, and 2 for the respective harmonics of response.

3.2.3 Bulk Data Preparation

The structural model and transient analysis parameter data defined in the Bulk Data deck are input via standard NASTRAN data cards. (See NASTRAN User's Manual.) The properties of the fluid and overall geometric variables of the fluid/structure interface are defined with IMPACT and IMPLIST or SLPLIST bulk data. The format and data field specification for these cards is given in the card description section to follow. In order to provide an efficient and consistent structure/fluid definition, the following special rules are imposed for the three impact conditions allowed.

Cylinder (Broadside) Impact

a. One-half of the cylindrical shell structure representing the booster motor case is modeled. A set of single point constraints is imposed on the vertical axis to represent the symmetric motion.

b. Planar constraints defined by MPC bulk data cards must be utilized when QUAD1 elements are used for modeling.

c. Physical properties represent a section of the cylindrical shell (of length ΔZ) and dynamic response is assumed localized at this section, i.e., axial interaction effects are ignored.

d. Evenly spaced grid points ($\Delta\theta$ = constant) are required in the region of penetration.

Nozzle (Tail-First) Impact

a. Axisymmetric (CØNEAX) elements only are allowed for modeling the structure, including booster motor case, nozzle, extension, and assorted hardware.

b. Harmonic values 0 and 1, defined on the AXIC data card, are permitted (0 = vertical entry).

c. The canted impact angle (γ) between the concial axis and local vertical must be small and less than the semi-apex angle (α) of the cone.

d. Evenly spaced points (RINGAX) are required along the nozzle in the region of penetration.

Slapdown Impact

a. The structure is modeled with axisymmetric (CØNEAX) elements. The portions of the structure not involved with the slapdown loads such as the nozzle, nose cone, and internal bulkheads, are also modeled with CØNEAX elements. However, these degrees of freedom should be partitioned from the matrices via ØMITAX data cards for accuracy and more economical processing.

b. Up to 20 harmonics are allowed on the AXIC card. The structure displacements are represented by a Fourier series around the circumference and the accuracy of the results is dependent on the number of terms. However, the running time increases proportionally to the number of harmonics.

c. Although the stations along the structure axis may be arbitrarily spaced, it is recommended that wide spacing be avoided. Because the pressure is assumed to vary linearly between stations, that distance should be less than the radius of the cylinder.

All Cases

a. Time step changes in the integration loop are not permitted.

b. The iterations performed to refine the water loads within each time step are controlled by the convergence criteria parameters ITER, ED, and EP. A large value of ITER in conjunction with small ED and EP values will improve the accuracy of the results but will increase the running time. The use of a smaller time step size with more time steps is a less effective alternate.

3.2.4 IMPACT, IMPLIST, and SLPLIST Bulk Data Descriptions

As mentioned, new bulk data sets must be supplied when executing the hydroelastic water impact analyses. The first set, IMPACT, specifies geometric and fluid property data uniquely for each of the impact orientations of NØZL, BDSD, or SLAP (i.e., tail-first, broadside, or slapdown entry, respectively). The second set, either IMPLIST or SLPLIST, defines a set of grid point identification numbers corresponding to structural grid positions on the impacting shell for which hydrodynamic forces may be expected to be applied. The SLPLIST card contains, in addition to the grid point numbers, their locations along the shell.

Definitions of the new bulk data cards are given on the following pages. They have been prepared in accordance with the format of the NASTRAN User's Manual and may be directly inserted.

3.2.5 Slapdown Example Problem

An example problem is used to illustrate the basic data deck setup and program output. The basic problem is described in Figure 7. The NASTRAN data deck is shown in Figure 8. Two CØNEAX elements were used to define a flexible cylindrical shell. The three stations on the vehicle are defined by the RINGAX data cards. With the exception of the IMPACT and SLPLIST data cards, all of the other bulk data are standard NASTRAN cards. The only non-standard NASTRAN card in the case control deck is the "NØNL = 99999" card.

The basic output format is shown in Figures 9 and 10. Figure 9 illustrates the printout of the CG motions and the pressure distribution which is output for each time step. The position, velocity, and acceleration for each of the three rigid body motions is followed by a printout of the pressure at a series of circumferential angles for each submerged station. The station number corresponds to the entry number in the SLPLIST data (i.e., the first SLPLIST entry is station 1, etc.). Only stations that are less than one-half submerged produce pressure output.

Figure 10 illustrates the standard NASTRAN displacement, velocity, or acceleration output as printed versus time. Each particular point corresponds to a harmonic number for a RINGFL point as encoded by the equation given in Section 3.2.2. Although the element stress output was not requested, it may be obtained with the case control request "STRESS =" and with the following ALTER cards in the executive control deck:

```
ALTER 164,164
ØFP ØEF1,ØES1,,,, // V,N,CARDNØ $
ENDALTER
```

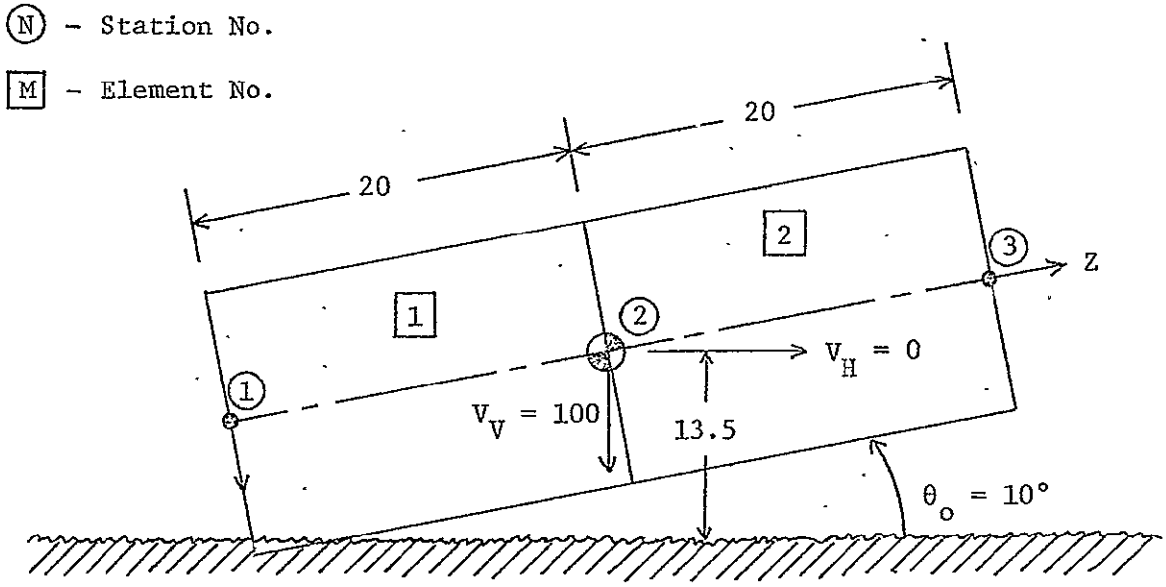

Initial Conditions

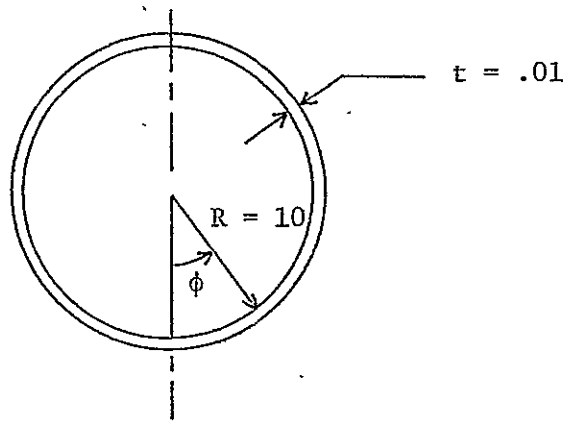

Cross Section

FIGURE 7. SLAPDOWN EXAMPLE PROBLEM

Executive Control Deck

```
ID      SLAPTEST, EXAMPLE
APP     DISP
SOL     9,0
TIME    2
CEND
```


Case Control Deck

```
$
TITLE =    SLAP DOWN EXAMPLE PROBLEM
LABLE =     VV = 100, THETA = 10, HT = 13.0, FLEXIBLE
$
NONLINEAR = 99999
AXISYM = COSINE
TSTEP = 20
SDISP = ALL
SACCE = ALL
HARMONICS = ALL
BEGIN BULK
```

Bulk Data Deck

```
.   1  ..   2  ..   3  ..   4  ..   5  ..   6  ..   7  ..   8  ..   9  ..  1
AXIC     4
CCONEAX  1        100      1        2
CCONEAX  2        100      2        3
IMPACT   SLAP     10.0     10.0     -13.0    100.0    .0       .0       386.4    +IMP
+IMP     1.0-4    0.0      0.0      10.0     2        5        .01      .001
MAT1     10       30.0+6            .333     9.9474-4
PCONEAX  100      10       .10      10       .0833
RINGAX   1                 10.0     -20.0                              46
RINGAX   2                 10.0     .0                                 46
RINGAX   3                 10.0     20.0                               46
SLPLIST  1        -20.0    2        .0       3        20.0
TSTEP    20       20       .005     1
ENDDATA
```

FIGURE 8. DATA DECK LISTING FOR EXAMPLE PROBLEM

SLAP DOWN EXAMPLE PROBLEM FEBRUARY 14, 1975 NASTRA

VV = 100, THETA = 10, HT = 13.0, FLEXIBLE

T R A N S I E N T S L A P D O W N I M P A C T O U T P U T D A T A

TIME STEP 14 TIME = 0.06500

CENTER OF GRAVITY PARAMETERS

	HORZ	VERT	ANGLE
DISP	-2.073647E-01	-6.945362E+00	1.397416E-01
VEL	-7.107086E+00	7.699167E+01	-7.293285E-01
ACC	-1.220751E+02	-6.897356E+02	1.898289E+01

PRESSURE DISTRIBUTION

STAT NO	ANGULAR POSITION ,DEGREES							
	0.0	10.00	20.00	30.00	40.00	50.00	60.00	70.00
1	0.18	0.18	0.16	0.13	0.10	0.09	0.19	
2	0.09	0.11	0.17	0.32	0.83			
3	0.58	11.17						

FIGURE 9. PRINTOUT FOR CG MOTION AND PRESSURE DISTRIBUTIONS IN SLAPDOWN ANALYSIS

SLAP DOWN EXAMPLE PROBLEM

VV = 100, THETA = 10, HT = 13.0, FLEXIBLE

POINT-ID = 3000002

D I S P L A C E M E N T V E C T O

TIME	TYPE	T1	T2	T3
0.0	G	0.0	0.0	0.0
4.999999E-03	G	-3.337381E-05	1.562295E-05	-5.448777E-06
9.999998E-03	G	-5.290190E-05	2.476525E-05	-8.673081E-06
1.500000E-02	G	-3.491776E-05	1.634615E-05	-5.722513E-06
2.000000E-02	G	-4.995339E-05	2.338371E-05	-8.136020E-06
2.499999E-02	G	-6.605833E-05	3.092452E-05	-1.083659E-05
2.999999E-02	G	-2.293197E-05	1.073573E-05	-3.784134E-06
3.499999E-02	G	-3.603128E-05	1.686538E-05	-5.816296E-06
3.999999E-02	G	-1.778503E-04	8.325704E-05	2.377610E-06
4.499999E-02	G	-3.793927E-05	1.776441E-05	-1.311220E-06
4.999999E-02	G	-3.036800E-05	1.421037E-05	-3.830696E-06
5.499999E-02	G	-1.610777E-04	7.540616E-05	4.345326E-06
5.999999E-02	G	-3.698806E-05	1.732202E-05	-9.455930E-07
6.499994E-02	G	-6.636641E-06	3.097447E-06	-4.093784E-06
6.999993E-02	G	-1.979546E-04	9.266942E-05	2.582348E-05
7.499993E-02	G	-1.074725E-05	5.042681E-06	-3.289360E-06
7.999992E-02	G	3.076275E-05	-1.441590E-05	-8.021927E-06
8.499992E-02	G	-1.704164E-04	7.977920E-05	2.295915E-05
8.999991E-02	G	7.411800E-07	-3.309819E-07	-3.935992E-06
9.499991E-02	G	5.938699E-05	-2.782156E-05	-1.004688E-05
9.999990E-02	G	-1.551779E-04	7.264697E-05	2.107906E-05

FIGURE 10. NASTRAN PRINTOUT FOR WATER IMPACT ANALYSIS

Input Data Card IMPACT (Parameters for Water Impact Problem)

Description: Defines initial conditions, physical constants, and solution parameters for transient water impact problems. The basic data card has three forms corresponding to the three impact cases.

FORM 1 (BDSD Case) Broadside Case

1	2	3	4	5	6	7	8	9	10
IMPACT	TYPE	RC	L	VØ	RHØ		THMAX		abc
IMPACT	BDSD	10.	238.	240.	.00012		20.		ABC

+bc					MM	ITER	ED	EP	
+BC					8	4	.01	.001	

Field	Contents
RC	Radius of cylinder (real, inches)
XL	Length of section of cylinder (real, inches)
VØ	Initial vertical velocity (real, in/sec)
RHØ	Mass density of fluid (real, lb-sec^2/in^4)
THMAX	Circumferential location of last point on IMPLIST data (real, degrees)
MM	Number of terms in Fourier series fluid solution (integer, default = 10)

Integration control parameters (see remarks)

ITER	Maximum number of iterations on fluid loads per time step (default = 4)

ED — Convergence criteria on displacement vector, ε_d, magnitude difference (real, default: $\varepsilon_d = .01$)

EP — Parallel vector test criteria, ε_p, absolute difference between each term (real, default: $\varepsilon_p = .001$)

FORM 2 (NØZL Case) Inverted Cone Case

1	2	3	4	5	6	7	8	9	10
IMPACT	TYPE		RC	VØ	RHØ	ALPHA	THMAX	HMAX	abc
IMPACT	NØZL		100.0	240.	.00012	15.	1.0	460.	ABC

+bc	GAMA	VØL	PAMB		NPØLY	ITER	ED	EP	
+BC	.16	.1E8	14.7		10	4	.01	.001	

Field	Contents
RC	Radius of base of nozzle (real, inches)
VØ	Initial velocity (real, in/sec) (See Remark #4)
RHØ	Mass density of fluid (real, lb-sec^2/in^4)
ALPHA	Half cone angle of nozzle (real, degrees)
THMAX	Uniform longitudinal distance between nodes on IMPLIST card (real, inches)
HMAX	Depth below water surface for which $\phi = 0$ assumption is made (real, inches)
GAMA	Impact angle from vertical oblique entry (degrees)
VØL	Initial volume of contained air (real, in^3)
PAMB	Absolute ambient air pressure (real, lb/in^2)
NPØLY	Number of terms in polynomial fluid solution (integer, default = 5)

Integration control parameters are the same as for Form 1.

FORM 3 (SLAP Case) Slapdown Case

1	2	3	4	5	6	7	8	9	10
IMPACT	TYPE	RC	THETA	H	VVERT	VHØR	VTHETA	G	abc
IMPACT	SLAP	10.	-5.	-10.	200.	0.0	0.0	386.4	ABC

+bc	RHØ	CDR	CDZ	PRT	MM	ITER	ED	EP	
+BC	.001	0.0	0.0	5.0	4	4	.01	.001	

Field	Contents
RC	Radius of cylinder (real, inches)
THETA	Orientation angle (real, degrees)
H	Initial height (from CG to waterline) (real, inches)
VVERT	Initial vertical velocity (real, in/sec)
VHØR	Initial horizontal velocity (real, in/sec)
VTHETA	Initial rotational velocity (real, radians/sec)
G	Gravitational constant (real, in sec/sec)
RHØ	Mass density of fluid (real, lb-sec^2/in^4)
CDR	Drag coefficient in radial direction (real, dimensionless)
CDZ	Drag coefficient in axial direction (real, dimensionless)
NM	Number of terms in fluid series equations (integer, default = 4)
PRT	Increment at which pressures are outputed (real, degrees) (only if DIAG 12 is not set)

Integration control parameters are the same as for Form 1.

Remarks:

1. The continuation card is required for TYPE = NØZL and SLAP. The default value will be used if a field is blank.
2. One and only one IMPACT card is allowed in the bulk data deck.

3. An IMPLIST bulk data card is required for TYPE = NØZL or BDSD. A SLPLIST (slap list) data card is required for TYPE = SLAP.

4. The iteration ITER defines the maximum number of iterations performed at each time step. The actual number of iterations may be less if the actual error is less than the convergence criteria ε_p or ε_d. When the maximum is reached a closed-form solution is calculated.

5. If the iteration error on the load vector is less than ε_p, the vector is assumed to be correct and is used as the final value. If the error vectors for two iterations are proportional (i.e., only one error mode exists) a closed-form solution is calculated.

6. The value of the ITER data may be changed to correct for instabilities or numerical problems when they occur. It is recommended that with small time steps ITER should be decreased. With large time steps ITER may be increased for better accuracy. For any given problem, the optimum time step size is obtained by experimentation.

Input Data Card IMPLIST (Grid Point Identification - Impact of Shells on Fluid)

Description: Defines the grid point identification numbers for either the impact of an inverted cone or horizontal impact of cylinder onto a fluid.

Format and Example:

1	2	3	4	5	6	7	8	9	10
IMPLIST	SID	G1	G2	G3	G4	G5	G6	G7	+abc
IMPLIST	2	105	104	103	102	101	100	99	ABC
+abc	G8	G9	G10	-etc-					
+BC	98	97	96						

Alternate Form

IMPLIST	SID	G1	"THRU"	GM					
IMPLIST	1	105	THRU	1					

Field	Contents
SID	Grid point set identification number (Integer > 0)
G1,...,GM	Grid point identification numbers (Integer > 0)

Remarks:

1. In the broadside problem (BDSD) the grid points interacting with the fluid must be equally spaced around the circumference, starting at the bottom ($\theta = 0$), with the last point at location θ_{max} defined on the IMPACT card.

2. In the nozzle impact problem (NØZL) the Gi values refer to RINGAX type grid points. The first point lies at the bottom with subsequent points at equally spaced locations along the surface. The last point (GM) corresponds to the last node which may be submerged in the impact analysis.
3. The grid-point set ID (SID) is arbitrary and may be used to identify a particular run or class of runs.

Input Data Card SLPLIST (Grid Point Identification and Location - Slapdown of Cylinder on Fluid)

Description: Defines the grid point identification numbers and axial location for the slapdown of a cylinder on a fluid surface.

Format and Example:

1	2	3	4	5	6	7	8	9	10
SLPLIST	G1	Z1	G2	Z2	G3	Z3	G4	Z4	abc
SLPLIST	100	0.0	1.0	10.	102	15.	103	25.	ABC
+bc	G5	Z5	G6	Z6	-etc-				
+BC	104	35.	105	45.					

Field	Contents
G1,...,GM	Grid point identification numbers (integer > 0)
Z1,...,ZM	Axial locations of grid points

Remarks:

1. The SLPLIST card is used only for the slapdown case.
2. The grid points must be entered such that the Z values are ascending. (Smallest value is Z1 and largest is ZM.)

4.0 EXPERIMENTAL CORRELATION AND PARAMETRIC STUDIES

To measure the validity of the analytic method, accuracy of the program, and provide additional insight into the slapdown impact problems, a series of computer runs were made to simulate both a test vehicle and the actual final design vehicle. For experimental comparison, a substantial amount of experimental data was available from drop tests of a 120-inch diameter (77% scale) test vehicle. After correlating with the experimental results, the program was applied to a NASTRAN model of the full scale design to determine the effects of design differences and parameter changes. This chapter summarizes this effort and describes the results.

Section 4.1 below presents details of the analysis correlation with the test. The overall comparison between the test data and the computer results was very good and indicates the reasonableness in the engineering assumptions made in the analysis.

Parametric studies, performed using both the 77% and full-scale models, to test effects of changes in physical parameters are presented in Section 4.2. This investigation included program executions with various values of structural stiffness, structural damping, initial impact position, and initial velocities. The effects of the differences between the test vehicle and the actual structure were also studied.

Conclusions reached from the experimental correlation and parametric studies are given in Section 4.3.

4.1 CORRELATION WITH TEST

The objective of the test program was to provide load and response data for derivation of design parameters for the recoverable Solid Rocket Booster (SRB) for the Space Shuttle project. The scale model test vehcile, referred to as the 120-inch or 77% model, was tested to measure the pressures and loads on the vehicle for initial impact, cavity collapse, and slapdown impacts. The vehicle consisted of six 120-inch diameter cylindrical sections with a thickness of 0.375 inches and having the nose, aft bulkhead, and nozzle fabricated from existing hardware.

Because of practical limitations on the instrumentation and occasional malfunctions, the experimental data was limited. The instrumentation channels had to be divided between the nozzle and the casing. The actual measured data from slapdown consisted of 6 diameter deflection gauges, 10 pressure transducers, and 54 strain gauges. Further details of the test program are given in Reference 4.

From the analytic viewpoint, the test data was valuable. The measured deflections and strains indicated low frequency or nearly static response to the changing loads. This provided the practical limits as to time steps and frequency content in the analysis. The fluid pressures indicated concentrated loads near the waterline. This indicated that a fine finite element mesh was necessary. These results guided the modeling and selection of integration parameters for both the scale model and full SRB analyses.

The NASTRAN finite element model of the 120-inch diameter test booster used for the test comparisons is shown in Figure 11. A listing of the input data deck is given in Appendix B. Finite elements, defined with CØNEAX input data, were connected to RINGAX points. In this analysis method the displacements, forces, stresses, etc. are expanded and solved in terms of their

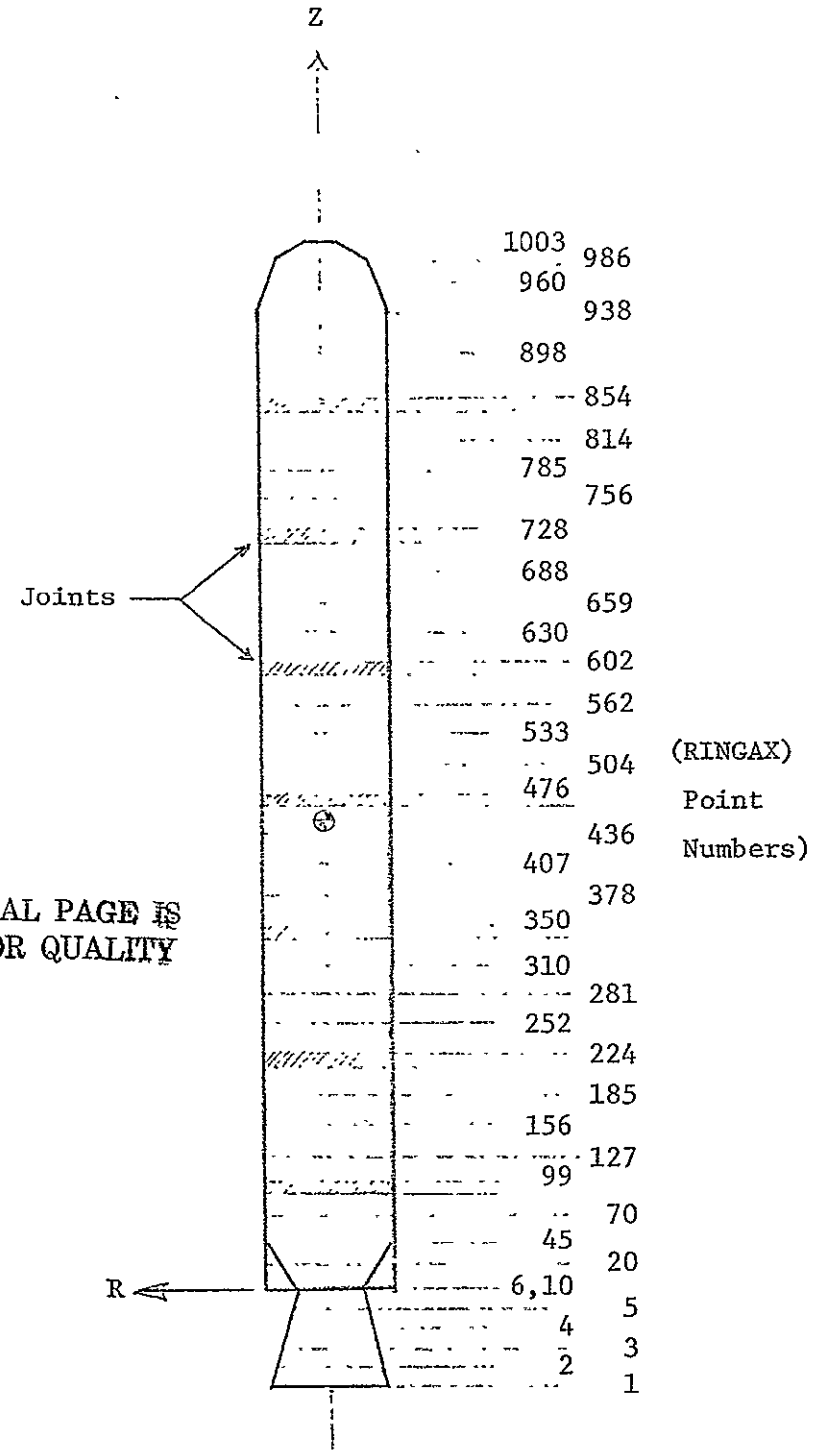

FIGURE 11. DEMONSTRATION PROBLEM FINITE ELEMENT MODEL
120-INCH DIAMETER VEHICLE

Fourier series coefficients around the circumference. In the structural model each harmonic, n, of the Fourier series is uncoupled from the other harmonics. This allows economical matrix decomposition and vector solutions. Five harmonics were used in the flexible structure analysis (n = 0,1,2,3,4). The fifth and higher harmonics were assumed to contribute negligible deformation due to their large stiffness.

The resulting structural mass and stiffness matrices were of order 1410. Using structural partitioning, controlled by the ØMITAX data cards, the matrices were reduced to 741 degrees of freedom. The computer-calculated weight on the structure was 90,176 pounds compared to the actual structure weight of 87,500 pounds. The location of the center of gravity was within two inches of the actual vehicle. In order to restrain spurious structure oscillations and simulate the viscous damping of entrapped water, a structural damping factor of 5% was added. Although the true damping may be higher, the use of the small value was expected to produce conservative results.

Initial positions and velocities for the demonstration slapdown problem were taken from the optical trajectory data of drop test C145-020 [Ref. 4]. In this test the vehicle was dropped at an initial angle of 30 degrees with an initial vertical impact velocity of 52.6 feet per second. Initial conditions for the slapdown analysis were chosen at a later point in time, when the side of the vehicle was just entering the water. The discussion below presents typical results from the correlation study. Test data for the C145-020 drop was obtained from References 4 and 5; Appendix B contains additional correlation data.

Figure 12 shows the time history of vertical height of the vehicle nose. The close comparison of trajectories indicates validity of initial conditions and accuracy of resultant loads.

FIGURE 12. HEIGHT VS. TIME AT OPTICAL REFERENCE POINT
120-INCH DIAMETER MODEL

Figure 13 presents diameter deflections along the vehicle at 3.0 seconds after initial impact. This time corresponds to maximum deflections at nearly all points in the test vehicle; however, the analytical model deflections had not yet peaked. The time shift is believed to be due to the bow wave which causes the peak pressures to occur sooner.

Figure 14 shows the envelope of maximum diameter deflections obtained in the drop test. The analytical result shows a comparable magnitude (8 inches) but occurrence at a location 120 inches forward of the test result. This forward displacement is again attributed to the bow wave effect.

In Figure 15 the pressure time histories at a particular station are shown for the centerline (keel), the average over the wetted circumference, and the experimental results measured at the keel. The experimental data contained considerable noise (± 10 psi) and a smooth curve was fitted to these results. Although the pressures at the centerline were less than the test results, the average pressures are generally higher.

Figure 16 shows pressures versus axial station and circumferential location at 3.1 seconds after impact. Note that with the assumption of a flat water surface, the pressures theoretically approach infinity at the waterline. In the real case of surface waves, the water is moving away from the vehicle at the waterline and the pressures are finite. In the analysis the large computed pressures at the waterline compensate for the smaller computed pressures at the centerline. Unfortunately, no test data was available for pressures off the centerline (keel).

The above correlation studies have shown that the analytic results are of sufficient quality to use the computer program as a working tool to provide analytic backup for the experimental loads program. The overall loads and dynamic response and structure deflections appear to match the physical data

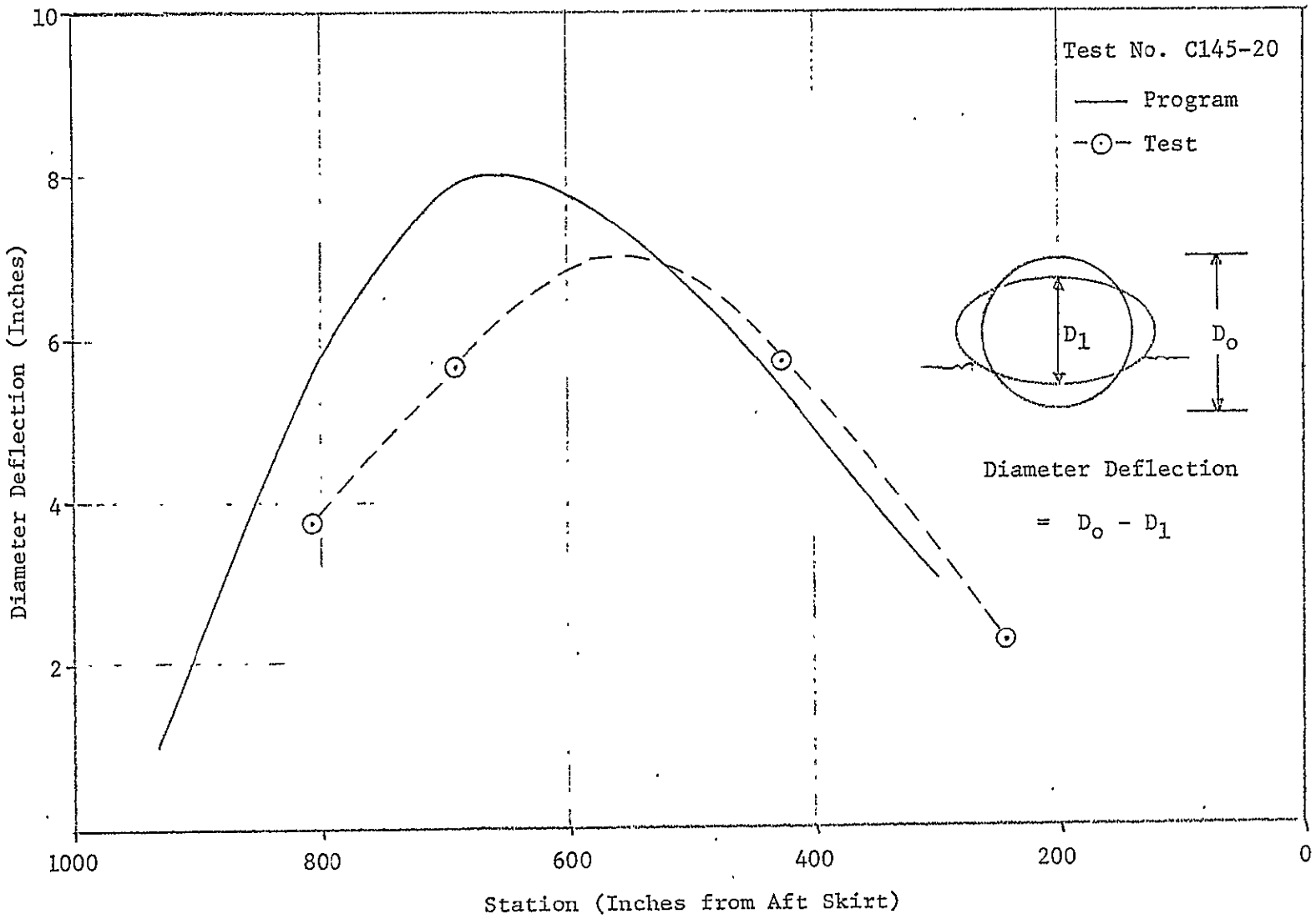

FIGURE 13. DIAMETER DEFLECTIONS AT T = 3.0 SEC.
120-INCH DIAMETER MODEL

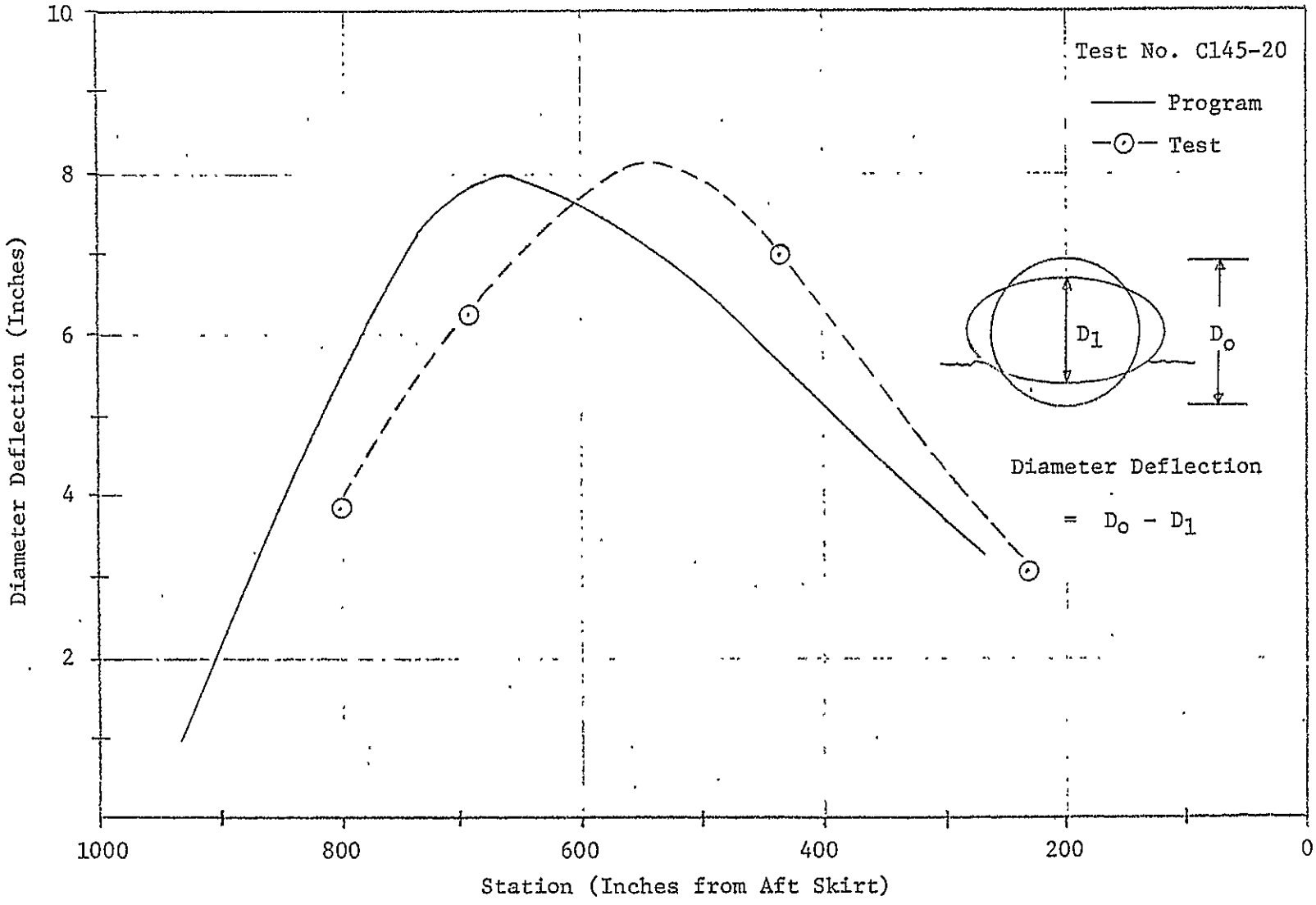

FIGURE 14. MAXIMUM DIAMETER DEFLECTIONS VS. LOCATION
120-INCH DIAMETER MODEL

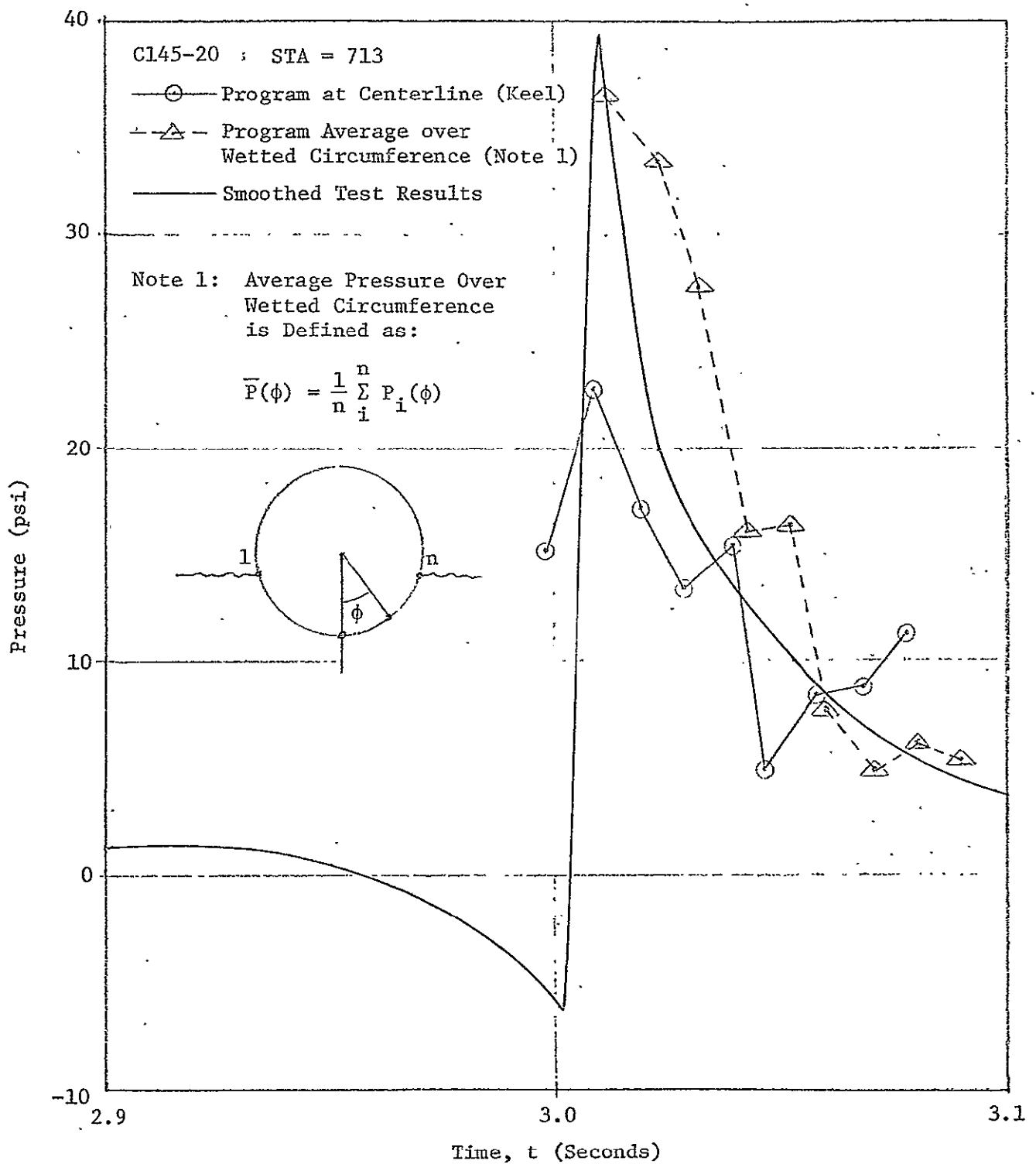

FIGURE 15. FLUID PRESSURE COMPARISONS VS. TIME
120-INCH DIAMETER MODEL

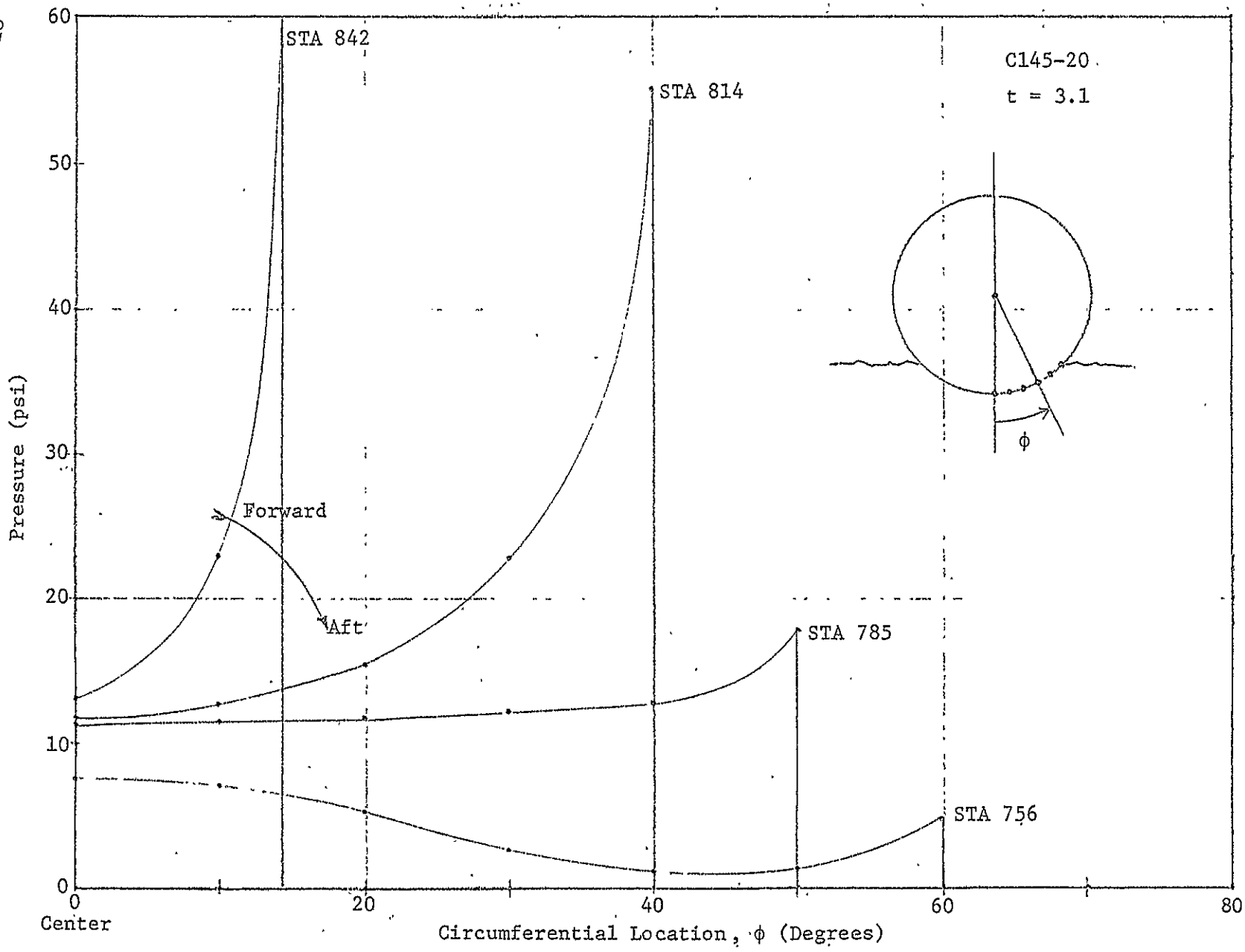

FIGURE 16. PRESSURE DISTRIBUTIONS AT TIME = 3.1 SEC.
120-INCH DIAMETER MODEL

within 20 percent. Primary data differences occurred in the pressure distributions and the time phase of the loads. Both of these differences may be attributed to the effects of surface waves, which cause the following effects:

1. The existence of a forward bow wave caused the application of pressure loads to occur sooner in the test. This was observed in both the pressure and deflection results.
2. The motion of the water along the side of the vehicle probably modified the circumferential pressure distributions, causing lower pressures at the waterline and higher pressures at the keel during the actual test.

4.2 PARAMETRIC STUDIES

The objective of the experimental correlation studies was to measure the differences between the test vehicle and the computer results. Analysis of the actual SRB structure could then proceed with a known confidence level and qualitative understanding of the problem. In conjunction with this analysis, the actual structure will be tested with static loads, obtained from experiment for the tested cases. In order to predict the trends of these loads and aid in the definition of criteria, additional parametric studies were performed on a NASTRAN model of the actual vehicle as discussed below. First, details of the NASTRAN model of the full scale vehicle will be presented.

Illustrated in Figure 17 is the actual rocket booster design, modeled by NASA contract support personnel, using the NASTRAN axisymmetric finite elements. The fine detail of the nose and nozzle structures was included for the purpose of analyzing several loading conditions other than the slapdown water impact. This procedure resulted in a rather large order analysis with 3480 degrees of freedom. However, for the slapdown analysis, matrix partitioning was used to reduce the problem to 1033 degrees of freedom.

The physical characteristics of the larger booster modified both the initial impact of the nozzle and the slapdown dynamics. Although the diameter was increased from 120 inches to 146 inches, the overall length went from approximately 1000 inches to a much larger 1535 inches. This and the design of the skirt surrounding the nozzle increased the rotary inertia and decreased the angular accelerations. Other significant differences included a larger skin thickness of 0.5 inches (vs. 0.375) and stiffer joints between the sections. Although the overall size was increased, the shell mode frequencies also increased due to these increases in stiffness.

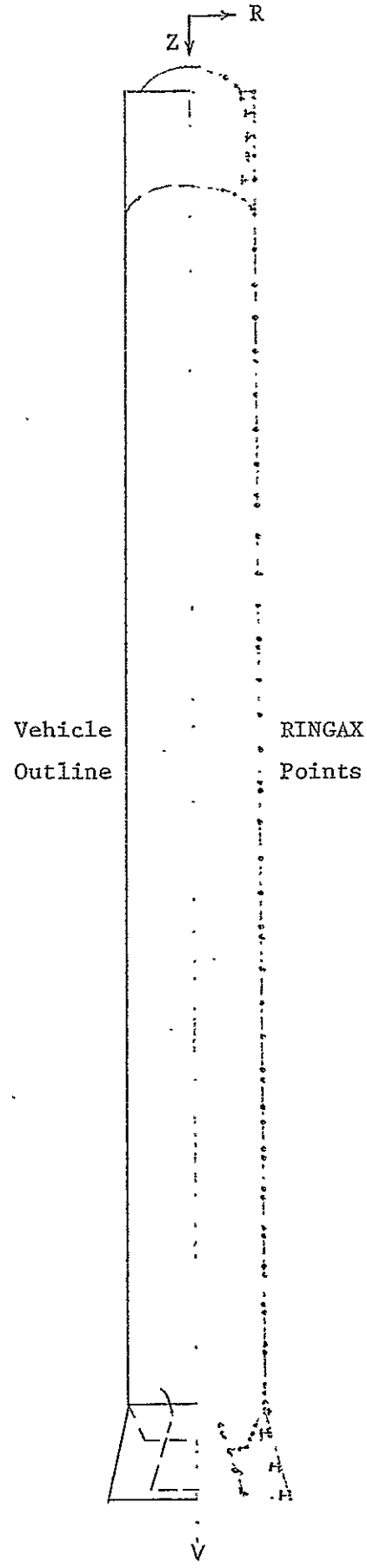

FIGURE 17. PROTOTYPE SRB STRUCTURE FINITE ELEMENT MODEL

The analysis of the full scale vehicle was performed both by UAI and by Teledyne-Brown personnel located near NASA - MSFC. The effort is being continued at MSFC. Because of the computer costs involved with the use of a commercial data center, the UAI effort was limited.

The effects of the various physical parameters defining the water impact were studied for both the 77% scale model (120-inch diameter) and a computer model of the actual SRB (146-inch diameter). Parameters included shell flexibility, damping, and initial conditions.

Variation of Shell Flexibility

The 77% structural model was stiffened by truncating the number of harmonics to 0 and 1, which results in no circumferential bending deflection. The effect on pressures is shown in Figure 18. In the rigid structure, the pressures rise to their peak immediately. In the flexible case, the structure motion delays the immediate pressure peak. However, when maximum deflection is reached, the pressures and forces may be larger in the flexible case.

Several analyses of the full SRB model were made using more severe impact conditions, scaled from the 77% model tests. An example of the calculated pressures for the flexible structure, compared to the rigid case, is shown in Figure 19. The small differences indicate that the pressures on the actual vehicle are relatively insensitive to deflections for the stiff full size vehicle.

Effect of Entrapped Water

Because of the design differences, the full scale vehicle entrapped more water than the scale test model. This will cause a substantial change in overall weight, as well as increasing damping on the full scale structure. The added mass will also lower the angular decelerations and cause higher velocities in the forward end of the vehicle. The estimated mass of the entrapped water was added to the structure as a fixed distributed mass.

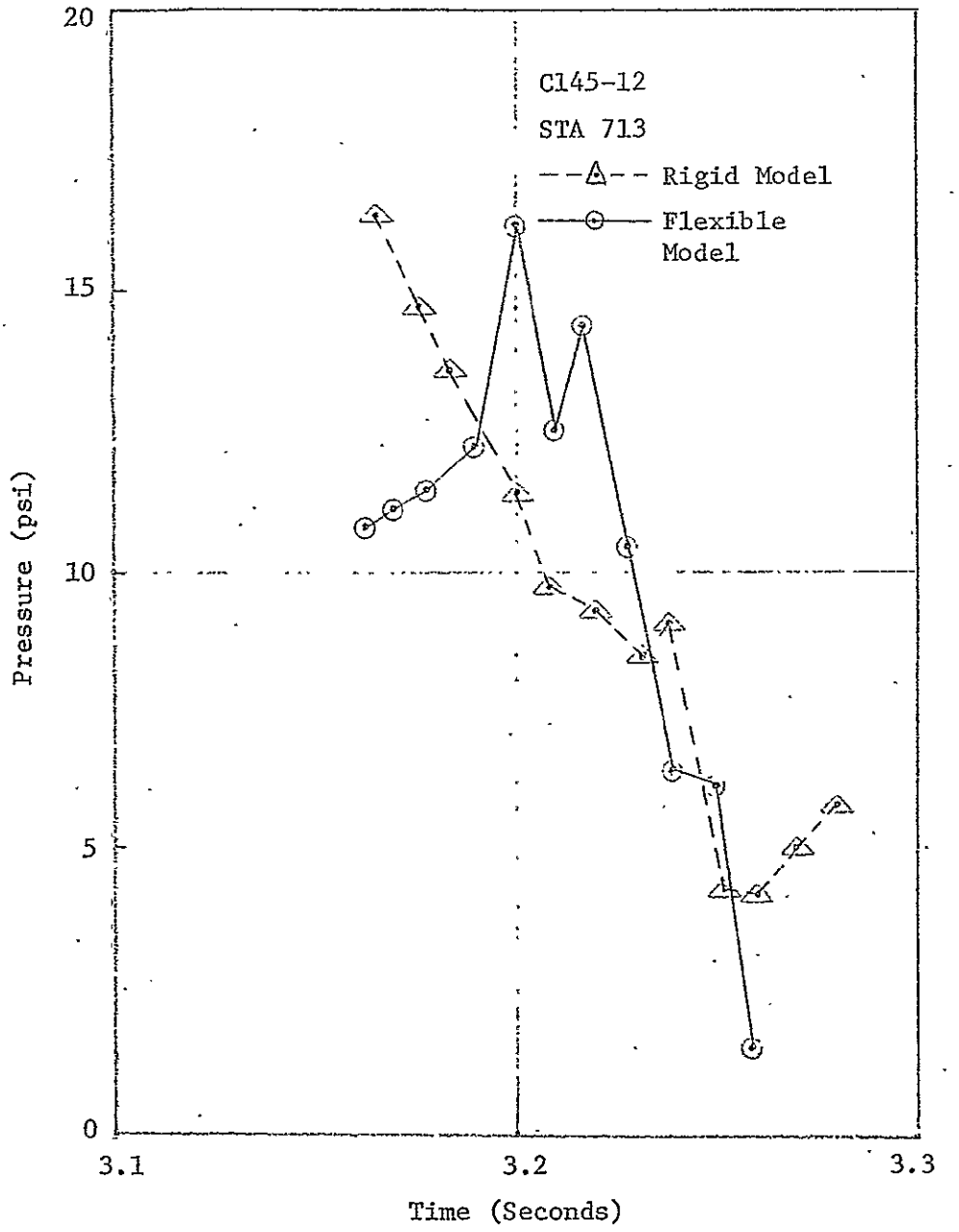

FIGURE 18. EFFECTS OF STRUCTURAL STIFFNESS ON PRESSURES 120-INCH DIAMETER MODEL

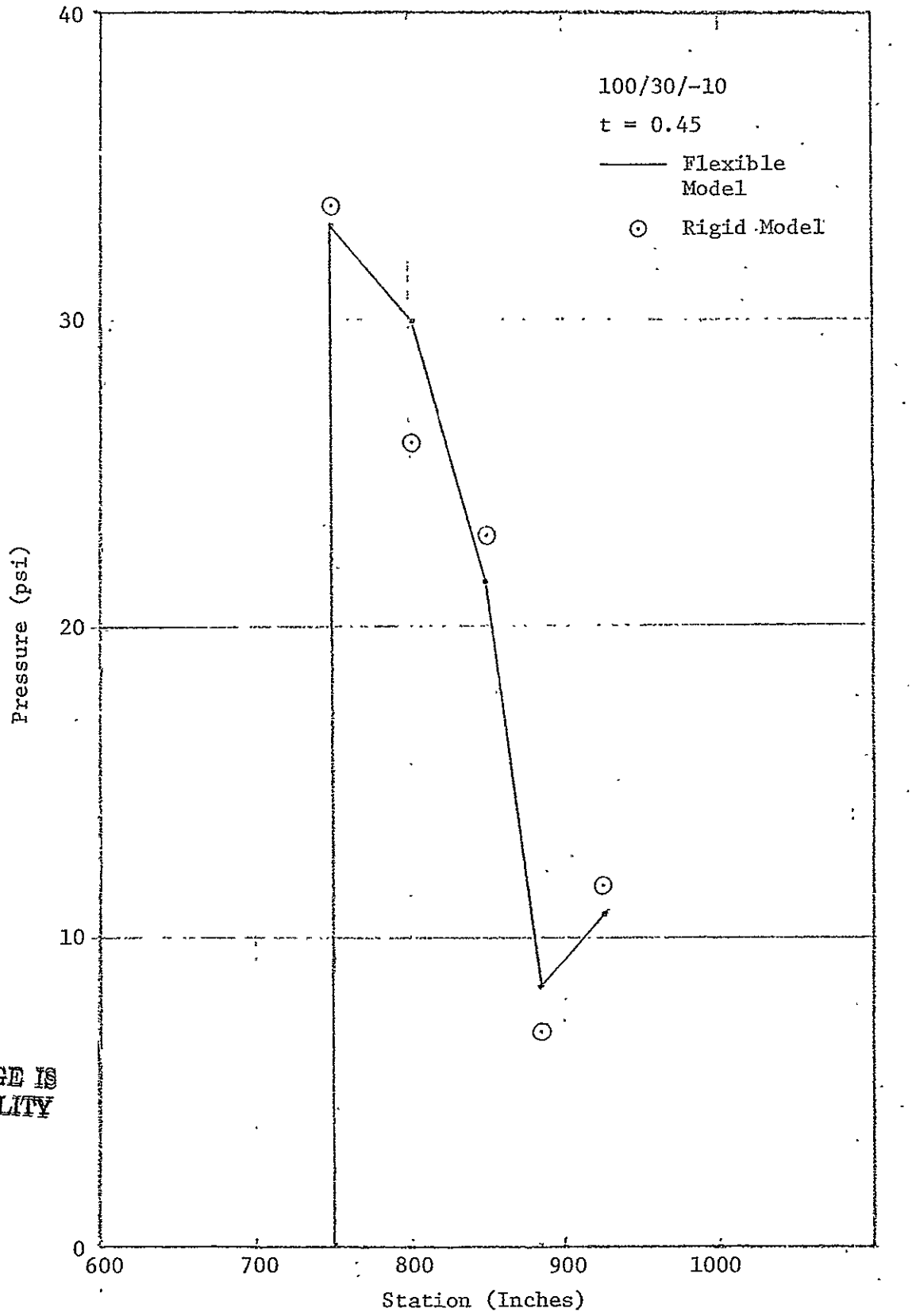

FIGURE 19. EFFECTS ON PRESSURES OF STRUCTURAL STIFFNESS
146-INCH DIAMETER VEHICLE

Variation of Structural Damping

Aside from the damping effects inherent in the fluid forces, the structure and any entrapped water will produce damping. These effects have been observed in the oscillations of the experimental data. For the 77% scale model, the undamped case is compared in Figure 20 with the results for a structural damping ratio of 5%. Although both cases appeared to oscillate more than the test data, the damped case more closely resembled the experimental results.

Effects of Initial Conditions

In order to investigate the effects of the initial conditions on the full SRB vehicle, a series of computer runs were made varying the initial height, vertical velocity, and angular velocity at the start of the slapdown process. The region of interest is, of course, when the velocities are high and the vehicle impacts in a nearly broadside angle. Knowing the effects of the different parameters in this region will aid in the future assessment of any changes in the vehicle trajectories prior to slapdown.

Maximum diameter deformation is plotted in Figure 21 versus vertical impact velocity for various combinations of height and angular velocities. The initial angle was fixed at 27 degrees and the horizontal velocity was 122 inches per second. Since a change in angle is equivalent to a change in height multiplied by the ratio of the angular velocity to the vertical velocity, it was unnecessary to vary the initial angle.

It was found that horizontal velocity which remains after initial impact had little effect upon results. A case having an increase of 50% in horizontal velocity was run for this configuration with insignificant changes in diameter deformation and CG accelerations.

Other output quantities such as vehicle accelerations, fluid pressures, and structural stresses are also affected by the initial conditions. However,

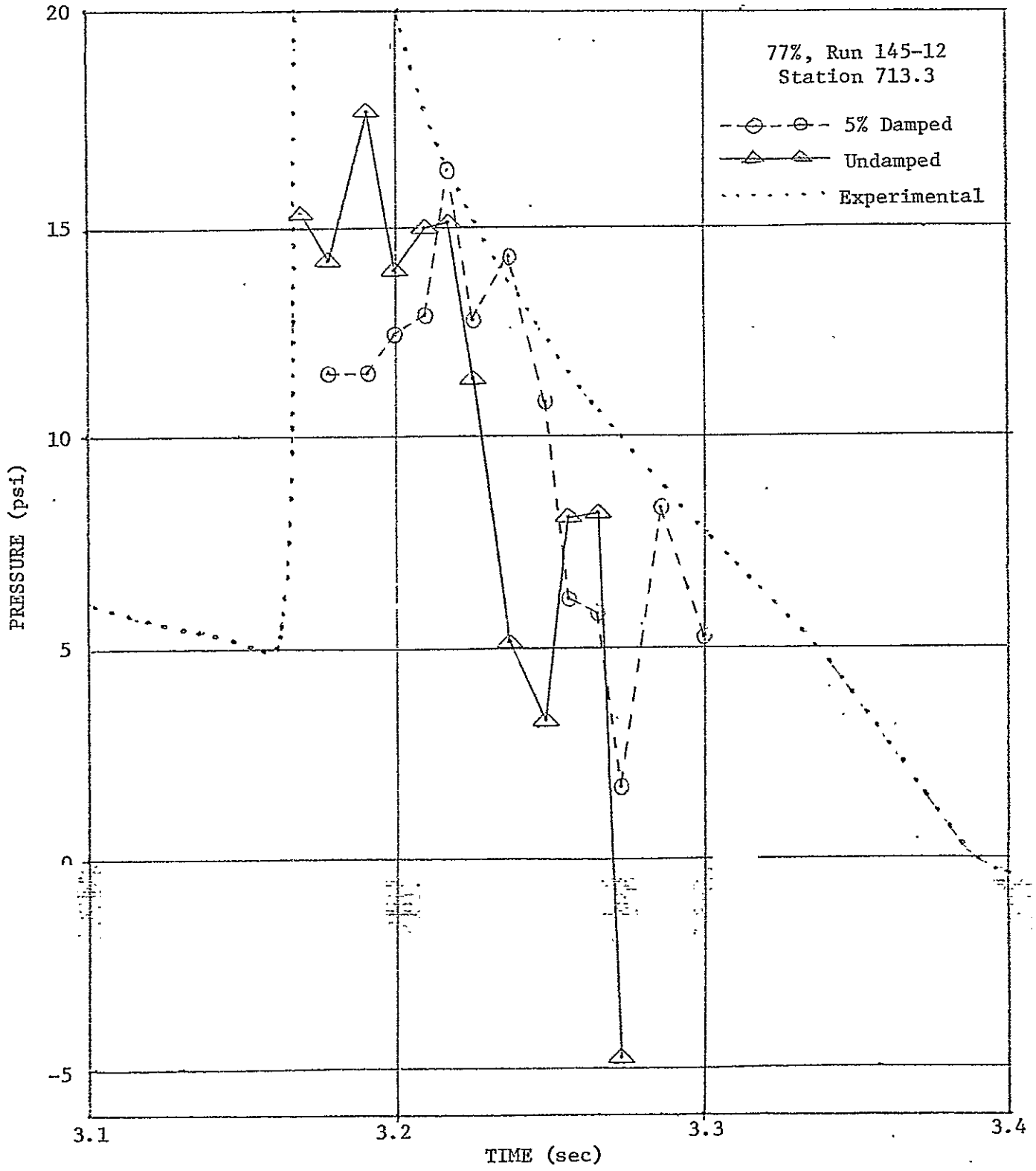

FIGURE 20. EFFECT OF STRUCTURE DAMPING ON FLUID PRESSURES

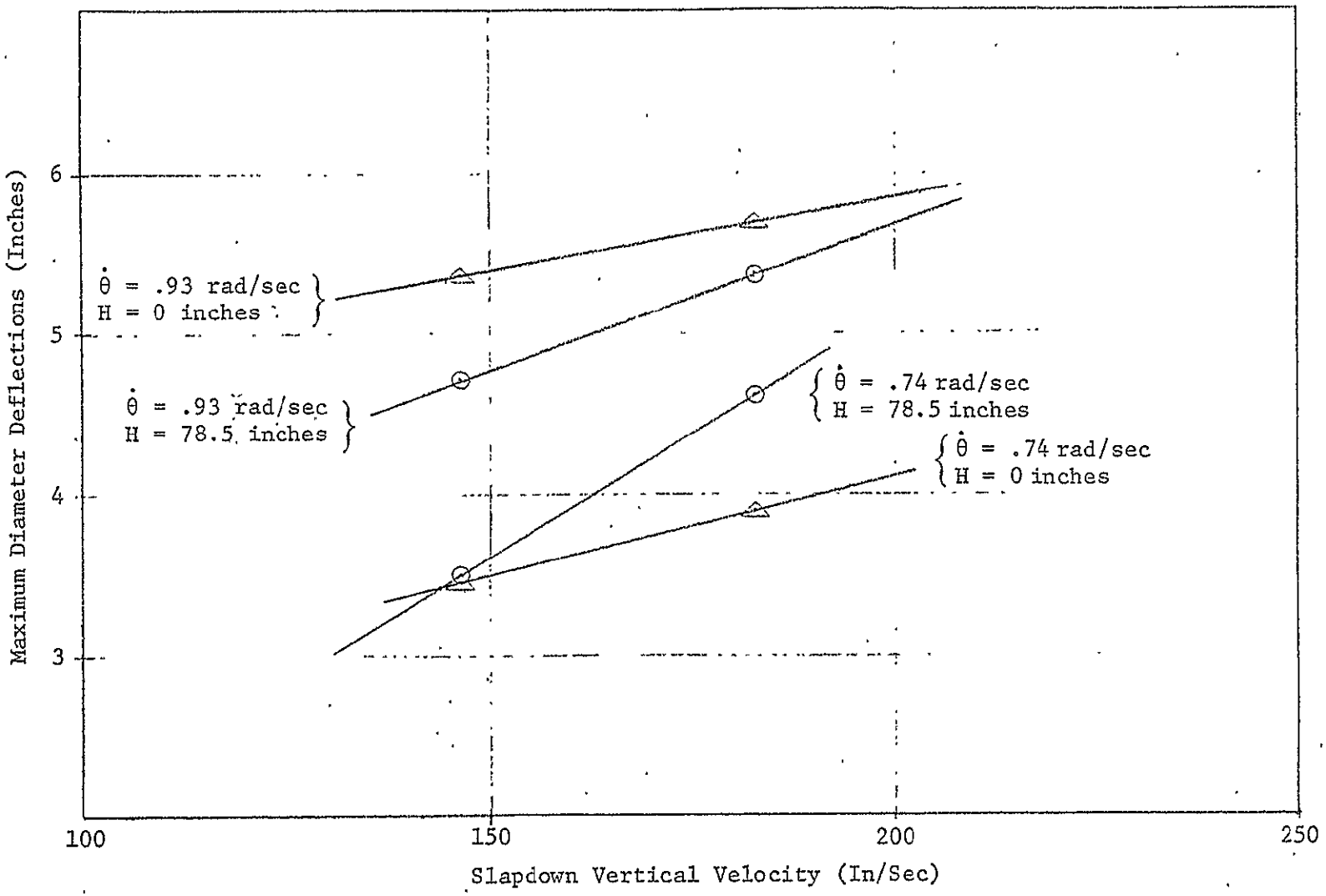

FIGURE 21. EFFECT OF SLAPDOWN INITIAL PARAMETERS ON MAXIMUM DIAMETER DEFLECTIONS

since the structural response is linear, and the structural vibrations are small, the stresses, loads, and thereby the accelerations are proportional to the deformations. For this reason only, the maximum deformation, which indicates the overall load, is discussed.

The study of these parameters indicates several interesting effects. The first is that the peak loads are not proportional to the square of the initial velocities as was expected, but rise more slowly. The second is that the increase in initial height above the water (or, in effect, a decrease in angle of impact) changes the growth rate of the load with velocity. Both of these effects may be explained by the fact that the peak loads occur in the forward region of the structure. By this time the impact velocities have been decreased by the previous loads on the aft and center of the vehicle. These self-cancelling effects insure that the changes in peak stresses and deformations will not grow radically with growth in slapdown impact velocities.

In starting the slapdown analysis with the modified NASTRAN program, the initial conditions may be selected at any time point in the test trajectory. However, because the initial structural deformation is assumed to be zero, it is necessary to start the analysis before any substantial slapdown loads and/or deflections have occurred. This point has generally occurred when the angle between the centerline and the water surface is thirty degrees or greater. If later initial conditions are specified, structural deflection overshoot can occur. Note that this dynamic overshoot only occurs when the structural deflections initially have a large value. In some cases, this effect was large enough to cause divergence in the numerical procedures because the local structural velocities became larger than the overall velocities. The remedy is to select earlier initial conditions corresponding to small deflections.

Comparison with 120-Inch Vehicle

The response of the full scale vehicle was compared to the response of the 120-inch test model for the same initial slapdown conditions. If L is the ratio of the model length to full scale length, the use of Froude scaling results in the following scale factors:

$$\text{gravity:} \qquad G = \frac{L}{T^2} = 1$$

$$\text{time:} \qquad T = \sqrt{L}$$

$$\text{velocity:} \qquad V = \frac{L}{T} = \sqrt{L}$$

$$\text{angular velocity:} \qquad A = \frac{1}{T} = \frac{1}{\sqrt{L}}$$

Note that the initial velocity for the full scale vehicle would be larger and the angular velocity would be smaller for direct comparisons.

It was found that the overall scaled pressures and loads in the two vehicles were similar, but the full scale model indicated 37% less deflection that the scaled test model results. This was due to the fact that the increase in skin thickness caused a 135% increase in shell bending stiffness (which is proportional to thickness cubed). This increase in stiffness resulted in a smaller coupling effect between the structure deflections and the fluid pressures.

4.3 CONCLUSIONS

The following comments apply to the comparison of the program to the test results and to the effects of the various parameters:

- The correlation studies have shown that peak, overall, water loads; structure deflections; and vehicle dynamics calculated by the program match the test data with error less than 20 percent.
- The calculated pressures differ from the experimental results both in the distribution over the surface and the time at which the initial peak occurs. These differences are probably due to the effects of surface waves with some additional second order effects of viscousity and finite element approximations.
- The effects of structural flexibility on the resultant fluid loads appeared to be small in the 120-inch diameter vehicle and negligible for the full scale SRB.
- The effects of damping due to internal fluid motion and external viscous flow are still unknown. These effects are extremely difficult to analyze and are not scaled in the small model tests.

4.4 RECOMMENDATIONS

The delivered computer program has served its basic purposes of providing analytic backup to the experimental testing and measuring the dynamic response of the flexible SRB. However, it has proved to be a useful tool for further studies of the SRB impact problem, beyond the original intentions and scope of the contract. The following are additions to the basic capability which could further improve the capabilities and usefulness.

- Refine the circumferential pressure distribution by including a vorticity correction in the potential function. This would remove the theoretically infinite free surface pressure and redistribute the circumferential pressure. Keel pressure will increase and probably show a better correlation to test values.
- Provide for longitudinal wave propagation in the potential function. This would involve the implementation of additional degrees of freedom for the definition of the three-dimensional surface waves. The pressure distribution and the definition of the waterline would be modified to account for the pressures and motion at the surface.
- Miscellaneous improvements could be made to refine the utility of the program. These would simplify the user's tasks of preparing the input data and simplify the production of output graphs and summaries. These would include additional printout of the waterline and diameter deflections at each station, printout of internal error criteria for assessing the numerical accuracy, and allowing for the definition of input geometry and initial conditions relative to any point on the structure.

REFERENCES

1. Flexible Body/Water Interaction During Water Impact, Universal Analytics, Inc., NASA-MSFC Contract No. NAS8-29665, Feb. 1974.

2. The NASTRAN Theoretical Manual, R. H. MacNeal, ed., NASA SP-221(01), April 1972.

3. R. E. Nichell, Nonlinear Dynamics by Mode Superimposition, AIAA/ASME/SAE 15th Structures, Structure Dynamics, and Materials Conference; April 1974, AIAA Paper No. 74-341.

4. Data Book for 120-Inch Diameter (77 Percent) Solid Rocket Booster Model Water Recovery Drop Test Program, NASA/MSFC, S&E-ASTN-ADC(73-45).

5. Remington, P. J., et al., Analysis of Selected Water Impact Loading on the Space Shuttle Solid Rocket Booster, Report No. 2870, Bolt Beranek and Newman, Inc. for NASA/MSFC.

APPENDIX A - PROGRAMMER'S MANUAL

A.1 IMPLEMENTATION INTO NASTRAN SYSTEM

The purpose of this appendix is to describe the programming tasks made to implement the hydroelastic water impact analysis into the NASTRAN computer program. In this chapter the overall solution algorithm is discussed, in A.2 the modifications to Data Blocks DYNAMICS and NLFT are described, and in chapter A.3 updates to the IFP, DPD and TRD modules are made. The remaining chapters describe newly developed fluid data and pressure generating subroutines.

The overall programming scheme has been designed to provide the user maximum convenience within the framework of the existing Level 15.5 NASTRAN System. Modifications and additions to the existing code have been kept to a minimum for the following reasons:

a. Level 15.5 NASTRAN may be updated to a new level and all changes to existing code will not require reprogramming.

b. The hydroelastic implementation within NASTRAN will not degrade the system for a normal structural transient analysis.

c. The reliability and flexibility of the systems is maintained; implemented changes involve only isolated subroutines.

The water impact problem is solved with rigid format 9 (Direct Transient Analysis) of the NASTRAN System. The necessary input data given by the user are briefly (see User's Manual for details):

a. A standard transient analysis structural model of the booster vehicle consisting of axisymmetric shell elements for the nozzle and slapdown entries and bar or quadrilateral plate elements for the cylindrical broadside entry.

b. A list of grid points and coordinate data for the idealized structure and points on the structure entering the water, and

c. Data defining the fluid properties and various geometric and system parameters.

Except for routine processing of the input data the only differences in the program flow from the normal transient analysis lies in the transient analysis module (TRD). The changes to the transient analysis module involve replacing the operations performed on the non-linear load functions (NØLINi) data cards) by the fluid impact operations (IMPACT, IMPLIST, and SLPLIST bulk data cards).

A simplified flow diagram for the implemented analysis within the TRD module is shown in Figure A.1. In order to activate the shell/fluid interaction analysis the control flag NØNLIN = 99999 is set in CASE CONTROL and processed in TRD1C.

A.2 DATA BLOCK DESCRIPTION UPDATES

The three new Bulk Data cards IMPACT, IMPLIST, and SLPLIST described in the User's Manual (Chapter 3) are processed by the IFP module and the card images or processed images written sequentially at the end of the DYNAMICS data block. The implementation of these new data by IFP are described in the following pages followed by the DATA BLOCK DESCRIPTION for the input DYNAMICS and output NLFT tables. These pages are prepared in a format suitable for direct insertion into the NASTRAN Programmer's Manual

A.2.1 Implementation in IFP (Table Entries)

The only code change to subroutine IFP within Level 15.5 NASTRAN consisted of a computed GØ TØ branch to the new bulk data. Implementation required updates to the IFP block data subroutines IFXiBD (i = 1, 2,..., 7) and subroutine

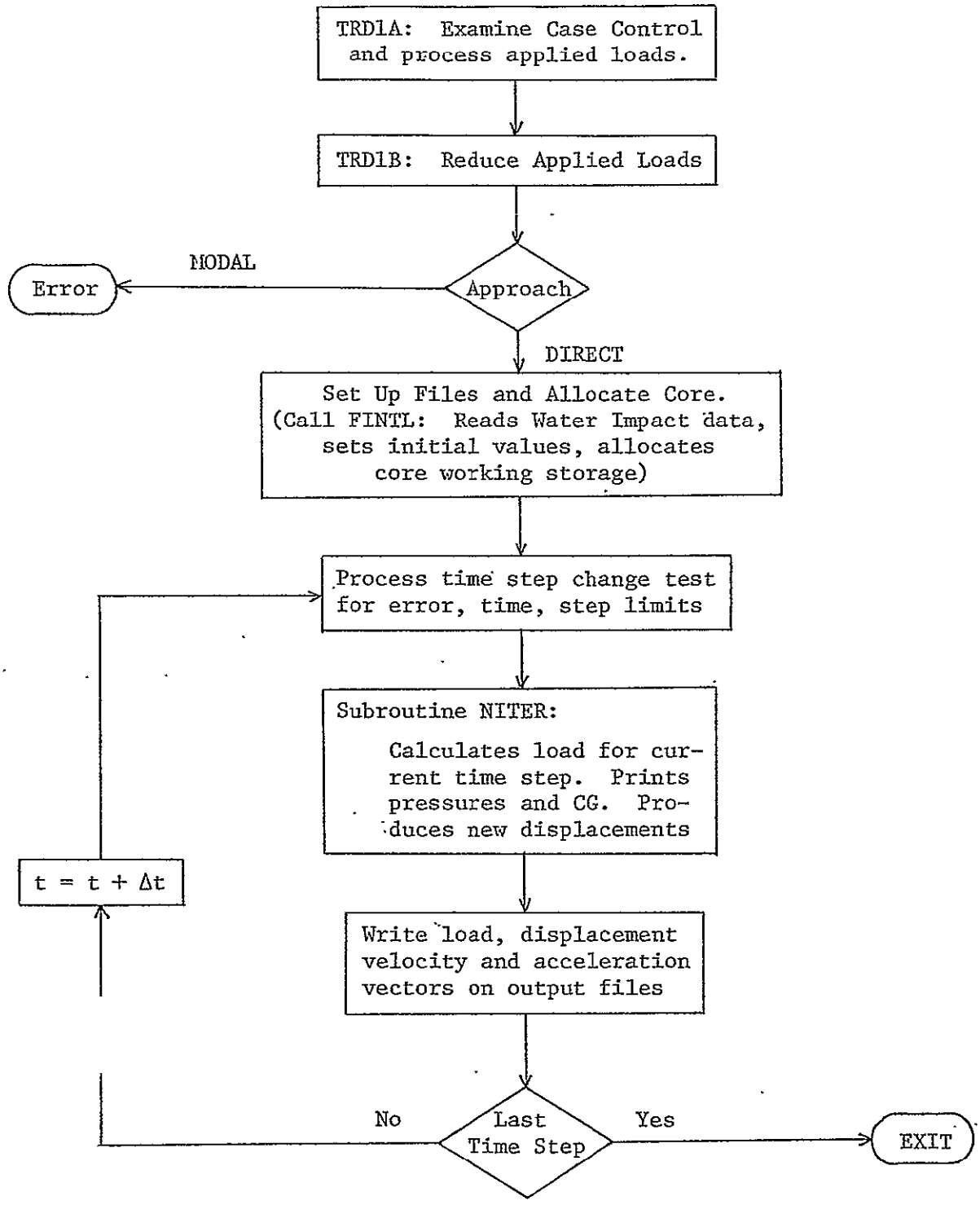

FIGURE A.1 TRD MODULE, SIMPLIFIED FLOW DIAGRAM

IFS3P which was recoded to interrogate the new bulk data cards. These changes were:

IFX1BD: Insert IMPACT, IMPLIST, and SLPLIST card ID titles into DATA I6//. These occur for card numbers 263 through 265, respectively.

IFX2BD: GINØ output file 7 and approach acceptability flag 0 set for the IMPACT, IMPLIST, and SLPLIST card entries.

IFX3BD: No change

IFX4BD: Required and allowable data items initialized as follows:

IMPACT	9, 17
IMPLIST	-4, 16
SLPLIST	-4, 9

(Note: IMPLIST and SLPLIST are open ended cards.)

IFX5BD: Entry statement numbers into IFX7BD field acceptability string set as follows:

IMPACT	991	(new string designed to accommodate 16 non-zero fields)
IMPLIST	-1	(no automated format checking)
SLPLIST	-1	" " " "

IFX6BD: IFP header information consisting of card type identification and bit position in a 96-bit trailer assigned as follows:

IMPACT	4307, 43
IMPLIST	4107, 41
SLPLIST	4507, 45

IFX7BD: Format code string entered for unique specification of IMPACT bulk data. No automated checking is done on IMPLIST and SLPLIST cards.

2.3.2.9 DYNAMICS (TABLE)

Card Types and Header Information:

Card Type	Header Word 1 Card Type	Header Word 2 Trailer Bit Position	Header Word 3 Internal Card Number
DAREA	27	17	182
DELAY	37	18	183
DLØAD	57	5	123
DPHASE	77	19	184
EIGB	107	1	86
EIGC	207	2	87
EIGP	257	4	158
EIGR	307	3	85
EPØINT	707	7	124
FREQ	1307	13	126
FREQ1	1007	10	125
FREQ2	1107	11	166
IMPACT	4307	43	263
IMPLIST	4107	41	264
NØLIN1	3107	31	127
NØLIN2	3207	32	128
NØLIN3	3307	33	129
NØLIN4	3407	34	130
RANDPS	2107	21	195
RANDT1	2207	22	196
RANDT2*	2307	23	197
RLØAD1	5107	51	131
RLØAD2	5207	52	132
SEQEP	5707	57	135
SLPLIST	4507	45	265
TF	6207	62	136
TIC	6607	66	137
TLØAD1	7107	71	138
TLØAD2	7207	72	139
TSTEP	8307	83	142

Card Type Formats:

DAREA (4 words)	SID	P	C
	A		
DELAY (4 words)	SID	P	C
	T		
DLØAD (open ended)	SID	S	S1
	L1	S2	L2
	...	S_n	L_n
	-1	-1	
PHASE (4 words)	SID	P	C
	TH		
EIGB (18 words)	SID	METHØD (2 words)	L1
	L2	NEP	NDP
	NDN	E	NØRM (2 words)
	G	C	0
	0	0	0
	0		

Card Type Formats Cont'd.:

EIGC (open ended)	SID	METHØD (2 words)	NØRM (2 words)
	G	C	E
	α_{a1}	ω_{a1}	α_{b1}
	ω_{b1}	ℓ_1	N_{e1}
	N_{d1}	α_{a2}	ω_{a2}
	α_{b2}	ω_{b2}	ℓ_2
	N_{e2}	N_{d2}	...
	α_{an}	ω_{an}	α_{bn}
	ω_{bn}	ℓ_n	N_{en}
	N_{dn}		-1
	-1		
	-1		
EIGP (4 words)	SID	α	
	M		
EIGR (18 words)	SID	METHØD (2 words)	F1
	F2	NE	ND
	NZ	E	NØRM (2 words)
	G	C	0
	0	0	0
	0		
EPØINT (1 word)	ID		
FREQ (open ended)	SID	F	F
	F	...	F
	-1		
FREQ1 (4 words)	SID	F1	DF
	NDF		
FREQ2 (4 words)	SID	F1	F2
	NF		
IMPACT (17 words)	TYPE (2 words)	DATA (12 words, type dependent)	
	ITER	ED	EP
IMPLIST (Open Ended)	SID	G(1)	G(2)
	G(3)	G(4)	G(5)
	...	G(M-1)	G(M)
	-1		
NØLIN1 (8 words)	SID	GI	CI
	S	GJ	CJ
	T	0	
NØLIN2 (8 words)	SID	GI	CI
	S	GJ	CJ
	GK	CK	
NØLIN3 (8 words)	SID	GI	CI
	S	GJ	CJ
	A	0	

Card Type Formats Cont'd.:

NØLIN4 (8 words)	SID	GI	CI
	S	GJ	CJ
	A	0	
RANDPS (6 words)	SID	J	K
	X	Y	TID
RANDT1 (4 words)	SID	N	TO
	TMAX		
RANDT2* Not available			
RLØAD1 (6 words)	SID	L	M
	N	TC	TD
RLØAD2 (6 words)	SID	L	M
	N	TB	TP
SEQEP (2 words)	ID	SEQID	
SLPLIST (open ended)	G(1)	Z(1)	G(2)
	Z(2)	etc	G(M)
	Z(M)	-1	-1
TF (open ended)	SID	GD	CD
	BO	B1	B2
	G(1)	C(1)	AO(1)
	A1(1)	A2(1)	G(2)
	C(2)	AO(2)	A1(2)
	A2(2)	...	G(N)
	C(N)	AO(N)	A1(N)
	A2(N)	-1	-1
	-1	-1	-1
TIC (5 words)	SID	G	C
	UO	VO	
TLØAD1 (5 words)	SID	L	M
	0	TF	
TLØAD2 (10 words)	SID	L	M
	0	T1	T2
	F	P	C
	B		
TSTEP (open ended)	SID	N(1)	DT(1)
	NØ(1)	N(2)	DT(2)
	NØ(2)		N(N)
			-1

2.3.29.9 FRL (TAB

Description

Frequency Response List.

The FRL contains one logical record for each different frequency set defined in the bulk data. Each record contains a sorted list of the unique frequencies defined in the set.

Table Format

Record	Word	Type	Item
	1,2	B	Data block name
	3	I	Set ID_1
	⋮		⋮
	2+n	I	Set ID_n
1	1-m	R	Frequencies belonging to set ID_1
⋮			⋮
n	1-k	R	Frequencies belonging to set ID_n
n+1			End-of-file

Table Trailer

Word 1 = number of frequency sets.

Word 2-6 = zero.

2.3.29.10 NLFT (TABLE)

Description

Non-Linear Forcing Table.

The header record of the NLFT contains a sorted list of set identification numbers for all NØLIN sets defined in the bulk data. Each logical record of the NLFT contains all data for a single set. Point and component numbers on the NØLIN cards are converted to scalar index values in both the d- and e-displacement sets. Record 1 in this table is modified if a water impact hydrodynamic analysis is desired.

Table Format

Record	Word	Type	Item
0	1,2	B	Data block name
	3		Set ID
	⋮		⋮
	2+n		Set ID_n

Record	Word	Type	Item	
1	1	I	Type of nonlinear load (1≤type≤4)	repeated for each NØLIN card in set
	2	I	SIL value in d-set	
	3	I	SIL value in e-set	
	4	R	Scale factor	
	5	I	SIL value in d-set	
	6	I	SIL value in e-set	
	7	type = 1 =	Table ID (integer)	
		type = 2 =	SIL value in d-set (integer)	
		type = 3 =	Scale factor (real)	
		type = 4 =	Scale factor (real)	
	8	type = 1 =	Not defined	
		type = 2 =	SIL value in e-set (integer)	
		type = 3 =	Not defined	
		type = 4 =	Not defined	
⋮				
n			Same format as record 1. Data belongs to set ID_n.	
n+1			End-of-file	

Note

Within each record, the data is sorted on word 2 of each 8-word entry in the record.

For water impact problems the NLFT output file contains the following information:

Record	Word	Type	Item
1	1	BCD	Approach flag BDSD, NØZL, or SLAP
	2,3,...,13	R and I	Water impact parameters
	14, 15, 16	R and I	Integration control parameters
	17	I	Number grid points (ND)
	18	I	Number of SIL values (NDØF)
2	1,...,NDØF	I	SIL values in d-set
3	1,...,ND	R	Z values, axial locations of grid points. This record is present only for SLAP case.

Table Trailer

Word 1 = number of NØLIN sets.

Word 2-6 = zero.

A.3 MODIFICATION TO EXISTING MODULES

A.3.1 DPD Module

In addition to the bulk data processing IFP module described in A.2.1, it is necessary to convert external grid point locations specified on the IMPLIST or SLPLIST data card into internal identifiers locating the active degree-of-freedom locations in the u_d vector set. The following pages describe the modifications made to the DPD module for this conversion. These pages are prepared in a format suitable for insertion into the NASTRAN Programmer's Manual.

$$f_i = f_0 \; 10^{(i-1)\delta} \quad i = 1,2,\ldots, N+1 \tag{2}$$

where

$$\delta = \frac{1}{N} \log_{10} \left(\frac{f_e}{f_0}\right). \tag{3}$$

3. If the entry corresponds to a FREQ set, the frequencies in the set are sorted, and any duplicate frequencies are discarded. The sorted list is written as one logical record on the FRL.

The RANDPS cards are read into core (if no RANDPS data are present, the PSDL is not assembled). The RANDT1 and RANDT2 cards are read into core, and a list similar to that in the frequency processing is formed. This list is sorted on set identification number. The file containing the PSDL is opened to write, and the set identifications are written in the header record. The RANDPS data are written as the first logical record of the PSDL. The remainder of the PSDL contains one logical record per set. For RANDT2 sets, the data are sorted on time lag, and duplicates are discarded prior to writing the record. For RANDT1 sets, N + 1 time lags, τ_i, are written where

$$\tau_i = \tau_0 + (i-1)\Delta\tau \quad i = 1,2,\ldots, N+1 \tag{4}$$

4.47.7.5 Assembly of the NLFT and TRL

The NØLINi (i = 1,2,3,4) cards are read into core. Each referenced grid point and component code is converted to a scalar index value in the u_p-set. The data are sorted on set identification number. USETD is read into core. The file containing the NLFT data block is opened to write, and the set identifications are written in the header record. The remainder of the NLFT contains one logical record per set. Scalar index values within each set are converted to scalar index values in the u_d and u_e sets. The data within each set are sorted on the scalar index value to which the forcing function is applied.

The water impact data cards are processed in a manner similar to the NØLINi cards. If the DYNAMICS data block contains records for IMPACT and IMPLIST or SLPLIST cards, these data are read into core. The IMPACT data is copies to the NLFT file. The list of identification numbers on the IMPLIST (type equals BDSD or NØZL) or SLPLIST (type equals SLAP) are converted to scalar indices in the d-set with subroutine DPD4. In general, if the problem is asymmetric (TYPE = NØZL or SLAP), the identification numbers are converted to internal numbers by the equation

$$ID_{internal} = ID_{list} + 10^6 * (n + 1)$$

where n = 0, 1 for NØZL and n is user-specified for SLAP case.

The scalar indices are converted to degree of freedom locations in the u_d vector with data block USETD. Each internal point generates two entries: u_r and u_θ for the broadside and three entries: u_r, u_z, and u_θ for the NØZL and SLAP cases. The total number of u_d locations is written on the NLFT file followed by the table of u_d pointers (IDØF). For the SLAP case the list of axial locations taken from the SLPLIST card is also written to the NLFT file.

The TIC cards are read, referenced grid points and component codes are converted to scalar index values in the u_p-set, and the data are written on SCR1, one logical record per set. A list of the TIC set identifications is accumulated in core. USETD is read into core. The

file containing the TRL data block is opened to write. The set identifications are written in the header record. The last word of the header contains the degrees of freedom in the u_d-set. Data are read from SCR1. Scalar index values are converted to scalar index values in the u_d-set. Each TIC set is written as one logical record on the TRL. When all the TIC data have been processed, the TSTEP data are copied from DYNAMICS to the TRL, one logical record per TSTEP set.

4.47.7.6 Assembly of the EED and TFL

Processing of EIGB, EIGC, EIGP and EIGR cards is minimal. For each card type present, a corresponding logical record is written on EED. For each of the cards which specify PØINT, the referenced grid point and component code is converted to a scalar index value (u_a set for EIGB and EIGR cards, u_d set for EIGC cards).

Transfer function data are read from the TF record on DYNAMICS one set at a time. For each transfer function set, the point and component codes are converted to scalar index values in the u_p set, which in turn form row and column numbers of the transfer function matrices. The data are written on the TFL, one transfer function set per logical record. The set identification number is the first word of each logical record. Four word entries follow. The first word is 65536*column number plus row number; the next three words are the terms of the matrices.

4.47.8 Subroutines

Auxiliary subroutines DPD1, DPD2, DPD3, DPD4 are described above.

4.47.8.1 Subroutine Name: DPDAA

1. Entry Point: DPDAA

2. Purpose: To convert a grid point and component code to a scalar index value in the u_p set.

3. Calling Sequence: CALL DPDAA

4. Method: A flag called INEQ is maintained in /DPDCØM/. If the flag is zero, EQDYN is read into core and INEQ is set to one. The grid point and component to be converted is stored in BUF(L) and BUF(L+1) where BUF and L are in /DPDCØM/. A binary search is performed in EQDYN. If the point is found, the corresponding scalar index value is stored in BUF(L). Otherwise, an error message is queued, and an internal

A.3.2 TRD Module

Modifications made to the TRD module for inclusion of the hydroelastic analysis occur in several locations and consist of testing for the existence of water impact load data (NØNLIN = 99999 in CASE CONTROL) and specific calls to the new subroutines. The simplified flow diagram [Figure A.1] illustrates the insertion of new subroutines within the TRD module. The initialization subroutine, FINTL, reads and converts pertinent bulk data (IMPACT, IMPLIST, and SLPLIST). The routine then sets initial values and pointers suitable for one of the three water impact conditions and allocates block data and open core for the relative variables and arrays. Subroutine NITER performs the solution for each time step using an iterative procedure. Maximum number of iterations and convergency criteria are controlled from the IMPACT data card. The FPG routine which is called by NITER, is designed basically as a driver to either the FCØNE and LGNDR (nozzle entry), FCYLP (broadside cylinder), or FSLAP and PLØAD (slapdown) subroutines which calculate the load vectors at each iteration. The selection of impact type is activated by the first word (NØZL, BDSD, or SLAP) on the IMPACT bulk data card. The following pages describe the modifications made to the TRD functional module and furnishes descriptions of the new subroutines. They should be inserted into the NASTRAN Programmer's Manual, Section 4.65 at the appropriate place.

NØLIN3 loads are computed as,

$$P_i(t) = \begin{cases} S\ \{u_j(t)\}A, & u_j(t)>0 \\ 0, & u_j(t)\leq 0 \end{cases} \tag{19}$$

NØLIN4 loads are computed as,

$$P_i(t) = \begin{cases} -S\ \{-u_i(t)\}A, & u_i(t)< 0 \\ 0, & u_i(t)\geq 0. \end{cases} \tag{20}$$

For the shell/fluid interaction analysis, the resulting non-linear hydrodynamic forces, equivalent to loads processed by the NØLINi bulk data cards, are automatically calculated by activating data supplied on the IMPACT, IMPLIST, and SLPLIST bulk data cards. These non-linear loads are computed by subroutines FCØNE, FCYLP, or FSLAP, having been called through FPG from NITER within the time loop in TRD1C. The loads are output directly into open core /TRDC1/ for processing the transient analysis solution. The user specifies the set of times at which data is to be saved. If the current time is an output time, the displacement vector for time $t = t_i$ is output.

The velocity vector given by:

$$\{\dot{u}_i\} = \frac{1}{2\Delta t}\ [\{u_{i+1}\} - \{u_{i-1}\}], \tag{21}$$

is output.

The acceleration vector given by

$$\{\ddot{u}_i\} = \frac{1}{\Delta t_i^2}\ [\{u_{i+1}\} + \{u_{i-1}\} - 2\ \{u_i\}] \tag{22}$$

is output.

If the time step is scheduled to change at t_{i+1} from Δt_1 to Δt_2, the displacement for time i+1 has been calculated. $\{u_{i-1}\}$, $\{u_i\}$, and $\{u_{i+1}\}$ are saved along with $\{P_{i+1}\}$. The matrices are formed and decomposed as in Equations 9,10, and 11 for $\Delta t = \Delta t_2$.

The following equation is used for computing $\{u_{i+2}\}$,

$$[D]\{u_{i+2}\} = \frac{1}{3}\{P_i^1 + P_{i+1} + P_{i+2}\} + \{N_{i+1}\} + [C]\{u_{i+1}\} + [E]\{u_i^1\}. \quad (23)$$

The vectors $\{P_i^1\}$ and $\{u_i^1\}$ in the above equation are calculated as follows. Define

$$\{\dot{u}_{i+1}\} = \frac{1}{\Delta t_1}(\{u_{i+1}\} - \{u_i\}), \quad (24)$$

$$\{\ddot{u}_{i+1}\} = \frac{1}{\Delta t_1^2}(\{u_{i+1}\} - 2\{u_i\} + \{u_{i-1}\}), \quad (25)$$

$$\{\dot{u}_i^1\} = \{\dot{u}_{i+1}\} - \{\ddot{u}_{i+1}\}\Delta t_2,$$

then:

$$\{u_i^1\} = \{u_{i+1}\} - \Delta t_2\{\dot{u}_{i+1}\} + \frac{\Delta t_2^2}{2}\{\ddot{u}_{i+1}\}, \quad (27)$$

(28)

4. Solution of Uncoupled Modal Equation: If the method of matrix formulation is modal and no transfer functions or direct input matrices are used, the equations may be solved in a more accurate, more direct manner. The diagonal terms of MHH, BHH, and KHH are stored in core. The following data are necessary to solve the transient behavior of a modal coordinate (ξ_i).

m_i = Modal mass of mode (MHH)

b_i = Modal damping coefficient (BHH)

K_i = Modal stiffness (KHH)

$$\omega_{oi} = (K_i/m_i)^{1/2}, \quad (29)$$

$$\beta_i = \frac{b_i}{2m_i}, \quad (30)$$

$$\omega_i^2 = |\omega_{oi}^2 - \beta^2|, \quad (31)$$

time of the j^{th} time step,

A.4 FLUID DATA INITIALIZER (SUBROUTINE FINTL)

FUNCTIONAL MODULE TRD (TRANSIENT ANALYSIS - DISPLACEMENT)

4.65.8.12 Subroutine Name: FINTL

1. Entry Point: FINTL

2. Purpose: To initialize shell/fluid interaction data for calculation of hydrodynamics loads by the FPG Subroutine. Reads data for conical or cylindrical impact problems from NLFT file. Stores pertinent data into FPGX common block and initializes pointers for working storage in open core. Allocates open core for use by Subroutine FPG.

3. Calling Sequence: CALL FINTL (NLFT,IDATA,NDATA,NROW,NGROUP,NZ2,IU1, IU2,DELTAT)

COMMON/TRDC1/ - Open core in TRD

COMMON/FPGX/DELZ,DELTH,DT,PI,RC,TL,VØ,RHØ,ALFA,THMAX,H,GAMA,VØL,PAMB, SALFA,CALFA,TALFA,TALFA2,VØLD,BO,VCR,VCZ,NPY,MM,NP,ND,NK,IT,IPRNT,IPC, ICM,ICMS,IP,IRZ,IASØ,IBSØ,IPMU,IPMUP,IP1M,IP1MU,IAS,IBS,IASD,IBSD,IPZØ, IPZØP,IP1Z,IP1ZØ,IPØ,IP1O,TYPE,LAST,KHARM,G,CDR,CDZ,MP,IIP,UD(3),UDD(3),PRT

NLFT - File number for input data.

IDATA - Entry point into open core TRDC1 containing water impact data and arrays.

NDATA - Last entry point into open core TRDC1 containing water impact data and arrays.

NRØW, NGRØUP NZ2 } - Pertinent pointers in Subroutine TRD1C.

DELZ - Increment ΔZ between nodes along longitudinal axis of cylinder or cone.

DELTH – Increment $\Delta\theta$ between circumferential nodes for cylindrical broadside impact.

DT – Time increment Δt in integration scheme.

PI – 3.1415927

RC – Radius of cylinder

TL – Lentth of cone (for FCØNE) from apex to nozzle exit, or length of cylinder (for FCYL

VØ – Initial impact velocity, V_o.

RHØ – Mass density of fluid

ALFA – Semi-apex angle of cone for nozzle entry

THMAX – Circumferential angle θ_{max} of last point in IMPLIST list for broadside entry (ΔZ for nozzle entry).

H – Depth below surface of fluid for which assumption $\phi = 0$ holds. Used for nozzle entry only.

GAMA – Initial canted angle (γ) of nozzle (cone) from vertical (for FCØNE only).

VØL – Total volume of enclosed shell impacting vertically in inverted conical configuration (for FCØNE only).

PAMB – Ambient air pressure (for FCØNE only).

SALFA, CALFA, TALFA, TALFA2 – Sine, cosine, tangent and tangent squared functions of semi-apex angle of conical nozzle (for FCØNE only).

VØLD, VCR, VCZ – Initialized velocity parameters

BØ – Initialized submerged depth

NPY (NPØLY) - Number of terms in expansion of Legendre function for stream potential expansion (for FCØNE only).

MM - Number of Fourier terms in expression for stream potential (for FCYLP only).

NP, ND - Number of nodal points taken along cone or cylinder for which hydrodynamic pressures are considered.

NK - Number of submerged points on wetted surface for cone or cylindrical mathematical models.

IT - Time increment counter in integration scheme.

IPRNT - Flag which may be turned on if pressures at each submerged node and each time step are desired as output

IPC - IP1Ø - Pointers into TRDC1 common block for various data and working array.

TYPE - Water impact type (NØZL, BDSD or SLAP) set by first word on IMPACT card.

LAST - Logical value set to true when NITER calls FPG for the final time in each time step.

KHARM - Number of harmonics.

G - Gravitational constant.

CDR - Drag coefficient in radial direction.

CDZ - Drag coefficient in axial direction.

MP - Mass property of structure.

IIP - Inertia property of structure.

UD - Rigid body velocities calculated in FSLAP

UDD - Rigid body accelerations calculated in FSLAP

PRT - Increment at which pressures are printed for slapdown case (degrees)

Integration control parameters are passed to NITER in common block INTCRL.

CØMMØN/INTCRL/NTER,ED,EP

NTER - Maximum number of iterations.

ED - Displacement convergence test.

EP - Parallel vector convergence test.

4. Method: The input file (NLFT) is opened and Record 1 is read and stored in the appropriate locations in /FPGX/. Work 1 determines the approach and the core allocation (NØZL, BDSD, or SLAP). See subroutines FCYLP, FCØNE, and FSLAP for a description of the core-held data. The working data is allocated in open core, words IDATA to NDATA. The list of pointers to other working arrays and vector locations of the connected grid points (IDØF) is read from the NLFT file and stored in open core. For the slapdown case the list of axial locations for each grid point is read and stored into open core.

A.5 FLUID PRESSURE GENERATOR SUBROUTINES

FUNCTIONAL MODULE TRD (TRANSIENT ANALYSIS - DISPLACEMENT

4.65.8.13 Subroutine Name: FPG

1. Entry Point: FPG

2. Purpose: To calculate non-linear hydrodynamic loads for shell/fluid interaction transient response for either an inverted cone (nozzle) or horizontal cylinder impacting a fluid.

3. Calling Sequence: CALL FPG (DELTAT,ICØUNT,IU1,IU2,IP4,NRØW,LAST,ITP,IY)

CØMMØN/TRDC1/ - Open core in TRD

CØMMØN/FPGX/ - See FINTL

DELTAT(DT) - Time increment Δt of integration scheme.

ICØUNT(IT) - Iteration counter

IU1 - Index to first location of u_{i+1} in TRDC1.

IU2 - Index to first location of u_{i+2} in TRDC1.

IP4 - Index to first location of non-linear load vector in TRDC1.

NRØW - Length of displacement and load vectors.

LAST - Logical variable to indicate last call to FPG for this time step.

IY - Error flag. Returns integer (1) to FPG if inappropriate geometry or loads data is calculated and terminates transient response.

4. Method: FPG is the driver routine which generates the inverted concial (FCØNE), cylindrical (FCYLP), or slapdown (FSLAP) water impact

load vectors for transient response. Transmits data pointers into TRDC1 for displacements, loads and working arrays.

4.65.8.14 Subroutine Name: FCYLP (Load Vector Generator for Broadside Impact of Cylinder into a Fluid)

1. Entry Point: FCYLP

2. Purpose: Calculates non-linear dynamic load vector for the transient response of a cylinder impacting a fluid on its side.

3. Calling Sequence: CALL FCYLP (UD,UDP1,FN,IDØF,CM,CMS,P,IY)

CØMMØN/TRDC1/ - Open core in TRD

CØMMØN/FPGX/ - Contains variables which have been initialized in FINTL subroutine

UD - Array in TRD open core containing $\{u_i\}$ - real - input

UDP1 - Array in TRD open core containing $\{u_{i+1}\}$ - real - input

FN - Array in TRD open core containing hydrodynamic forces $\{N_{i+1}\}$ - real - output and accelerations ($\ddot{u}_i$) as input.

IDØF - Array of integer pointers. Each entry is the position into the UD, UDP1 and FN vector arrays.

CM, CMS - Arrays for C_m at current and past time steps

P - Array of hydrodynamic pressures

IY - Error flag - See FPG

4. Method

a. Find submerged depth of penetration, B, and width of wetted

$$B = V\Delta t + B_{previous}$$

$$A = \sqrt{2R_c B}$$

where for the first time step $B_{previous} = 0$, $V = V_o$

b. Obtain velocities at grid points from the structural displacements, U_{ir}, and the IDØF table:

$$\overline{V}_{in} = [U_{ir}(t) - U_{ir}(t - \Delta t)] / \Delta t$$

$$\overline{V}_{i\phi} = [U_{i\phi}(t) - U_{i\phi}(t - \Delta t)] / \Delta t$$

c. Calculate the average, or "rigid body" velocity

$$V = \frac{1}{M} \sum_{i=1}^{M} \{\overline{V}_{in} \cos \theta_i - V_{i\phi} \sin \theta_i\}$$

where M is the total number of grid points in the IMPLIST list and $\theta_i = (i - 1)\Delta\theta$.

d. Calculate the fluid coefficients C_m, m = 1, 2...MM using the following equations

$$\eta_i = \cos^{-1}\left(\frac{R_c \sin \theta_i}{A}\right)$$

$$\Delta\eta_i = -\frac{1}{2}(\eta_{i+1} - \eta_{i-1})$$

where $\eta_o = \eta_1 = \frac{\pi}{2}$ and $\eta_{N+1} = 0$

$$v_i = \overline{V}_{in} - \dot{V} \cos \theta_i$$

and

$$C_m = \sum_{i=1}^{N} v_i \, [\sin (2m + 1) \, \eta_i] \sin \eta_i \, \eta\Delta_i$$

where N is the index of the last wetted point.

e. Calculate the derivative of each C_m

$$\dot{C}_m = [C_m(t) - C_m(t - \Delta t)] \, / \, \Delta t$$

The values C_m are stored for use in the next time step.

f. Calculate the pressures P_i at each point with the equation:

$$P_i = \frac{\rho}{\sin \eta_i} \left[\frac{R_c V^2}{A} + A\dot{V} \sin^2 \eta_i \right]$$

$$+ \frac{4\rho}{\pi} \sum_{m=o}^{M} \frac{1}{2m + 1} \left\{ \left[\frac{R_c V}{A} C_m + A \dot{C}_m \right] \sin (2m + 1) \, \eta_i \right.$$

$$\left. + (2m + 1) \, C_m \frac{R_c V}{A} \frac{\cos \eta_i}{\sin \eta_i} \cos (2m + 1) \, \eta_i \right\}$$

where $\dot{V} = [V(t) - V(t - \Delta t)]/\Delta t$

g. The area factors S_i for the points are:

$$S_i = \frac{1}{2} R_c \Delta\theta L, \quad i = 1$$

$$S_i = R_c \Delta\theta L, \quad i = 2, 3, \ldots, N-1$$

$$S_i = \frac{1}{2} R_c L \left[\sin^{-1} \left(\frac{A}{R_c} \right) - \theta_{N-1} \right], \quad i = N$$

h. The forces on each point in the radial direction are:

$$N_i = P_i S_i + M_i^f \ddot{u}_i$$

The forces are placed in the load vector, FN, in positions determined by the IDØF table.

4.65.8.15 Subroutine Name: FCØNE (Load Vector Generator for Inverted Cone Impacting into a Fluid)

1. Entry Point: FCØNE

2. Purpose: To calculate fluid pressure at each submerged node in the case of an inverted cone impacting water and to find elements of the associated non-linear load vector.

3. Calling Sequence: CALL FCØNE (IDØF,UD,UDP1,FN,RZ,ASØ,BSØ,PMU,PMUP, P1MU,P1MUP,AS,BS,ASD,BSD,PZØ,PZØP,P1ZØ,P1ZØP,PØ,P1,IY)

CØMMØN/TRDC1/ - Open core in TRD

CØMMØN/FPGX/ - Contains variables which have been initialized in FINTL Subroutine.

IDØF,UD,UDP1 FN,IY } See Subroutine FCYLP, each entry of the IDØF array is the position in the UD, UDP1 and FN vectors, e.g., U_{ri}^n or U_{zi}^n for point i and harmonic n. (n = 0 and/or 1)

RZ - Array of R and Z coordinates of nodes on IMPLIST list contained in open core /TRDC1/ starting at IRZ.

ASØ - P1 - Working and storage arrays in open core set up in subroutine FINTL.

4. Method: The logic flow and pertinent mathematical equations are as follows:

a. Penetration depth, B and velocities B and $\dot{D}$ calculated and the number of submerged nodes on the cone (NK) determined.

b. Calculation of geometry (a,ζ_o) of the expanding ellipsoid for current time step made.

c. Calculate air pressure within entrapped motor case (P_a).

d. The velocities $(\dot{U}^o_r)_{i+1}$, $(\dot{U}^o_z)_{i+1}$, $(\dot{U}^1_r)_{i+1}$ and $(\dot{U}^1_z)_{i+1}$ are calculated from difference equations for all submerged nodes utilizing displacements obtained from the UD and UDP1 arrays and pointers from the IDØF array.

e. The velocities, normal to the shell, are calculated:

$$\overline{V}_n(\mu_i) = \dot{U}^o_r(\mu_i) \cos\alpha - \dot{U}^o_z(\mu_i) \sin$$

$$\overline{V}^1_n(\mu_i) = \dot{U}^1_r(\mu_i) \cos\alpha - \dot{U}^1_z(\mu_i) \sin$$

f. The Legendre polynomials and their first derivative, Namely, P^o_m, P^1_m, P'^o_m and P'^1_m are calculated for ζ_o and μ_i by calling subroutine LGNDR.

g. A_s and B_s are calculated as follows.

$$I_n^o = \sum_{i=1}^{NK-1} \left[\sqrt{\frac{\zeta_o^2 - \mu_{i+1}^2}{\zeta_o^2 - 1}} P_m^o(\mu_{i+1}) \bar{V}_n(\mu_{i+1}) + \sqrt{\frac{\zeta_o^2 - \mu_i^2}{\zeta_o^2 - 1}} P_m^o(\mu_i) \bar{V}_n(\mu_i) \right] \left(\frac{\mu_{i+1} - \mu_i}{2} \right)$$

$$I_m^1 = \sum_{i=1}^{NK-1} \left[\sqrt{\frac{\zeta_o^2 - \mu_{i+1}^2}{\zeta_o^2 - 1}} P_m^1(\mu_{i+1}) \bar{V}_n^1(\mu_{i+1}) + \sqrt{\frac{\zeta_o^2 - \mu_1^2}{\zeta_o^2 - 1}} P_m^1(\mu_i) \bar{V}_n^1(\mu_i) \right] \left(\frac{\mu_{i+1} - \mu_i}{2} \right)$$

Then:

$$A_s = -a(2m + 1) \left[P'^o_m(\zeta_o) \right]^{-1} I_m^o \qquad \text{where } m = 2s + 1$$

$$B_s = -a \frac{(2m + 1)}{m(m + 1)} \left[P'^1_m(\zeta_o) \right]^{-1} I_m^1 \qquad \text{where } m = 2s + 2$$

h. A_s and B_s are evaluated as differences with respect to time:

$$\dot{A}_s = \frac{A_s(t) - A_s(t - \Delta t)}{\Delta t}$$

$$\dot{B}_s = \frac{B_s(t) - B_s(t - \Delta t)}{\Delta t}$$

i. C_{11}, C_{21}, C_{12}, C_{22} and C_{33} are calculated for the submerged points as follows:

$$C_{11} = -\frac{(1-\mu_i^2)\mu_i}{a(\zeta_o^2-\mu_i^2)}\dot{a}$$

$$C_{21} = -\frac{(\zeta_o^2-1)\zeta_o}{a(\zeta_o^2-\mu_i^2)}\dot{a}$$

$$C_{12} = \frac{\mu_i\sqrt{(1-\mu_i)^2\,(\zeta_o^2-1)}}{a(\zeta_o^2-\mu_i^2)}V_o \sin\gamma$$

$$C_{22} = -\frac{\zeta_o\sqrt{(1-\mu_i^2)\,(\zeta_o^2-1)}}{a(\zeta_o^2-\mu_i^2)}V_o \sin\gamma$$

$$C_{33} = \frac{1}{R_i}V_o \sin\gamma$$

where $V_o \sin\gamma$ is the average lateral velocity of the nozzle.

j. $\tilde{P}_o$, $\tilde{P}_1$, $\tilde{P}_2$ and $\tilde{P}_3$ are calculated as follows:

$$\tilde{P}_o(\mu_i) = \sum_{s=o}^{NPY}\Big[\dot{A}_s P_m(\mu_i)\,P_m(\zeta_o) + A_s P_m'(\mu_i)\,P_m(\zeta_o)\,C_{21} + A_s P_m(\mu_i)\,P_m'(\zeta_o)\,C_{11}\Big]$$

$$\tilde{P}_1(\mu_i) = \sum_{s=o}^{NPY} \left\{ B_s P_n^1(\mu_i)\, P_n^1(\zeta_o) + A_s \left[C_{12} P'_m(\mu_i)\, P_m(\zeta_o) + C_{22} P_m(\mu_i)\, P'_m(\zeta_o) \right] + B_s \left[C_{11} P'^1_n(\mu_i)\, P_n^1(\zeta_o) + C_{21} P_n^1(\mu_i)\, P'^1_n(\zeta_o) \right] \right\}$$

$$\tilde{P}_2(\mu_i) = \sum_{s=o}^{NPY} B_s \left[C_{12} P'^1_n(\mu_i)\, P_n^1(\zeta_o) + C_{22} P_n^1(\mu_i)\, P'^1_n(\zeta_o) \right]$$

$$\tilde{P}_3(\mu_i) = \sum_{s=o}^{NPY} B_s \left[C_{33} P_m(\mu_i)\, P_m(\zeta_o) \right]$$

where

$$\left.\begin{aligned} m &= 2s + 1 \\ n &= 2s + 2 \end{aligned}\right\} \quad s = 0, 1, 2...$$

k. The harmonics, n = 0 and 1, of water pressure are evaluated for each submerged node from:

$$P_o(\mu_i) = P_o(\mu_i) + \frac{+}{2} \left[P_2(\mu_i) + P_3(\mu_i) \right]$$

$$P_1(\mu_i) = \tilde{P}_1(\mu_i)$$

l. Each harmonic of water pressure for an element is assumed to be the average of that of the adjacent grid points, and is linearly distributed to the adjacent grid point in such a manner that the

center of pressure is preserved. The n^{th} harmonic of generalized normal forces at grid points a and b is:

$$\left.\begin{aligned} F_{an} &= \pi L \left[\frac{r_a}{3} + \frac{r_b}{6}\right] P_{av_n} \\ F_{bn} &= \pi L \left[\frac{r_a}{6} + \frac{r_b}{3}\right] P_{av_n} \end{aligned}\right\} \quad n > 0$$

where L is the length of the conical element $\Delta z/\cos\alpha$ and P_{av_n} is the average of the n^{th} harmonic of the water pressure on this element. Note that for n = 0 the forces are multiplied by 2. The forces are transformed to the r and z directions, the virtual mass forces $M_i^f \ddot{u}_i$ are calculated, and both are added to the F_n vector in positions determined from the IDØF array. The coefficients A_s and B_s are saved in locations ASØ and BSØ for use in the next time step.

4.65.8.16 Subroutine Name: LGNDR

1. Entry Point: LGNDR

2. Purpose: To calculate the first N odd degree Legendre polynomials and first N even degree associated Legendre functions of order one and their first derivatives for variable X.

3. Calling Sequence: CALL LGNDR (N,X,PX,PPX,P1X,PP1X)

N - Polynomial's degree (No. of terms in expansion series) - integer - input

X - Given variable - real - input

PX - Value of polynomial - real - output

PPX - Value of derivative of polynomial - real - output

P1X - Value of function - real - output

PP1X - Value of derivative of function - real - output

4. Method: The following recursive formulae are used to calculate the value of the Legendre polynomials and their derivatives for orders 0 and 1.

$$P_m^n(X) = \frac{1}{m - n} \left[(2m - 1)\, XP_{m-1}^n(X) - (m + n - 1)\, P_{m-2}^n(X) \right], (n = 0, 1)$$

and

$$\frac{d}{dx} P_m^o(X) = \frac{m}{x^2 - 1} \left[XP_m^o(X) - P_{m-1}^o(X) \right]$$

$$P_m^1(X) = \sqrt{1 - X^2}\, \frac{d}{dx} P_m^o(X)$$

and

$$\frac{d}{dx} P_m^1(X) = \frac{1}{X^2 - 1} \left[mXP_m^1(X) - (m + 1)\, P_{m-1}^1(X) \right]$$

4.65.8.17 Subroutine Name MASSG

Purpose: To calculate mass and inertia properties at the CG of the structure for a slapdown water impact problem. The CG location is also calculated and the DLIST array (defined originally on the SLPLIST data card) is converted to locations relative to the CG.

Entry Point: MASSCG

Calling Sequence:

CALL MASSCG (NPTS,NHARM,R,ILIST,DLIST,IM,D,MP,IP,ZCG)

The variables are:

NPTS - Number of grid points (input)

NHARM - Number of harmonics (input)

R - Radius of cylinder (input)

ILIST - Array of SIL values (input)

DLIST - Z locations of grid points (input, output)

on input - relative to origin

on output - relative to CG

IM - Matrix control block for MASS file (input)

D - Working storage (real & integer)

MP - Mass property (output)

IP - Inertial property (output)

ZCG - CG location (output)

Method:

The rigid body matrix D is created as a core-held packed matrix. The rigid body mass matrix, $[\bar{M}]$, is calculated by the equation:

$$[\bar{M}] = [D]^T [M] [D]$$

where M is the structural mass matrix (M_{dd} file).

The total mass, m, the CG location, $\bar{z}$, and the inertia, I, about the CG are calculated by the following equations:

$$m = \frac{1}{2} (\bar{M}_{11} + \bar{M}_{22})$$

$$\bar{z} = -\frac{1}{m} \bar{M}_{13}$$

$$I = \bar{M}_{33} - m\bar{z}^2$$

The location of each station relative to the CG replaces the values z_i in the DLIST array, i.e.,

$$z_{iCG} = z_i - \bar{z}$$

4.65.8.18 Subroutine Names IJINT, GETIJ

Purpose: To precalculate the integral terms $I_{nm}(\alpha)$ and $J_{nm}(\alpha)$ for a selected range of n, m, and α values. The definition of the integrals is:

$$I_{mn} = \int_0^{\pi} \cos n\phi \sin (2m + 1)\, \eta \sin \eta \, d\eta$$

$$J_{mn} = \int_0^{\pi} \cos n\phi \cos (2m + 1)\, \eta \cos \eta \, d\eta$$

Entry Point: IJINT

Calling Sequence:

CALL IJINT (NA,NN,NM,R,Z,ALPHA)

The variables are:

Z - Array of open core, output (2*NA*NM*NN) in length

ALPHA - Array of α values, output

NA - Number of α points (= 2*MAX(NN/4 NM) + 2)

NM - Number of m values, 1,2,...,NM

NN - Number of n values, 0,1,...,NN-1

R - Radius

Method:

The routine will generate 2 NA matrices each of dimensions NN by NM and store them in the array z. Four nested loops are necessary to perform the required calculations. They are:

1. The outer loop sets the value $\alpha_i = R(\frac{i}{NA})$ and sets the matrices I_{nm} and J_{nm} to zero. The values sin α_i and cos α_i are also calculated.

2. The second loop changes the index k where η_k ($0 < \sin \eta_k < 1$) and $\Delta\eta_k$ are obtained from the Gaussian integration table. The values $\sin \eta_k$, $\cos \eta_k$, $\sin 2\eta_k$, and $\cos 2\eta_k$ are also calculated.

   The functions of ϕ are calculated from the equations:

$$\phi = \frac{\cos n}{\sin^{-1} \left(\frac{a}{R}\right)}$$

   The following functions are calculated and stored for $m = 1,2,\ldots,NM$.

$$CE(m) = \cos (2m + 1)\,\eta = CE(m - 1) \cos 2\eta - SE(m - 1) \sin 2\eta$$

$$SE(m) = \sin (2m + 1)\,\eta = SE(m - 1) \cos 2\eta - CE(m - 1) \sin 2\eta$$

   where $CE(0) = \cos \eta_k$ and $SE(0) = \sin \eta_k$ is implied.

3. The third loop is performed over the index n where $n = 0,1,2,\ldots,NN$. The following values are calculated and stored at each value of $n > 1$

$$CP(n) = \cos (n\phi) = \cos (n - 1)\,\phi \cos \phi - \sin (n - 1)\,\phi \sin \phi$$

   where

$$\sin (n\phi) = \sin (n - 1)\,\phi \cos \phi + \cos (n - 1)\,\phi \sin \phi$$

4. The inner loop is performed over the index m where $m = 1,2,3,\ldots,NM$. The following increments to the integrates are calculated and stored:

$$\Delta I_{nm} = \Delta\eta_k \cos n\phi \sin \eta \sin (2m + 1)\,\eta$$

$$\Delta J_{nm} = \Delta\eta_k \cos n\phi \cos \eta \cos (2m + 1)\,\eta$$

   or

$$\Delta I_{nm} = \Delta\eta_k \; CP(n) \; SE(0) \; SE(m)$$

$$\Delta J_{nm} = \Delta\eta_k \; CP(n) \; CE(0) \; CE(m)$$

Note that since the indices n and m have zero values, the actual program indices are larger by one.

Entry Point: GETIJ

Calling Sequence:

CALL GETIJ (A,N,M,INM,DINM,JNM)

The variables are:

A - Input, real - half width of water-line, a

N - Input, integer - harmonic index

M - Input, integer - fluid series index

INM - Output, real - I_{nm} integral

DINM - Output, real - $\partial I_{nm}/\partial a$ integral

JNM - Output, real - J_{nm} integral

Method:

The table α_i is searched until $a_i < A < a_{i+1}$. Linear interpolation is used for the corresponding values of I_{nm} and J_{nm}. The derivative term DINM uses the difference $\Delta I_{nm}/\Delta\alpha$.

4.65.8.19 Subroutine Name NITER

Purpose: To perform the solution of a displacement vector due to nonlinear loads for each time step in a transient analysis.

Entry Point: NITER

Calling Sequence:

CALL NITER (DELTAT,IU1,IU2,IU3,IP1,IP4,SCR1,BUF1,IY)

COMMON/TRDC1/ - Open Core

The variables are:

DELTAT	- Time step size
U1,U2,U3	- Pointers to displacement vectors in open core. U3 is output
IP1	- Pointer to applied load vector in open core
IP4	- Pointer to resultant load vector in open core, output
SCR1,BUF1	- GINØ scratch file and buffer
IY	- Error flag returned by calls to FPG

Method:

1. An estimate for the new displacement vector is obtained by linear extrapolation,

$$\{y_o\} = 2\{u_2\} - \{u_1\}$$

where u_2 is the current displacement vector, u_1 is the previous vector, and y_o is the estimate of the next vector.

2. The subroutine performs the iteration on the matrix equation,

$$[A_2]\ \{y_{i+1}\} = \{N(y_i)\} + \{C\}$$

where:

$$[A_2] = \left[\frac{1}{\Delta t^2} M + \frac{1}{2\Delta t} B + \frac{1}{3} K \right]$$

$$\{C\} = \left[\frac{2}{\Delta t^2} M - \frac{1}{3} K \right] \{u_2\} +$$

$$\left[\frac{-1}{\Delta t^2} M + \frac{1}{2\Delta t} B - \frac{1}{3} K \right] \{u_1\} + \{\bar{P}\}$$

$\{N(y_i)\}$ is the nonlinear load obtained by calling Subroutine FPG.

3. Starting with the second iteration, the following vectors are written to the scratch file for each iteration:

$$\{\delta_i\} = \{y_i - y_{i-1}\}$$

$$\{\Delta_i\} = \{f_i - f_{i-1}\}$$

where:

$$\{f_i\} = \{N(y_i) - N(y_{i-1})\}$$

4. The following tests are performed after each iteration:

a. The change in the magnitude of the force vector is checked.

If $|f_i| \Big/ |N(y_i)| < \varepsilon_p$,

the load has converged and the subroutine goes to Step 6.

b. The number of non-zero terms in the force vector is checked.

If $i \geq$ total number of non-zero terms in $\{N(y_i)\}$,

set $n = i$ and go to 5.

c. The two previous {f} are checked to ensure they are not parallel.

f_i and f_{i-1} are normalized such that

$$|f_i| = |f_{i-1}| = 1$$

and the largest term of each is positive.

If, for all non-zero terms in the vector,

$$\left| \frac{f_{ij} - f_{i-1,j}}{f_{ij}} \right| < \varepsilon_d \qquad j = 1,2.....NROW$$

If all terms pass the test, set n = i - 1 and go to 5.

d. The number of iterations performed is checked.

If $i = I_{max}$, set n = i and go to 5.

e. If none of the above, continue the iteration for $i = i + 1$.

5. This step is executed if the process is not converging. At least three iterations must have occurred.

a. The equation below is solved for $\{\alpha\}$,

$$[u]^T [A_\Delta] \{\alpha\} = [u]^T \{N(y_n)\}$$

where the vectors stored on the scratch file make up [u] and $[A_\Delta]$ as follows:

$$[u] = [\delta_2, \delta_3, ..., \delta_n]$$

$$[A_\Delta] = [\Delta_2, \Delta_3, ..., \Delta_n]$$

Note that the matrix to be inverted is of order η-1 and may be held in core. If the matrix to be inverted is singular, the maximum number of iterations, I_{max}, is decreased and processing begins at Step 1.

b. The final displacement vector is calculated,

$$\{y\} = \{y_n\} - [u] \{\alpha\}$$

c. The final load vector {N} is calculated by calling Subroutine FPG.

6. The final displacement and load vectors are placed in the output locations indicated by IU3 and IP4, and the subroutine exits.

4.65.8.20 Subroutine Name FSLAP

Purpose: To calculate the slapdown loads on the cylindrical shell structure for a given set of positions and velocities for slapdown analysis.

Entry Point: FSLAP

Calling Sequence:

CALL FSLAP (U1,U2,Y,PNL,ILIST,DLIST,TEMP)

The variables are:

U1,U2 - Core held displacement vectors (u_{1r}, $u_{1\phi}$, etc.; u_{2r}, $u_{2\phi}$, etc.)

Y - Current estimate of next vector

PNL - Load vector output, {N}

ILIST - List of position indices for the vector terms of each point

DLIST - List of the avial distances from the CG to each point (δ_i)

TEMP - Temporary working array

The common block /FPGX/ contains the control data, miscellaneous constants, rigid body accelerations and velocities, and total mass properties M and I. The displacement vector, U_2, contains three extra terms corresponding to the rigid body displacements U, W, and θ.

Method:

The FSLAP subroutine performs three basic steps: The water impact loads are calculated for each point for all harmonics and added to the overall load vector and to the loads on the CG. The CG accelerations are calculated from the basic momentum equations. Finally, the loads on the structure are corrected by adding the inertial forces due to the rigid body motion. The output load vector, PNL, contains the forces on the structure points plus the three total CG forces, F_x, F_z, and M_θ.

1. Estimated displacements and velocities are predicted from initial data. The displacements, velocities and accelerations of the structure are estimated from the previous time step,

$$y_i = \ddot{u}_i \Delta t^2 + 2u_{2i} - u_{1i}$$

where y is the estimate for displacement, u_1 and u_2 are the current or initial values from the previous time step, and $\ddot{u}_i$ is the estimated acceleration derived from rigid body considerations. When the final iteration is performed, then the last estimate for acceleration is calculated as:

$$\ddot{u}_i = (y_i + u_{1i} - 2u_{2i})/\Delta t^2$$

The detailed processing steps are listed below:

2. Load Vector Calculations:

A loop is performed over each station on the structure as defined by the tables ILIST and DLIST. The following steps are executed at each point.

a. The local velocity functions at point i are:

$$\dot{u}_r^n = \frac{1}{2\Delta t}\left(y_r^n - u_{1r}^n\right) \qquad (n \neq 1)$$

$$\dot{u}_r^1 = \frac{1}{2\Delta t}\left(y_r^1 - u_{1r}^1\right) + \dot{W}_{CG} \cos\theta + \dot{U}_{CG} \sin\theta - \delta_i \dot{\theta}_{CG} \qquad (n = 1)$$

where u_r^n is the displacement at point i in the r direction for harmonic n.

b. The accelerations are:

$$\ddot{u}_r^n = \frac{1}{\Delta t^2}\left(y_r^n - 2u_{2r}^n + u_{1r}^n\right) \qquad (n \neq 1)$$

$$\ddot{u}_r^1 = \frac{1}{\Delta t^2}\left(y_r^1 - 2u_{2r}^n + u_{1r}^1\right) + \ddot{W}_{CG}\cos\theta + \ddot{U}_{CG}\sin\theta - \delta_i\ddot{\theta}_{CG}$$

Note that these equations are best coded as function subroutines to be evaluated as they are needed rather than store all results in core.

c. Calculate the distance from the center line to the water, r_i, where

$$r_i = \frac{1}{\cos\theta}\left[\delta_i \sin\theta - W_{CG}\right] - u_{2r}^1$$

where u_{2r}^1 is the local displacement at point i in the r direction, harmonic 1.

If $r_i \geq R$, the station is "dry", no loads are produced, and the loop proceeds to the next point.

d. If $0 < r < R$, perform the following calculations:

$$a = \sqrt{R^2 - r^2}$$

$$\dot{r}_i = (r_i \tan\theta + \delta_i)\,\dot{\theta} - \frac{1}{\cos\theta}\dot{W}_{CG} - \frac{1}{2\Delta t}\left(y_r' - u_{1r}'\right)$$

$$\dot{a} = -\frac{r_i \dot{r}_i}{a}$$

$$\dot{X} = \dot{U}_{CG} + \dot{r}\sin\theta - W_{CG}\,\dot{\theta}$$

$$\Delta x = \frac{1}{2}\left(\delta_{i+1} - \delta_{i-1}\right) / \cos\theta$$

Note $\delta_o = \delta_1$ and $\delta_{N+1} = \delta_N$ at the end points 1 and N.

Evaluate the loads P_r^k using Subroutine PLØAD. The integrals I_{nm}, $\frac{\delta I_{mn}}{\delta a}$ and J_{mn} are obtained by interpolating the tables using the current value of a. The derivatives of the velocities are obtained from the velocities of the adjoining stations:

$$\frac{\delta \dot{u}_r^n}{\delta x} = \frac{1}{2\Delta x}\left(\dot{u}_r^n\Big|_{i+1} - \dot{u}_r^n\Big|_{i-1}\right)$$

where the end values are zero.

e. The impact loads are distributed to the adjoining stations using the equations below:

$$\left.\begin{aligned} F_{i-1}^k &= -\frac{1}{4} P_r^k \\ F_i^k &= -\frac{1}{2} P_r^k \\ F_{i+1}^k &= -\frac{1}{4} P_r^k \end{aligned}\right\} \quad 1 < i < N_i$$

The end points on the cylinder are a special case:

$$F_1^k = F_2^k = -\frac{1}{2} P_r^k \qquad (i = 1)$$

$$F_N^k = F_{N-1}^k = -\frac{1}{2} P_r^k \qquad (i = N)$$

where F_i^k is the load in the r direction at point i in the k^{th} harmonic. The F_i^k forces are added to the appropriate position in the PNL vector.

f. If $r_i \leq 0$, the loads are calculated from the virtual mass of the attached fluid. The net force on each harmonic k is:

$$P_r^k = \frac{\rho R \Delta x}{2k} (R - r_i)) \ \ddot{u}_r^k \qquad (k > 0)$$

$$P_r^o = \rho R \Delta x \ (R - r_i)) \ \ddot{u}_r^o \qquad (k = 0)$$

The loads are distributed to the adjacent stations as in step e. If $r_i \leq -R$, then y_i is set equal to -R.

During the execution of step 'f' above, the mass matrix containing the effective inertia terms relative to the CG is added to the running sums M_w, δ_w, and I_w. These are added to the mass of the structure giving a total rigid body mass matrix, $\bar{M}$, where:

$$[\bar{M}] = \begin{bmatrix} m & & \\ & m & \\ & & I \end{bmatrix} + \begin{bmatrix} M_w & 0 & -M_w\delta_w \\ 0 & 0 & 0 \\ -M_w\delta_w & 0 & I_w \end{bmatrix}$$

The new rigid body acceleration in vehicle coordinates is:

$$\begin{Bmatrix} \ddot{u}_r \\ \ddot{u}_z \\ \ddot{\theta} \end{Bmatrix} = [\bar{M}]^{-1} \begin{Bmatrix} F_r \\ F_z \\ M \end{Bmatrix}$$

where F_r, F_z, and M are the net forces acting at the CG with the acceleration loads removed.

4. Inertial Reaction Loads:

In order to keep the structural displacements small and manageable, the structure loads are calculated to produce only motions relative to the coordinates fixed on the CG. Centrifugal and Coriolis forces are ignored. The procedure for calculating these corrective loads is:

a. The mass matrix file is opened to be read a column at a time; each column corresponds to a displacement for a given point and harmonic. Only the zero and first harmonics are used to produce inertial loads.

b. The loads are generated one point, i, at a time. The accelerations due to the CG motion at each point are:

$$\ddot{u}^1_{r_{CG}} = \frac{1}{2}\bar{\ddot{u}}_r - \delta_i \ddot{\theta}_j$$

$$\ddot{u}^1_{\phi_{CG}} = -\ddot{u}^1_{r_{CG}}$$

$$\ddot{u}^o_{z_{CG}} = \bar{\ddot{u}}_z$$

$$\ddot{u}^1_{z_{CG}} = R\ddot{\theta}_j$$

Note the superscript indicates the harmonic number and the subscript indicates the direction.

c. The columns of the mass matrix corresponding to u^1_r, u^1_ϕ, u^o_z, and u^1_z are multiplied by the <u>negative</u> of the corresponding acceleration and added to the load vector PNL in core. This load vector will be in equilibrium with respect to rigid body motion and will produce only relative structural displacements.

4.65.8.21 Subroutine PLØAD

Purpose: To evaluate the loads P_r^k for slapdown analysis. The equation to b be used is:

$$P_r^k = \frac{2\,\rho R^2\, a^2\, \Delta X \cos\theta}{\pi\,(R^2 - a^2)} \sum_n \sum_m \left\{ \left[\left(\ddot{u}_r^n + \frac{\partial \dot{u}_r^n}{\partial X}\,\dot{X} \right) + \left(\frac{a}{I_{mn}} \left(\frac{\partial I_{mn}}{\partial a} \right) + \frac{R^2}{R^2 - a^2} \right) \frac{\dot{a}}{a}\,\dot{u}_r^n \right] \frac{I_{mn}\, I_{mk}}{2n+1} + \left[\dot{u}_r^n\, \frac{\dot{a}}{a} \right] I_{mn}\, J_{mk} \right\}$$

Entry Point: PLØAD

Calling Sequence:

CALL PLØAD (PR,K,MM,XDØT,ADI,UXRD,URDØT,DEN,R,AI,DELX,TH,PI,URDD)

The variables are:

PR - Harmonic load (P_r^k)

K - Number of harmonics

XDØT - $\dot{X}$

ADI - $\dot{a}$

UXRD - $\frac{\dot{u}_r^n}{x}$

URDØT - $\dot{u}_r^n$

DEN - ρ density

R - Radius

AI - a

DELX - ΔX

TH - θ

PI - π

URDD - $\ddot{u}_r^n$

MM - Number of polynomials in series

Method:

The routine will precalculate the leading constants. Then two nested loops will be used for the summations. Each loop has an entry point for the integral subroutine GETIJ. The integral functions I_{nk}, I_{mn}, J_{mk} are precalculated and are obtained from tables using the current value of a. The following equations are executed inside the loop

$$x_1 = \ddot{U}_R^n + \frac{\partial U_r^n}{\partial x} \dot{X}$$

$$x_2 = \frac{1}{I_{mn}} \left(\frac{\partial I_{mn}}{\partial a} \right) + \frac{1}{\sqrt{R^2 - a^2}}$$

$$x_3 = x_2 \dot{a} \dot{u}_r^n$$

$$x_4 = (x_1 + x_3) \left(\frac{I_{mn} I_{mk}}{2m + 1} \right)$$

$$x_5 = \dot{u}_r^n \left(\frac{\dot{a}}{a} \right) I_{mn} J_{mk}$$

$$C\emptyset N3 = \frac{2\rho R^2 \Delta x \cos \theta}{\pi} \sin^{-1} \left(\frac{a}{R} \right)$$

$$SUM = x_4 + x_5$$

$$P_{R_k}^n = C\emptyset N3 * SUM$$

APPENDIX B

ANALYTICAL AND EXPERIMENTAL DATA COMPARISONS

Test Run C145-20

The following plots are given:

- Height and Angle vs. Time
- Pressure vs. Time ($\theta = 0°$ and average pressure)
- Circumferential Pressure Distribution
- Diameter Deflection vs. Time
- Diameter Deflection vs. Station
- Maximum Deflection vs. Station

Run C145-20

Height and Angle vs. Time

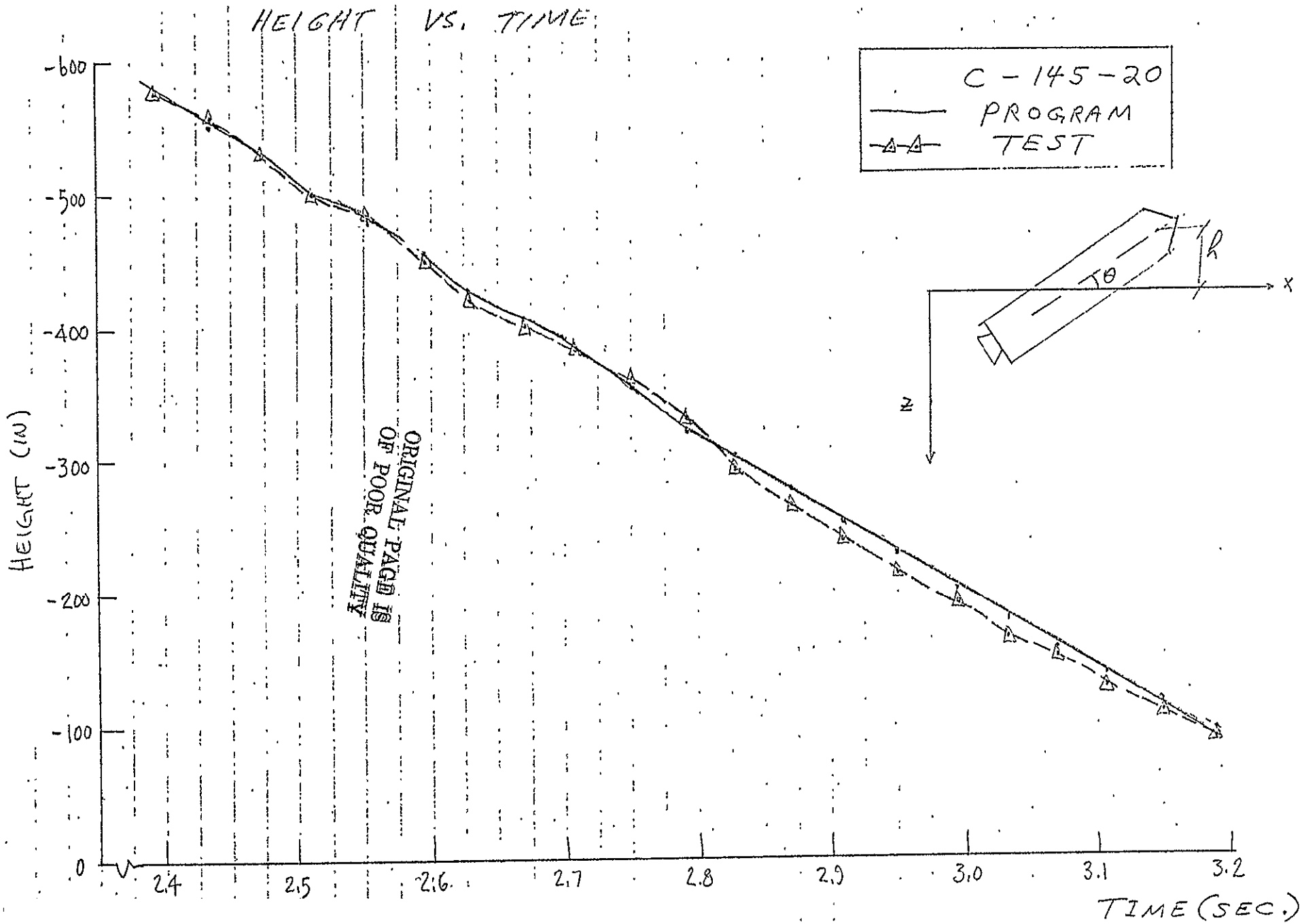

HEIGHT Vs. TIME

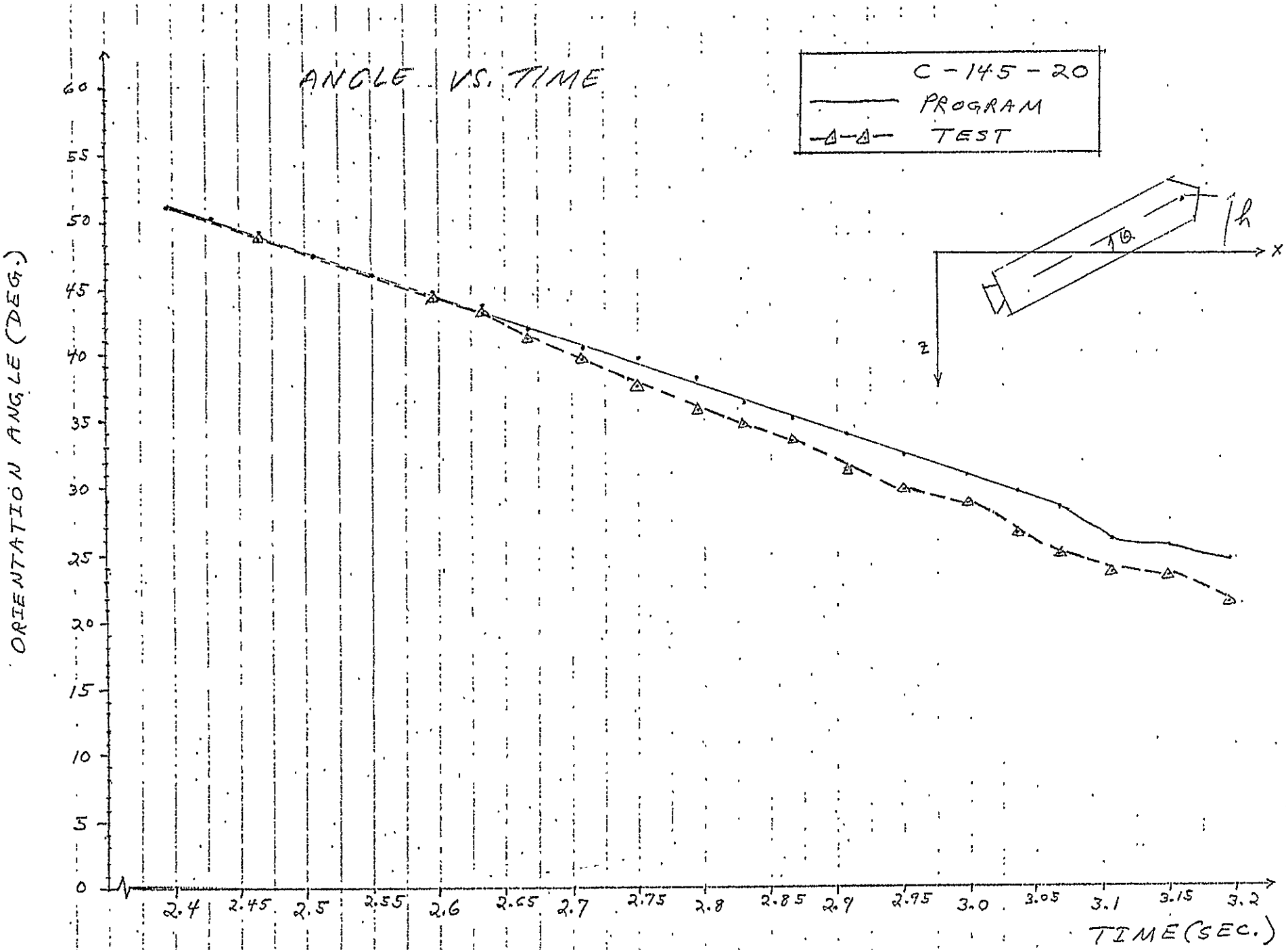
ANGLE VS. TIME
C-145-20
PROGRAM
TEST
ORIENTATION ANGLE (DEG.)
TIME (SEC.)
0
5
10
15
20
25
30
35
40
45
50
55
60
2.4
2.45
2.5
2.55
2.6
2.65
2.7
2.75
2.8
2.85
2.9
2.95
3.0
3.05
3.1
3.15
3.2
h
θ
x
z

Run C145-20

Pressure vs. Time

At Centerline and Average Over Wetted Area

Note: Test results are plotted as envelopes bounded by dashed lines.

77% Water Recovery 145-20

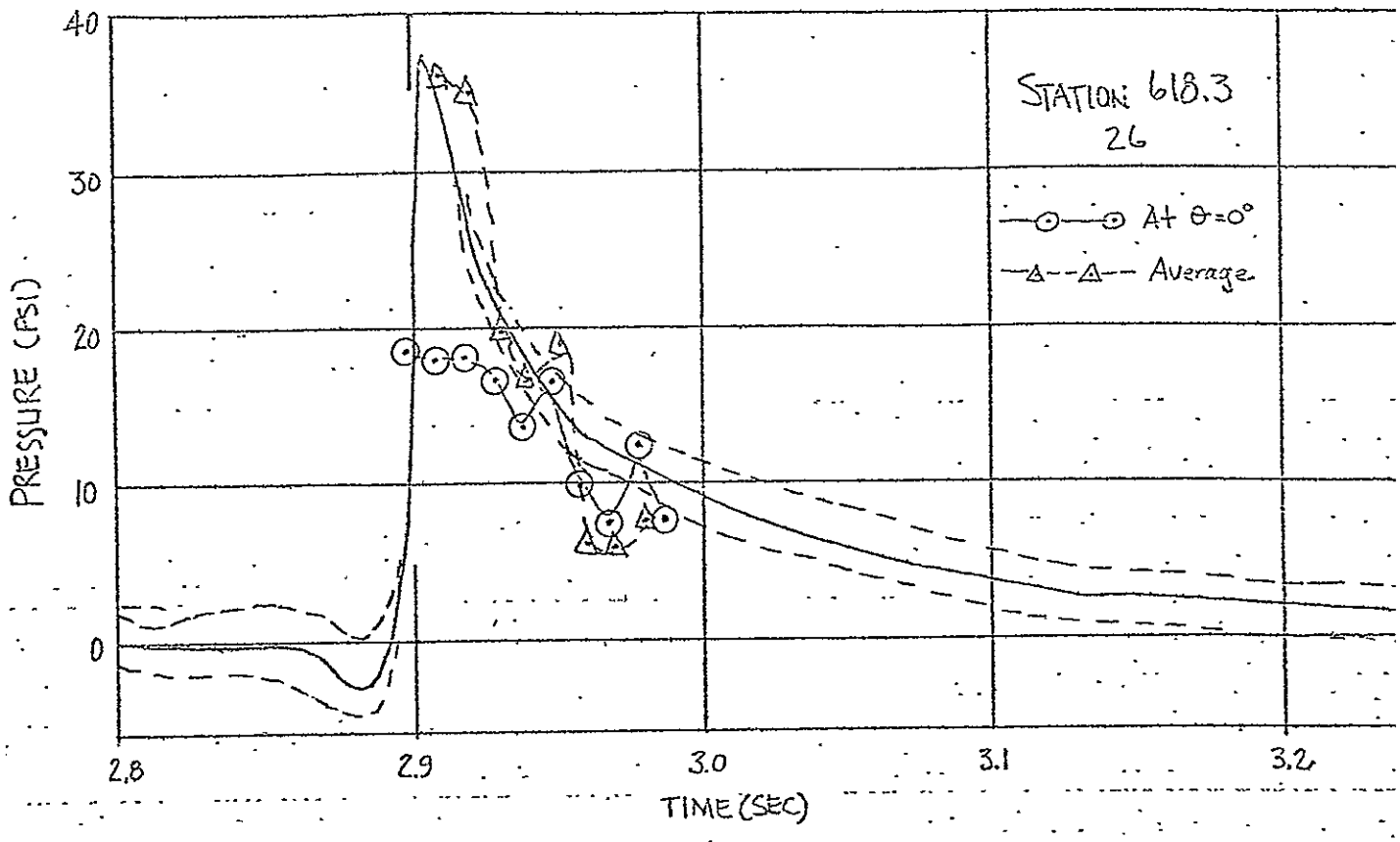

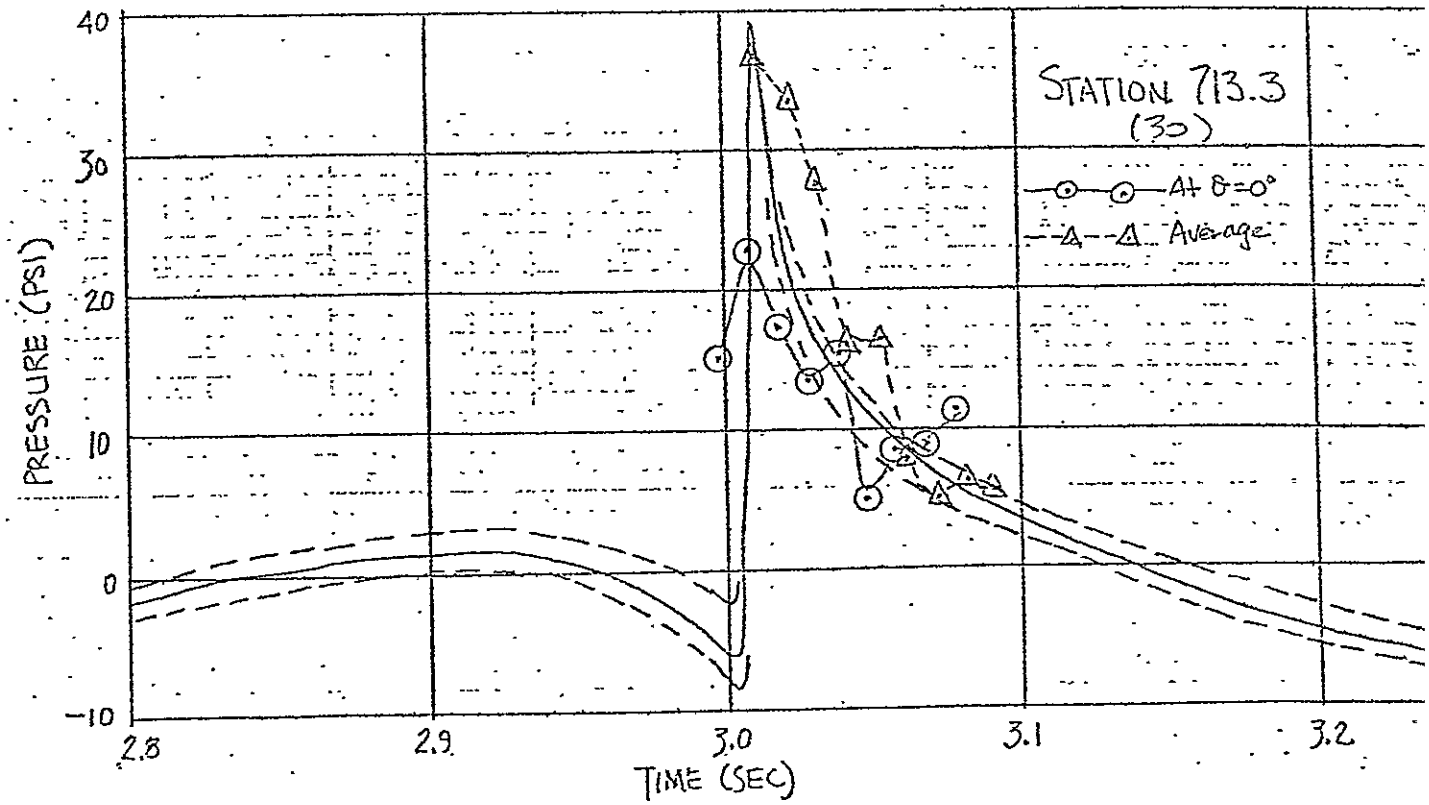

Run 31.c.

77% Water Recovery 145-20

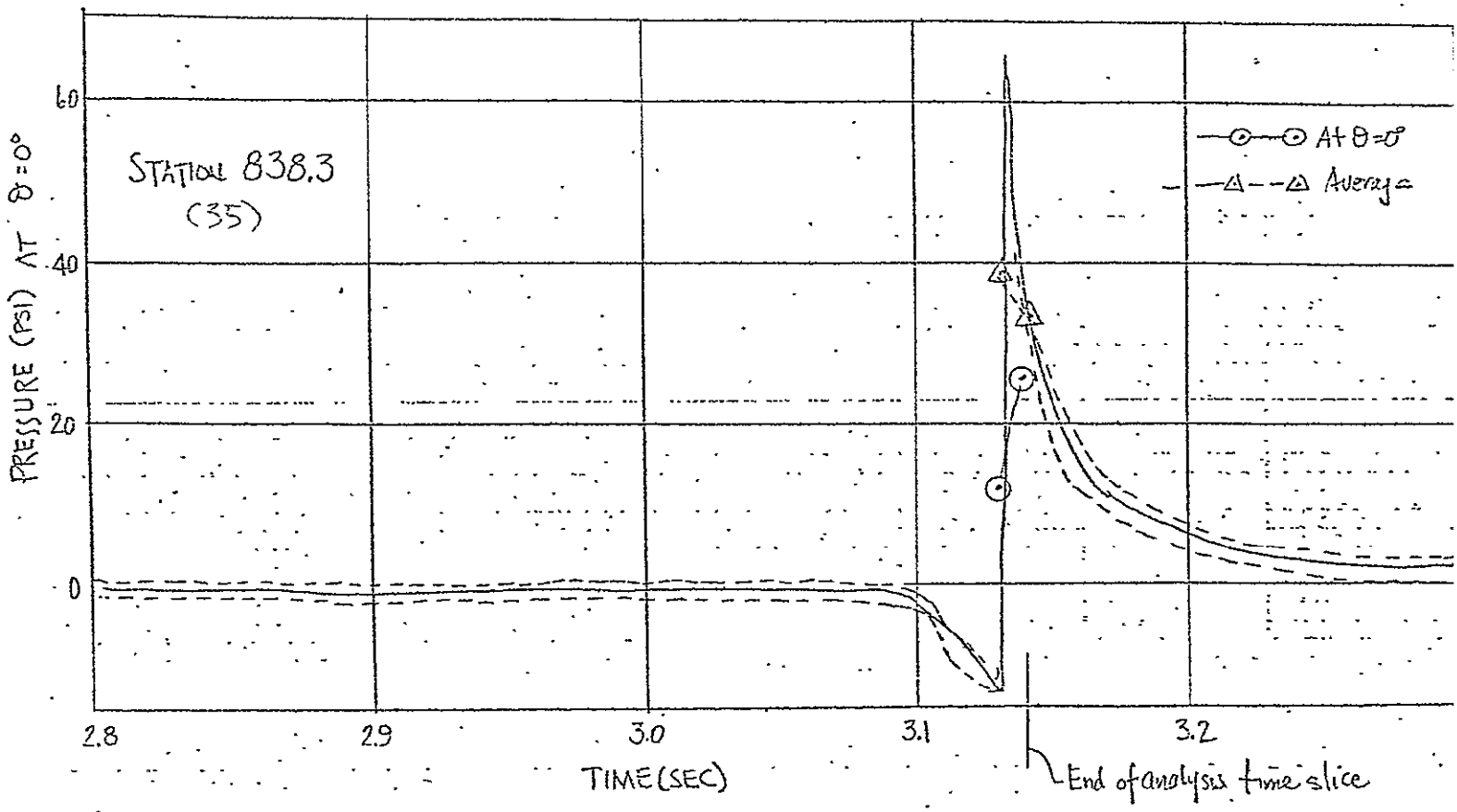

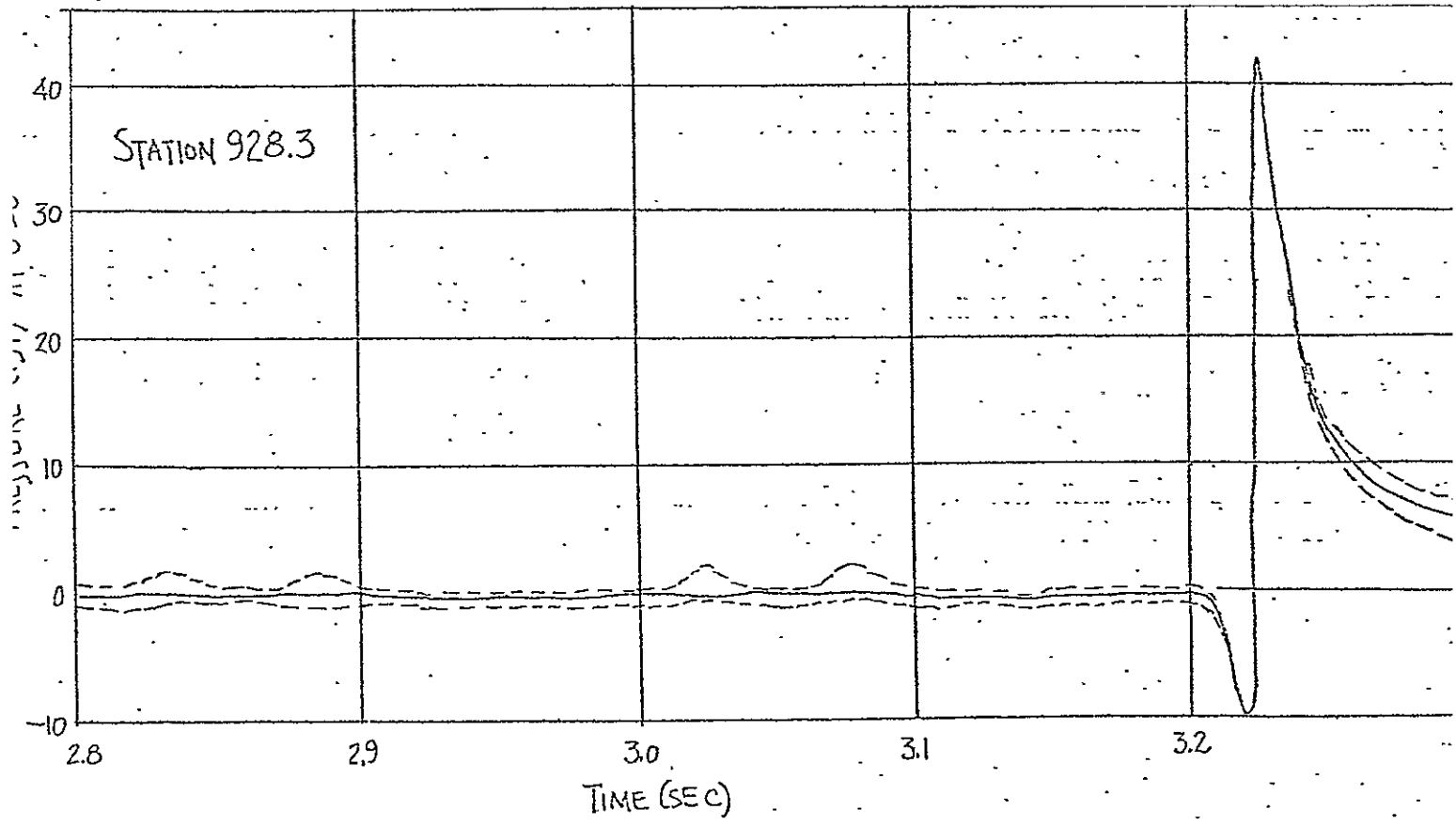

Run 3 I.C.

77% Water Recovery 145-20

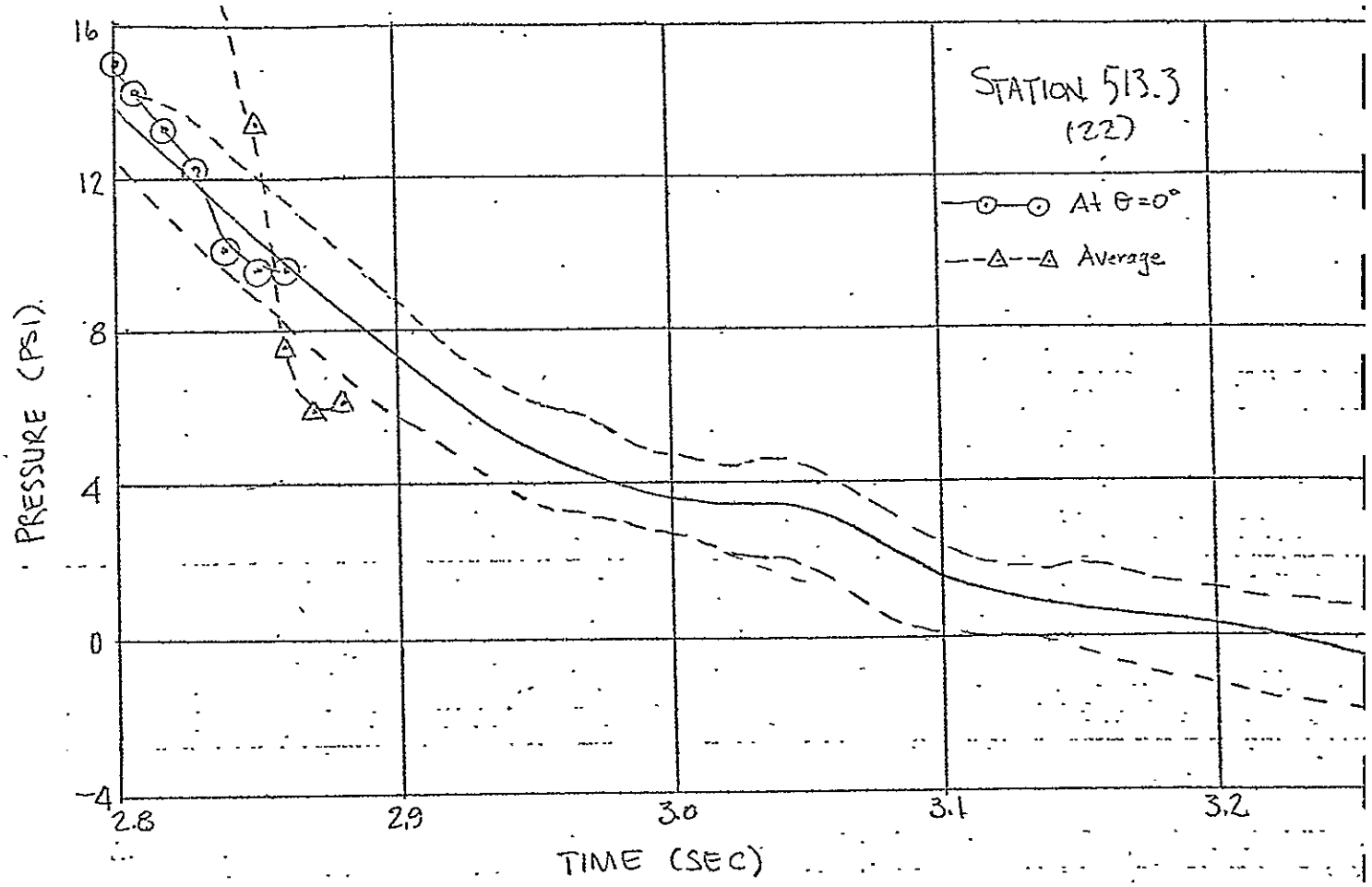

Run C145-20

Pressure vs. Station

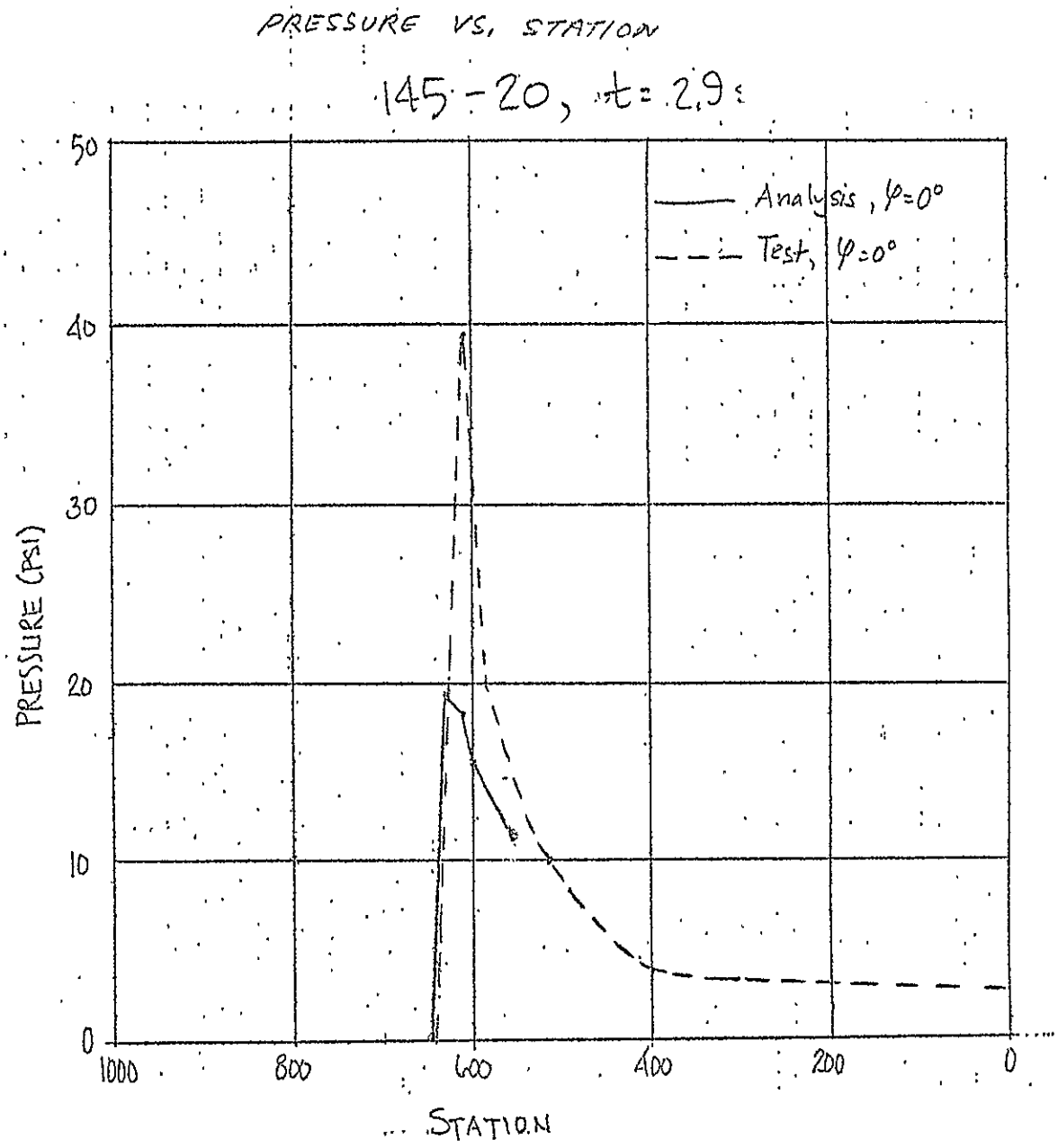
PRESSURE VS. STATION
145 - 20, t = 2.9 s
Analysis, φ=0°
Test, φ=0°
PRESSURE (PSI)
50
40
30
20
10
0
1000
800
600
400
200
0
STATION

PRESSURE VS. STATION

145-20, t=3.0 sec

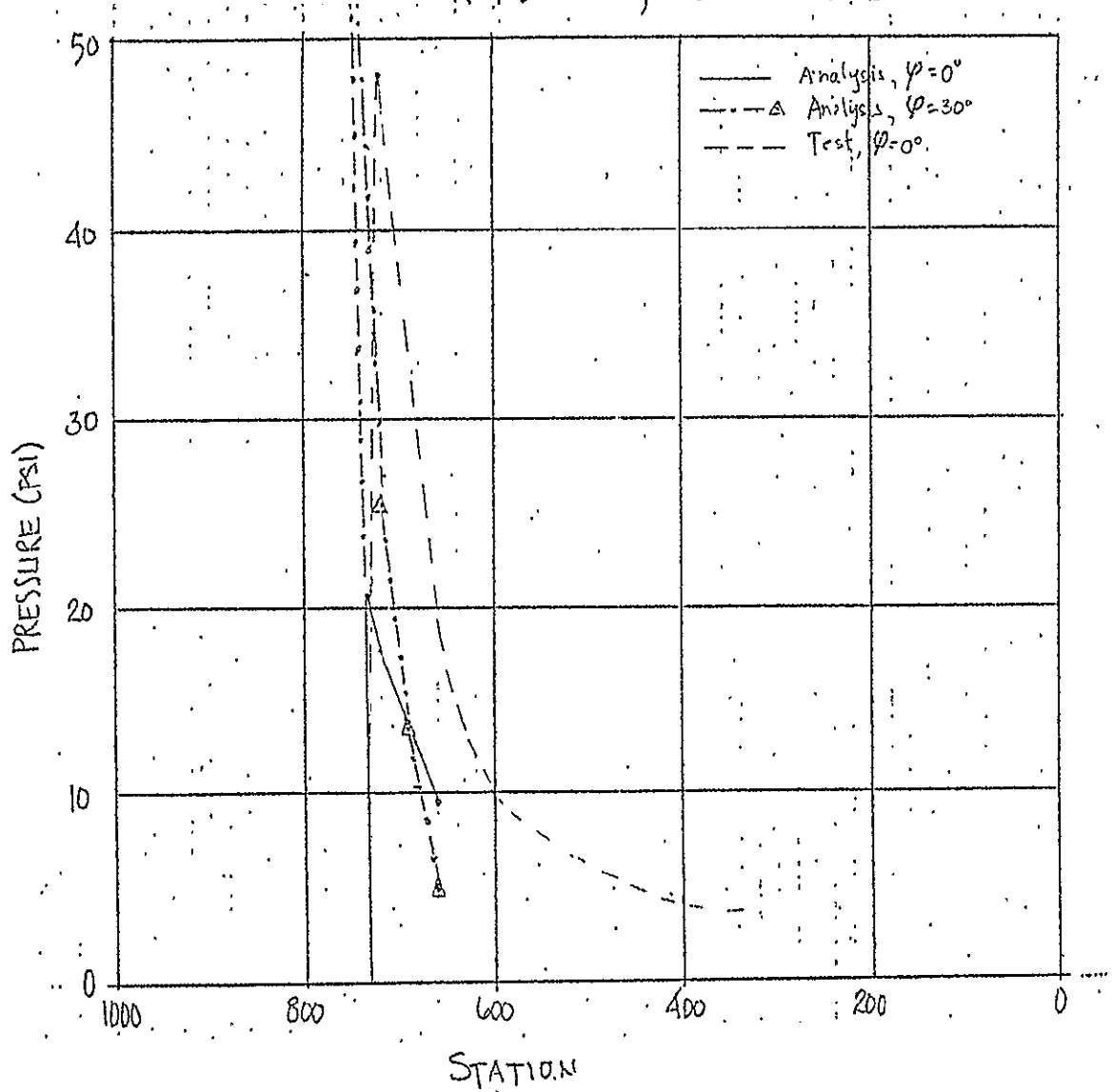

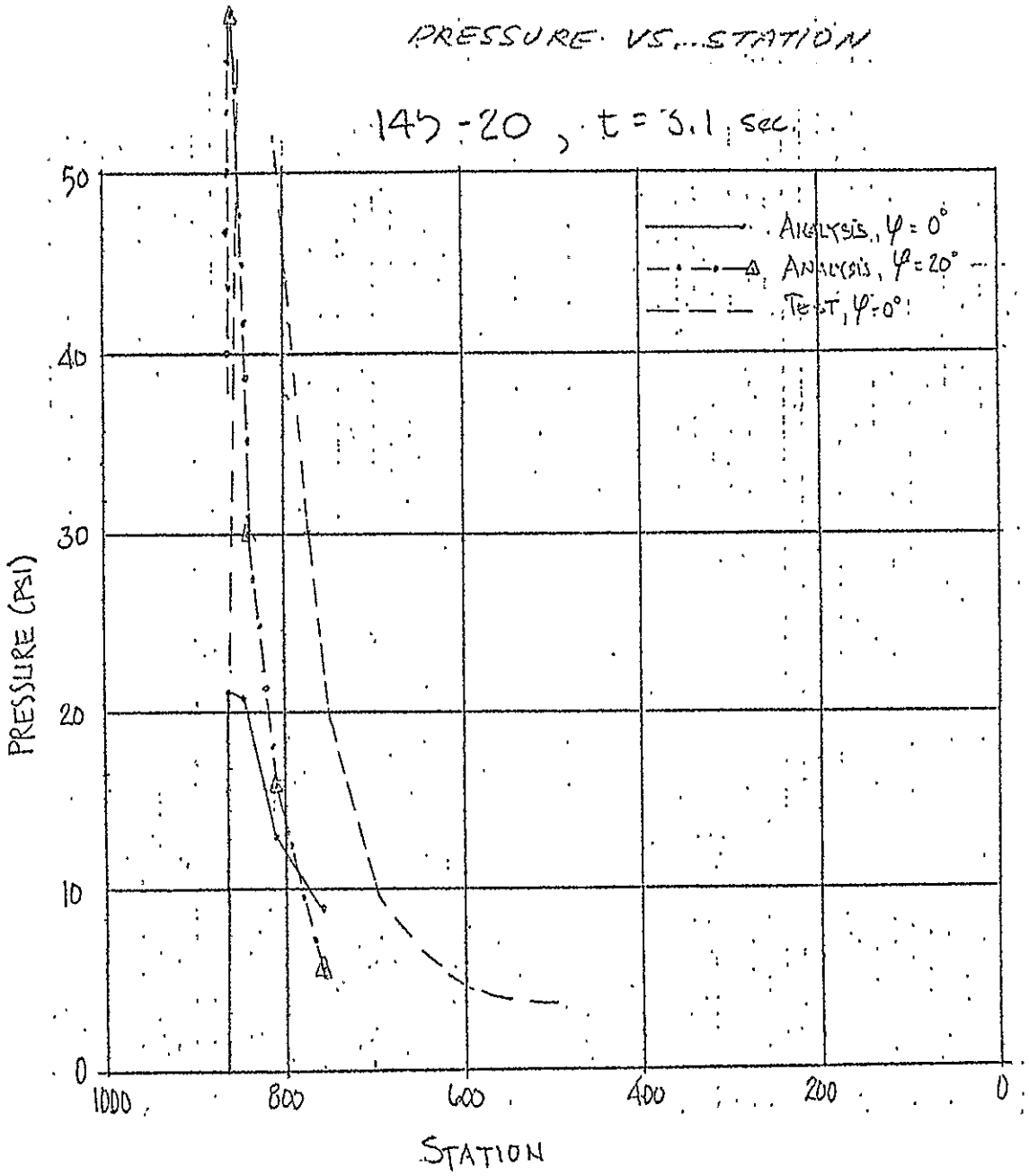
PRESSURE VS. STATION
145-20, t = 3.1 sec.
ANALYSIS, ψ = 0°
ANALYSIS, ψ = 20°
TEST, ψ = 0°
PRESSURE (PSI)
50
40
30
20
10
0
1000
800
600
400
200
0
STATION

Run C145-20

Circumferential Pressure
Distribution

145-20

TIME = 2.9 SEC

CIRCUMFERENTIAL PRESSUR
DISTRIBUTION

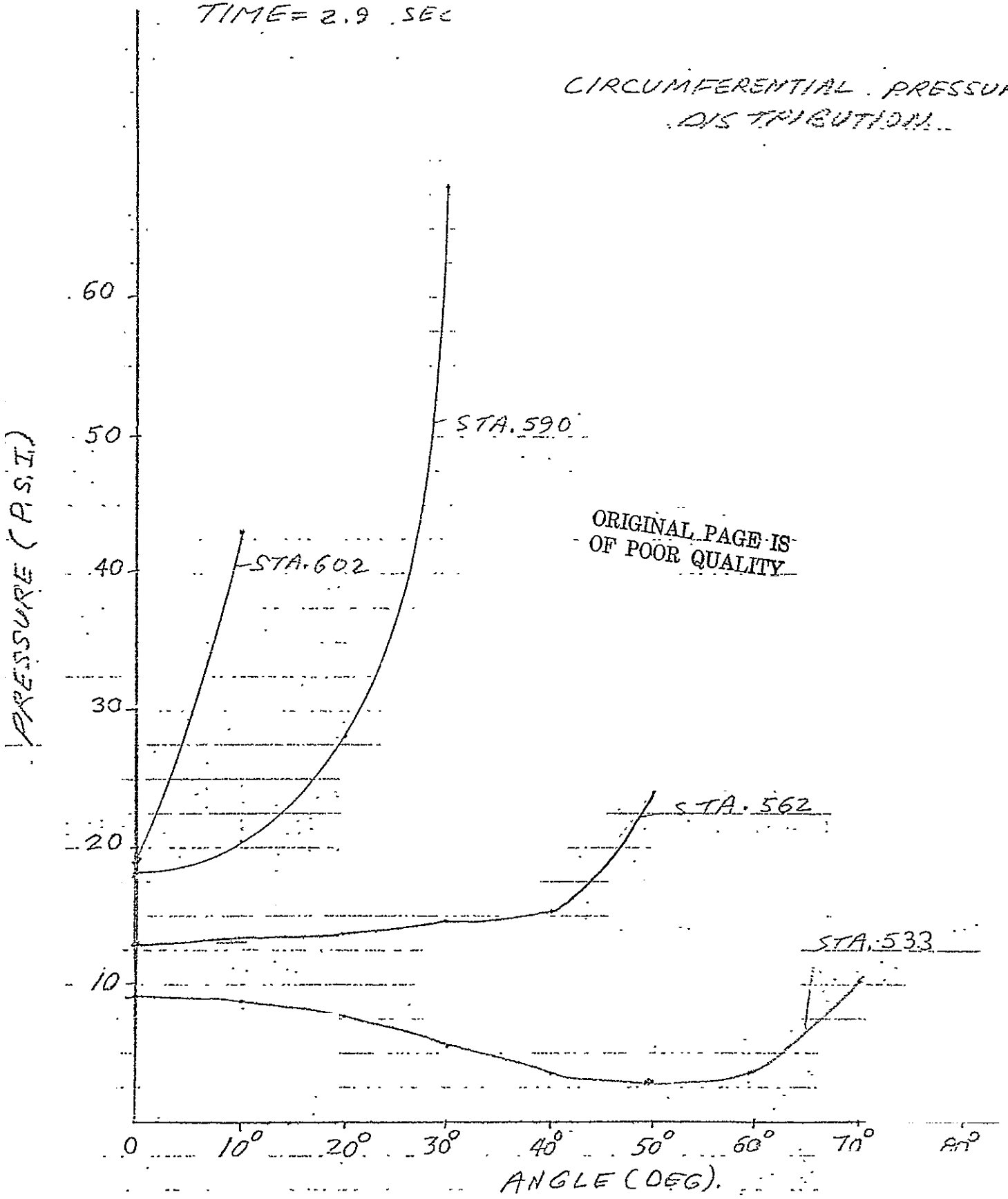

CIRCUMFERENTIAL PRESSURE DISTRIBUTION.

145-20

TIME = 3.0 SEC

CIRCUMFERENTIAL PRESSUR
DISTRIBUTION

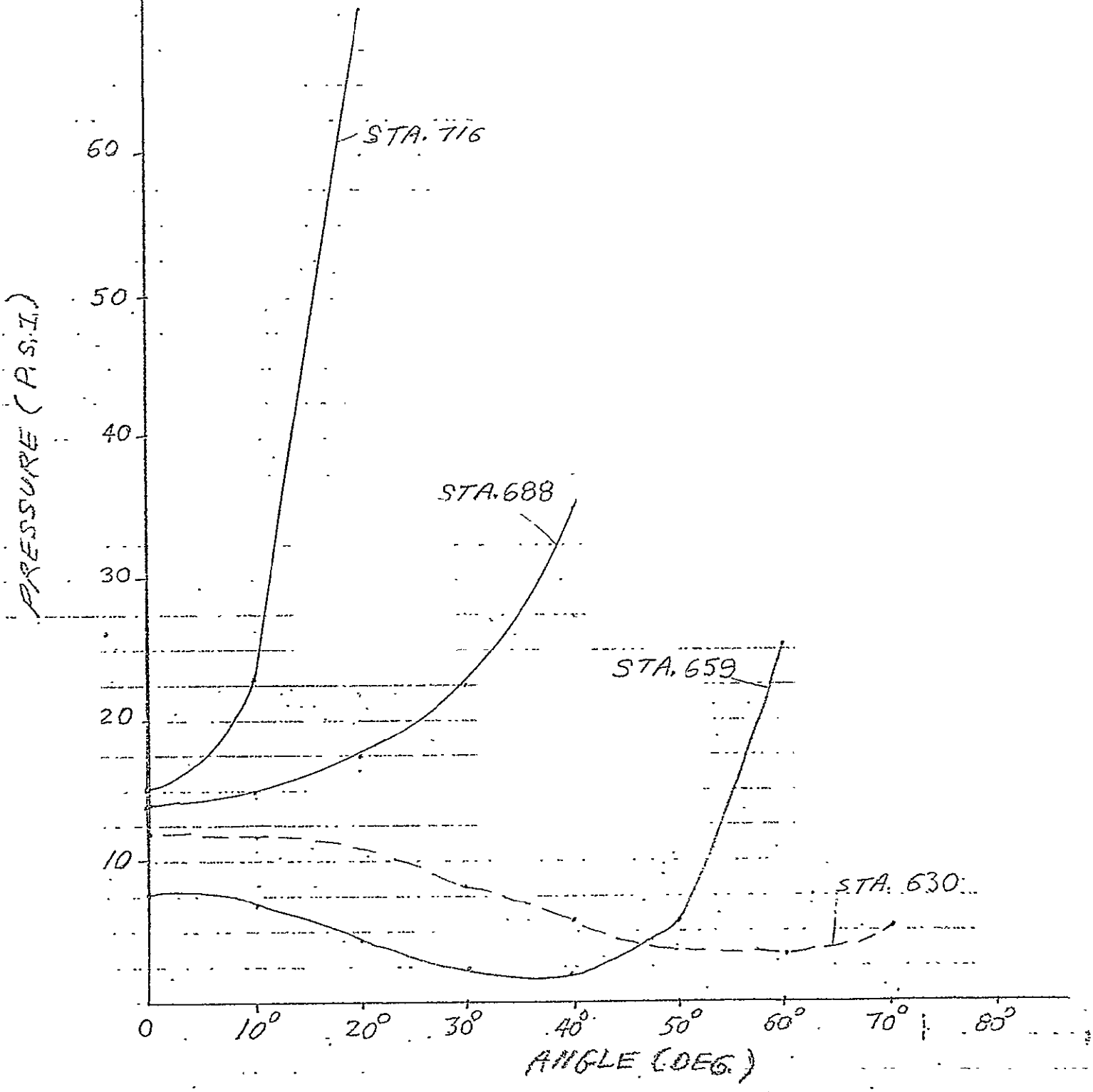

CIRCUMFERENTIAL PRESSURE DISTRIBUTION

145-20

TIME = 3.1 SEC

CIRCUMFERENTIAL PRESSURE DISTRIBUTION

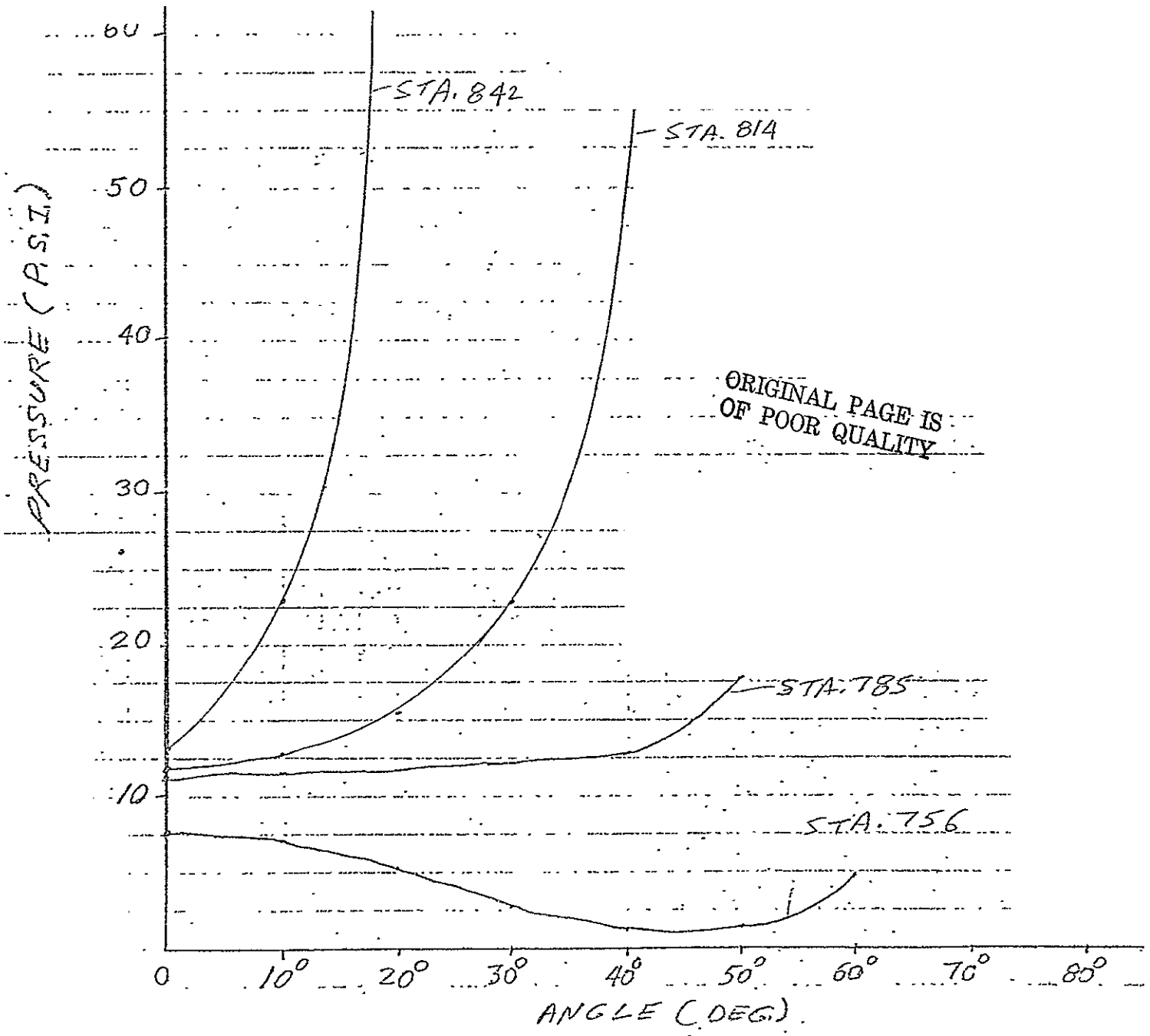

CIRCUMFERENTIAL PRESSURE DISTRIBUTION

Run C145-20

Diameter Deflection

vs.

Time

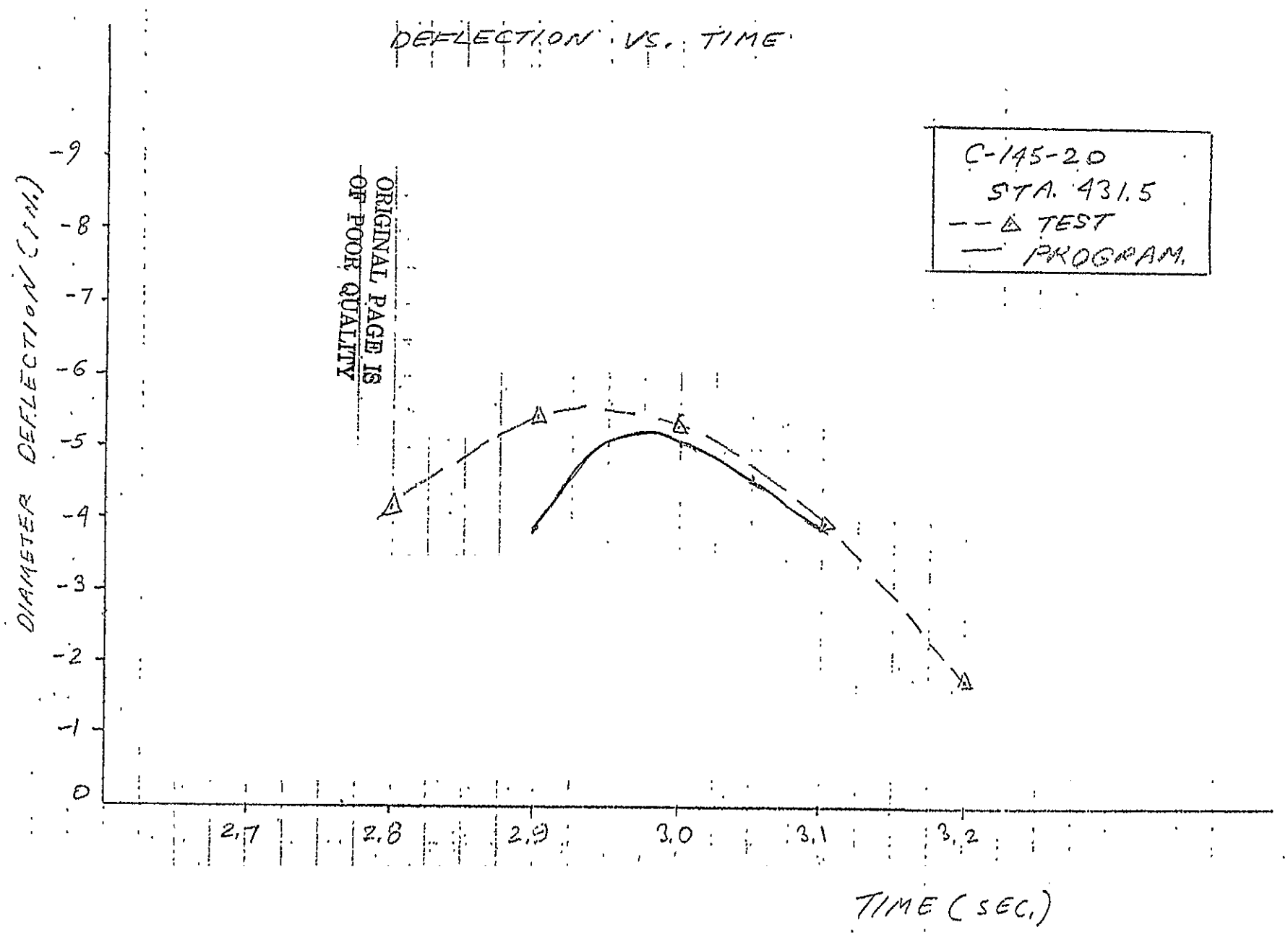

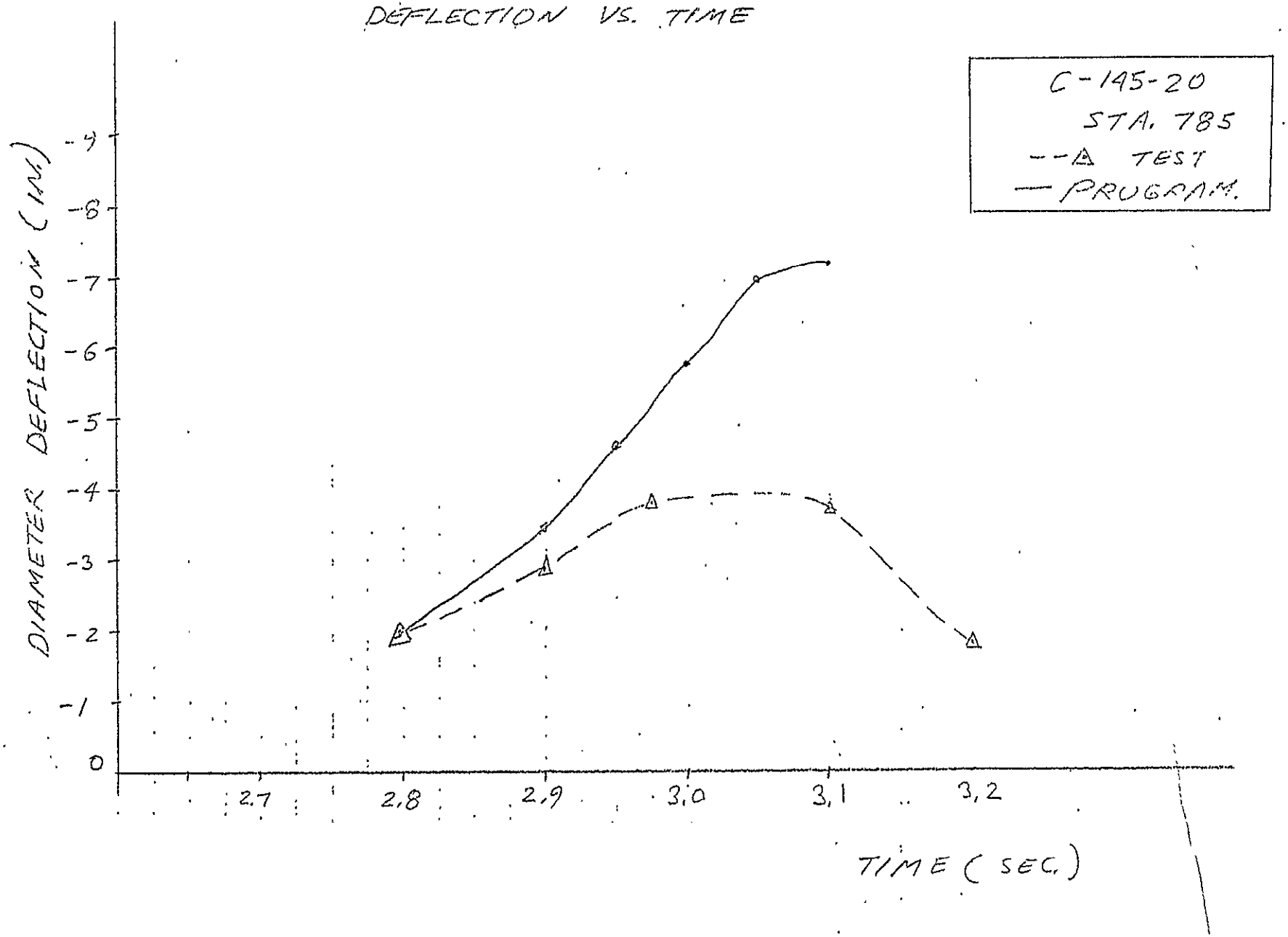
DEFLECTION VS. TIME
C-145-20
STA. 785
--△ TEST
— PROGRAM.
DIAMETER DEFLECTION (IN.)
-9
-8
-7
-6
-5
-4
-3
-2
-1
0
2.7
2.8
2.9
3.0
3.1
3.2
TIME (SEC.)

Run C145-20

Diameter Deflection

vs.

Station

DEFLECTION VS. STATION

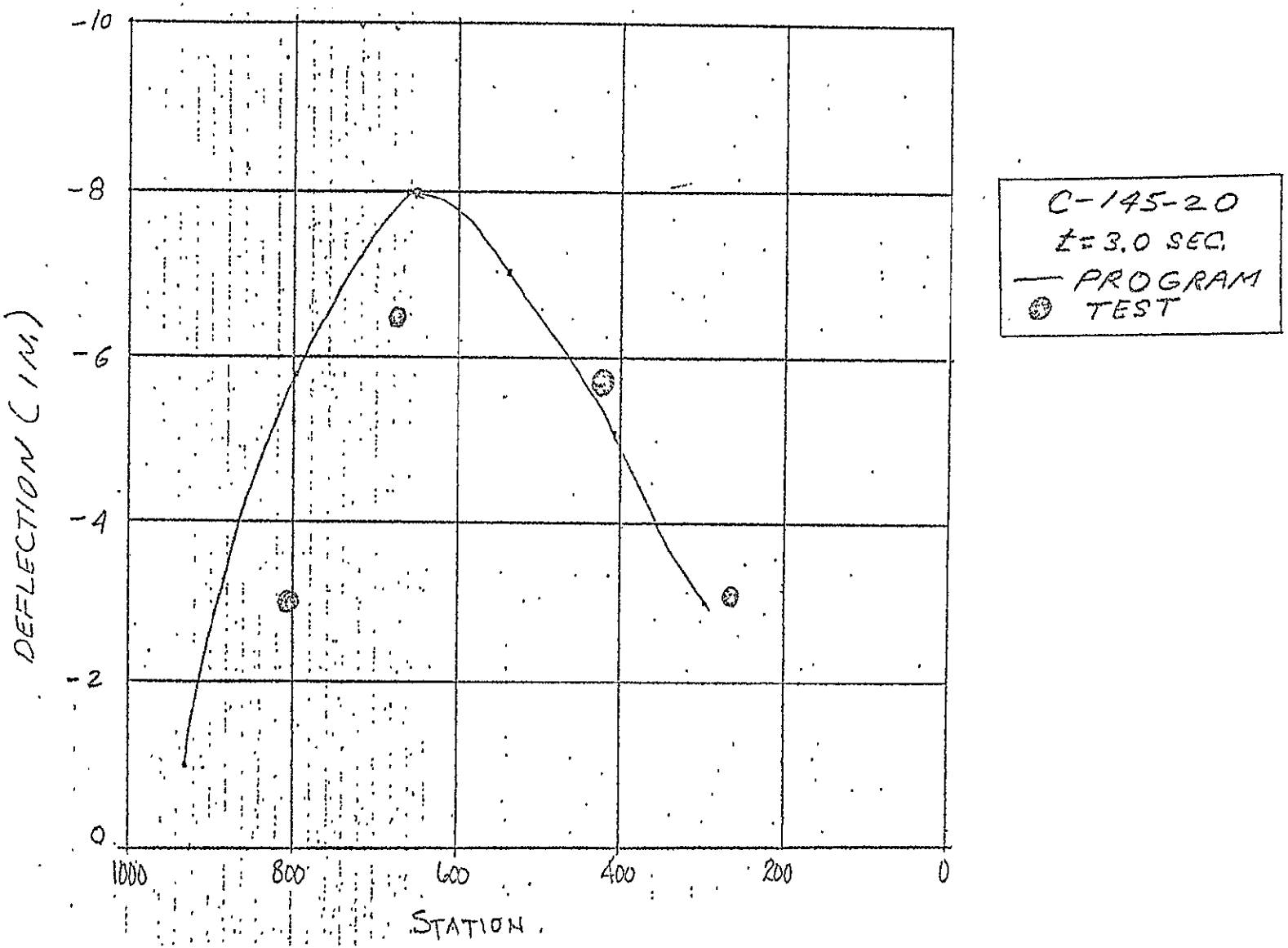

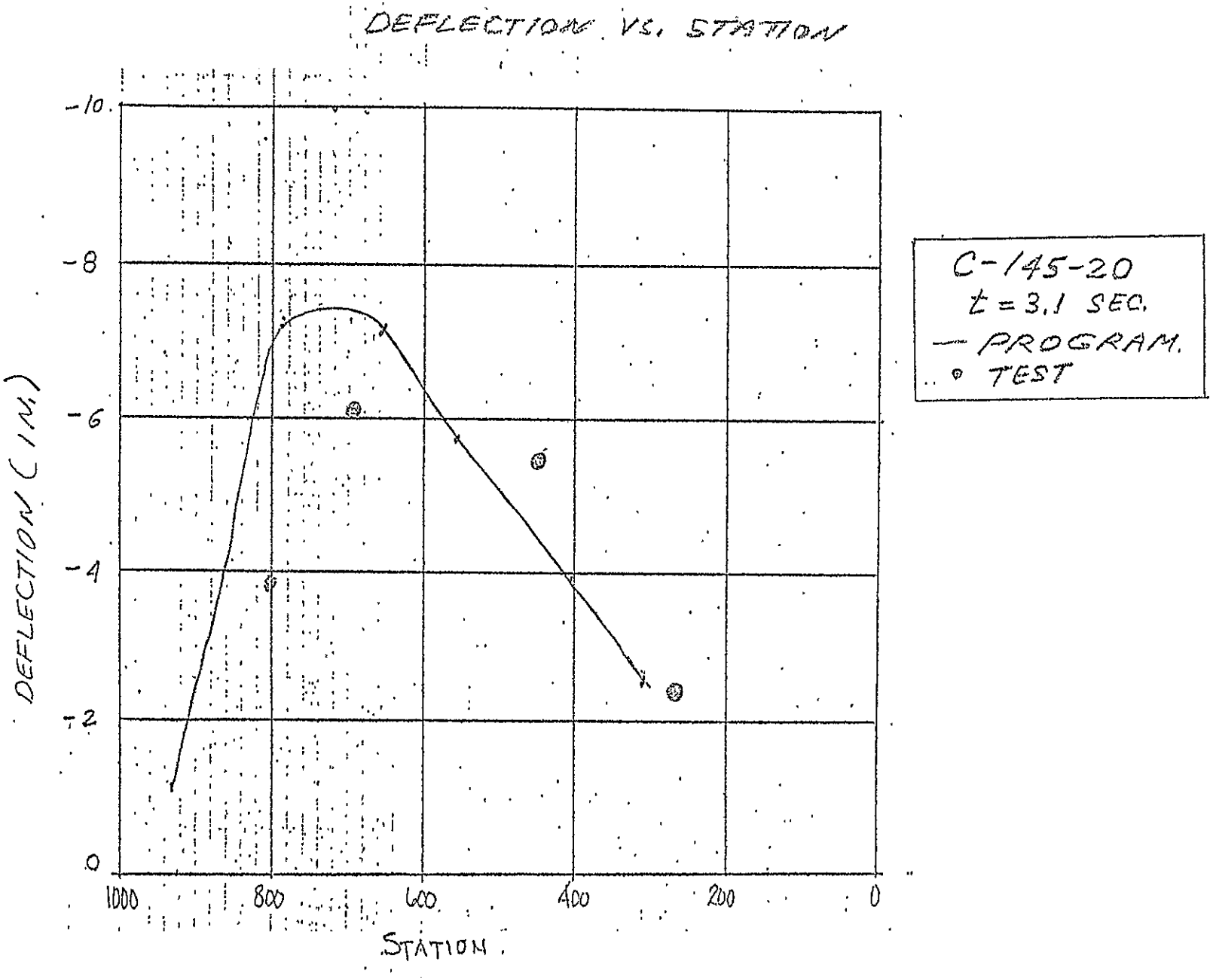

Run C145-20

Maximum Deflection

vs.

Station